GROUNDWATER QUALITY AND VULNERABILITY ASSESSMENT OF SEAWATER INTRUSION IN KHAMBHAT COASTAL REGION

A Thesis submitted to Gujarat Technological University

for the Award of

Doctor of Philosophy

in

Civil Engineering

By

Bhavsar Zalak Aalap

Enrollment No.: 209999912008

under supervision of

Dr. Jayeshkumar S. Patel

Principal, Vadodara Institute of Engineering,

Vadodara, Gujarat

GUJARAT TECHNOLOGICAL UNIVERSITY

AHMEDABAD

June – 2025

DECLARATION

I declare that the thesis entitled **Groundwater Quality and Vulnerability Assessment of Seawater Intrusion in Khambhat Coastal Region** submitted by me for the degree of Doctor of Philosophy is the record of research work carried out by me during the period from February 2021 to February 2025 under the supervision of Dr. Jayeshkumar S. Patel and this has not formed the basis for the award of any degree, diploma, associateship, fellowship, titles in this or any other University or other institution of higher learning.

I further declare that the material obtained from other sources has been duly acknowledged in the thesis. I shall be solely responsible for any plagiarism or other irregularities, if noticed in the thesis.

Signature of the Research Scholar: ..... Date: 20-06-2025

Name of Research Scholar: **Bhavsar Zalak Aalap**

Place: GTU, Chandkheda, Ahmedabad

CERTIFICATE

I certify that the work incorporated in the thesis **Groundwater Quality and Vulnerability Assessment of Seawater Intrusion in Khambhat Coastal Region** submitted by Mrs. Bhavsar Zalak Aalap was carried out by the candidate under my supervision/guidance. To the best of my knowledge: (i) the candidate has not submitted the same research work to any other institution for any degree/diploma, Associateship, Fellowship or other similar titles (ii) the thesis submitted is a record of original research work done by the Research Scholar during the period of study under my supervision, and (iii) the thesis represents independent research work on the part of the Research Scholar.

Signature of the Research Supervisor: ..... Date: 20-06-2025

Name of Supervisor: Dr. Jayeshkumar S. Patel

Place: GTU, Chandkheda, Ahmedabad

Course-work Completion Certificate

This is to certify that Mrs. Bhavsar Zalak Aalap enrolment no. 209999912008 is enrolled for PhD program in the faculty Civil Engineering of Gujarat Technological University, Ahmedabad.

(Please tick the relevant option(s))

☐ He/She has been exempted from the course-work (successfully completed during M.Phil Course)

☐ He/She has been exempted from Research Methodology Course only (successfully completed during M.Phil Course)

☑ He/She has successfully completed the PhD course work for the partial requirement for the award of PhD Degree. His/ Her performance in the course work is as follows-

Grade Obtained in Research Methodology [PHD22-01]	Grade Obtained in Research and Publication Ethics [PHD22-02]	Grade Obtained in Self-Study Course/ Contact Program [PHD22-03]
BC	AA	AA

Supervisor's Sign

(Name of the Research Supervisor: Dr. Jayeshkumar S. Patel)

Originality Report Certificate

It is certified that PhD Thesis titled **Groundwater Quality and Vulnerability Assessment of Seawater Intrusion in Khambhat Coastal Region** by Mrs. Bhavsar Zalak Aalap has been examined by us. We undertake the following:

a. Thesis has significant new work / knowledge as compared already published or are under consideration to be published elsewhere. No sentence, equation, diagram, table, paragraph or section has been copied verbatim from previous work unless itis placed under quotation marks and duly referenced.

b. The work presented is original and own work of the author (i.e. there is no plagiarism). No ideas, processes, results or words of others have been presented as Author own work.

c. There is no fabrication of data or results which have been compiled / analyzed.

d. There is no falsification by manipulating research materials, equipment or processes, or changing or omitting data or results such that the research is not accurately represented in the research record.

e. The thesis has been checked using **Turnitin software** (copy of originality report attached) and found within limits as per GTU Plagiarism Policy and instructions issued from time to time (i.e. permitted similarity index <=10%).

Signature of the Research Scholar: ..... Date: 20-06-2025

Name of the Research Scholar: Mrs. Bhavsar Zalak Aalap

Signature of the Research Supervisor: ..... Date: 20-06-2025

Name of the Research Supervisor: Dr. Jayeshkumar S. Patel

Place: GTU, Chandkheda, Ahmedabad

Thesis_209999912008.pdf

ORIGINALITY REPORT

7%	1%	6%	1%
SIMILARITY INDEX	INTERNET SOURCES	PUBLICATIONS	STUDENT PAPERS

PRIMARY SOURCES

1	Zalak Bhavsar, Jayeshkumar Patel. "Assessing potability of groundwater using groundwater quality index (GWQI), entropy weighted groundwater pollution index (EGPI) and geospatial analysis for khambhat coastal region of Gujarat", Groundwater for Sustainable Development, 2023 Publication	1%
2	Sankar Loganathan, Mahenthiran Sathiyamoorthy. "Groundwater quality assessment for drinking, irrigation purposes and fuzzy logic-based water quality index for industrial suitability in Walajapet taluk, Ranipet district, Tamil Nadu, India", AQUA — Water Infrastructure, Ecosystems and Society, 2024 Publication	<1%
3	B. Suvarna, V. Sunitha, Y. Sudharshan Reddy, B. Muralidhara Reddy, A. K. Kadam, M. Ramakrishna Reddy. "Groundwater quality assessment using multivariate statistical approach and geospatial modelling around cement industrial corridor, South India", International Journal of Environmental Science and Technology, 2022 Publication	<1%
4	Rohitashw Kumar, Kanak N. Moharir, Vijay P. Singh, Chaitanya B. Pande, Abhay M. Varade. "Sustainability of Natural Resources - Planning, Development, and Management", CRC Press, 2024 Publication	<1%
5	Dimple Dimple, Pradeep Kumar Singh, Mahesh Kothari, Kamal Kishore Yadav, Sita Ram Bhakar, Jitendra Rajput, Anvesha. "Assessing groundwater quality in Nand Samand catchment, Rajasthan, India: a GIS-based multi indices approach for drinking and irrigation water suitability", Water Practice & Technology, 2024 Publication	<1%
6	"Groundwater of South Asia", Springer Science and Business Media LLC, 2018 Publication	<1%
7	Vinay Kumar Gautam, P. K. Singh, Mahesh Kothari, Ahmed Elbeltagi. "Spatial interpolation and mapping groundwater quality using geostatistical method: case study in Jakham River Basin", Environmental Earth Sciences, 2024 Publication	<1%

8	S. Chidambaram, U. Karmegam, M. V. Prasanna, P. Sasidhar, M. Vasanthavigar. "A study on hydrochemical elucidation of coastal groundwater in and around Kalpakkam region, Southern India", Environmental Earth Sciences, 2011 Publication	<1%
9	link.springer.com Internet Source	<1%
10	Nizar Troudi, Fadoua Hamzaoui-Azaza, Ourania Tzoraki, Fatheddine Melki, Mounira Zammouri. "Assessment of groundwater quality for drinking purpose with special emphasis on salinity and nitrate contamination in the shallow aquifer of Guenniche (Northern Tunisia)", Environmental Monitoring and Assessment, 2020 Publication	<1%
11	Submitted to University of Zululand Student Paper	<1%
12	"Groundwater Resources Development and Planning in the Semi-Arid Region", Springer Science and Business Media LLC, 2021 Publication	<1%
13	Naidu L.S., G. Rao V.V.S., T. Rao G., Mahesh J., Padalu G., Sarma V.S., Prasad P.R., Rao S.M., R. Rao B.M.. "An integrated approach to investigate saline water intrusion and to identify the salinity sources in the Central Godavari delta, Andhra Pradesh, India", Arabian Journal of Geosciences, 2012 Publication	<1%
14	Berihu Abadi Berhe. "Evaluation of groundwater and surface water quality suitability for drinking and agricultural purposes in Kombolcha town area, eastern Amhara region, Ethiopia", Applied Water Science, 2020 Publication	<1%
15	P. Prusty, S.H. Farooq. "Seawater intrusion in the coastal aquifers of India - A review", HydroResearch, 2020 Publication	<1%
16	"Groundwater in the Coastal Zones of Asia-Pacific", Springer Science and Business Media LLC, 2013 Publication	<1%
17	M. V. Prasanna, S. Chidambaram, G. Senthil Kumar, AL Ramanathan, H. C. Nainwal. ", تقييم المياه الجوفية في حوض Neyveli Hydrogeochemical مقاطعة آودالور ، جنوب الهند", Arabian Journal of Geosciences, 2010 Publication	<1%
18	N. Subba Rao, A. Dinakar, B. Karuna Kumari, D. Karunanidhi, T. Kamalesh. "Seasonal and	<1%

Spatial Variation of Groundwater Quality Vulnerable Zones of Yellareddygudem Watershed, Nalgonda District, Telangana State, India", Archives of Environmental Contamination and Toxicology, 2020
Publication

19	www.mdpi.com Internet Source	<1 %
20	C. Singaraja, S. Chidambaram, Noble Jacob, E. Ezhilarasan, C. Velmurugan, M. Manikandan, S. Rajamani. "Taxonomy of groundwater quality using multivariate and spatial analyses in the Tuticorin District, Tamil Nadu, India", Environment, Development and Sustainability, 2015 Publication	<1 %
21	K.S. Anil Kumar, C.P. Priju, N.B. Narasimha Prasad. "Study on Saline Water Intrusion into the Shallow Coastal Aquifers of Periyar River Basin, Kerala Using Hydrochemical and Electrical Resistivity Methods", Aquatic Procedia, 2015 Publication	<1 %
22	Arun Prasun, Anshuman Singh. "Assessment of groundwater contamination in Aurangabad, Bihar using WQI and geostatistical modeling", Stochastic	<1 %

Environmental Research and Risk Assessment, 2025
Publication

23	Anjali Malan, Hardeep Rai Sharma. "Groundwater quality in open-defecation-free villages (NIRMAL grams) of Kurukshetra district, Haryana, India", Environmental Monitoring and Assessment, 2018 Publication	<1 %
24	Victor Fanuel Sanga, Christina Fabian Pius, Fikira Kimbokota. "Heavy metals pollution in leachates and its impacts on quality of groundwater around Iringa municipal solid waste dumpsite.", Research Square Platform LLC, 2022 Publication	<1 %
25	M. Rhishi Hari Raj, D. Karunanidhi, Priyadarsi D. Roy, T. Subramani. "Fluoride enrichment in groundwater and its association with other chemical ingredients using GIS in the Arjunanadi River basin, Southern India: Implications from improved water quality index and health risk assessment", Physics and Chemistry of the Earth, Parts A/B/C, 2025 Publication	<1 %
26	S.O. Academe, P.C. Emenike, P. Unokiwedi, C.C. Nnaji, M.A. Etim. "Suitability and hydrogeochemical imprints of groundwater in	<1 %

residential location around Abeokuta, southwestern Nigeria", IOP Conference Series: Earth and Environmental Science, 2022
Publication

27 S. Selvam, G. Manimaran, P. Sivasubramanian, N. Balasubramanian, T. Seshunarayana. "GIS-based Evaluation of Water Quality Index of groundwater resources around Tuticorin coastal city, south India", Environmental Earth Sciences, 2013 <1%
Publication

28 M. Vasanthavigar, K. Srinivasamoorthy, M. V. Prasanna. "Evaluation of groundwater suitability for domestic, irrigational, and industrial purposes: a case study from Thirumanimuttar river basin, Tamilnadu, India", Environmental Monitoring and Assessment, 2011 <1%
Publication

29 P. Arulbalaji, B. Gurugnanam. "Groundwater quality assessment using geospatial and statistical tools in Salem District, Tamil Nadu, India", Applied Water Science, 2016 <1%
Publication

30 Qiying Zhang, Hui Qian, Panpan Xu, Kai Hou, Faxuan Yang. "Groundwater quality assessment using a new integrated-weight water quality index (IWQI) and driver analysis in the Jiaokou Irrigation District, China", Ecotoxicology and Environmental Safety, 2021 <1%
Publication

31 Rabindranath Barik, Sanjaya Kumar Pattanayak. "Assessment of groundwater quality for irrigation of green spaces in the Rourkela city of Odisha, India", Groundwater for Sustainable Development, 2019 <1%
Publication

32 S. M. Sadat-Noori, K. Ebrahimi, A. M. Liaghat. "Groundwater quality assessment using the Water Quality Index and GIS in Saveh-Nobaran aquifer, Iran", Environmental Earth Sciences, 2013 <1%
Publication

33 Subhankar Ghosh, Madan Kumar Jha. "Hydrogeochemical characterization of groundwater and critical assessment of its quality in a coastal basin", Environment, Development and Sustainability, 2023 <1%
Publication

34 Submitted to University of Philadelphia - Jordan <1%
Student Paper

35 "Proceedings of International Conference on Remote Sensing for Disaster Management", Springer Science and Business Media LLC, 2019 <1%

Publication

36	Akshay Kumar, Varun Narayan Mishra, Rahul Ratnam, Chaitanya B. Pande, Akhouri Pramod Krishna. "Chapter 3 Assessment of Groundwater Quality in South Karanpura Coalfield Region, Jharkhand, India Using WQI and Geospatial Approach", Springer Science and Business Media LLC, 2023 Publication	<1 %
37	c.coek.info Internet Source	<1 %
38	ia601301.us.archive.org Internet Source	<1 %
39	Gyampo, Maxwell Anim-, Musah Saeed Zango, and Boateng Ampadu. "Assessment of Drinking Water Quality of Groundwaters in Bunpkurugu-Yunyo District of Ghana", Environment and Pollution, 2014. Publication	<1 %
40	"Landslides in the Himalayan Region", Springer Science and Business Media LLC, 2024 Publication	<1 %
41	Huan Wang, Xinyu Wang, Yuanxing Yin, Xiaojun Deng, Muhammad Umair. "Evaluation of urban transportation carbon footprint – Artificial intelligence based solution", Transportation Research Part D: Transport and Environment, 2024 Publication	<1 %
42	Rui Cao, Ji Dor, YongQiang Cai, XiaoLin Chen, Xiang Mao, Hui-ren Meng. "Geochemical and H–O–Sr–B isotope signatures of Yangyi geothermal fields: implications for the evolution of thermal fluids in fracture-controlled type geothermal system, Tibet, China", Geothermal Energy, 2023 Publication	<1 %

Exclude quotes On
Exclude bibliography On
Exclude matches < 14 words

Ph.D. Thesis Non-Exclusive License to

GUJARAT TECHNOLOGICAL

UNIVERSITY

In consideration of being a Research Scholar at Gujarat Technological University, and in the interests of the facilitation of research at the University and elsewhere, I, Mrs. Bhavsar Zalak Aalap having (Enrollment No.) 209999912008 hereby grant a non- exclusive, royalty free and perpetual license to the University on the following terms:

a. The University is permitted to archive, reproduce and distribute my thesis, in whole or in part, and/or my abstract, in whole or in part (referred to collectively as the "Work") anywhere in the world, for non-commercial purposes, in all forms of media;
b. The University is permitted to authorize, sub-lease, sub-contract or procure any of the acts mentioned in paragraph (a);
c. The University is authorized to submit the Work at any National / International Library, under the authority of their "Thesis Non-Exclusive License";
d. The Universal Copyright Notice (©) shall appear on all copies made under the authority of this license;
e. I undertake to submit my thesis, through my University, to any Library and Archives. Any abstract submitted with the thesis will be considered to form part of the thesis.
f. I represent that my thesis is my original work, does not infringe any rights of others, including privacy rights, and that I have the right to make the grant conferred by this non-exclusive license.
g. If third party copyrighted material was included in my thesis for which, under the terms of the Copyright Act, written permission from the copyright owners is required, I have obtained such permission from the copyright owners to do the acts mentioned in paragraph (a) above for the full term of copyright protection.
h. I understand that the responsibility for the matter as mentioned in the paragraph (g) rests with the authors / me solely. In no case shall GTU have any liability for any acts/ omissions/errors/copyright infringement from the publication of the said thesis or otherwise.
i. I retain copyright ownership and moral rights in my thesis, and may deal with the copyright in my thesis, in any way consistent with rights granted by me to my University in this non-exclusive license.

j. GTU logo shall not be used /printed in the book (in any manner whatsoever) being published or any promotional or marketing materials or any such similar documents.

k. The following statement shall be included appropriately and displayed prominently in the book or any material being published anywhere: "The content of the published work is part of the thesis submitted in partial fulfilment for the award of the degree of Ph.D. in Civil Engineering of the Gujarat Technological University".

l. I further promise to inform any person to whom I may hereafter assign or license my copyright in my thesis of the rights granted by me to my University in this nonexclusive license. I shall keep GTU indemnified from any and all claims from the Publisher(s) or any third parties at all times resulting or arising from the publishing or use or intended use of the book / such similar document or its contents.

m. I am aware of and agree to accept the conditions and regulations of Ph.D. including all policy matters related to authorship and plagiarism.

Date: 20-06-2025

Place: GTU, Chandkheda, Ahmedabad

Signature of the Research Scholar
Bhavsar Zalak Aalap

Recommendation of the Research Supervisor: Recommended

Recommendation of the Co-Supervisor (if any): .....

Signature of the Research Supervisor
Dr. Jayeshkumar S. Patel

Signature of the Co-Supervisor (if any)

Thesis Approval Form

The viva-voce of the PhD Thesis submitted by Mrs. Bhavsar Zalak Aalap (Enrollment No. 209999912008) entitled **Groundwater Quality and Vulnerability Assessment of Seawater Intrusion in Khambhat Coastal Region** was conducted on ....20/06/2025..... (day and date) at Gujarat Technological University.

(Please tick any one of the following option)

☑ The performance of the candidate was satisfactory. We recommend that he/she be awarded the PhD degree.

☐ Any further modifications in research work recommended by the panel after 3 months from the date of first viva-voce upon request of the Supervisor or request of Independent Research Scholar after which viva-voce can be re-conducted by the same panel again.

(briefly specify the modifications suggested by the panel)

—

☐ The performance of the candidate was unsatisfactory. We recommend that he/she should not be awarded the PhD degree.

(The panel must give justifications for rejecting the research work)

—

Dr. Jayeshkumar S. Patel

Name and Signature of Supervisor with Seal

Dr. A.D. Ghare

1) (External Examiner 1) Name and Signature

Dr. Mahendra Kumar Choudhary

2) (External Examiner 2) Name and Signature

Vadodara Institute of Engineering Kotambi

ABSTRACT

Gujarat is privileged to possess an extensive coastline. Along the coast of the state, various villages, industrial settlements, and urban centres are situated. Since freshwater availability is essential for supporting household, industrial, and agricultural demands, water resources in coastal areas are significant for any development activity. Groundwater, the primary source of freshwater in coastal areas, is utilized extensively to satisfy increasing demands for various purposes. However, the quality of groundwater in the region near the coast is negatively impacted by several natural and human activities. Furthermore, the coastal area is confronting a substantial issue caused by increased groundwater salinity resulting from the migration of saline seawater into freshwater resources. Agriculture is the primary occupation of the Khambhat coastal villages, which significantly depend on groundwater extraction. The unrestricted withdrawal of groundwater leads to the region's susceptibility to salty water intrusion. The current research assesses groundwater quality for potability and agriculture applications in 62 coastal villages of Khambhat and Borsad taluka of Gujarat. Moreover, the study region is categorized into two distinct zones of seawater vulnerability by employing the GALDIT method.

Groundwater sampling was carried out for two seasons of the year, and the samples were tested in the laboratory for the various water quality indicator parameters. High concentrations of the salinity indicator parameters such as EC, TDS, Na, and Cl in the PRM period represent the seawater mixing. However, the concentration of the salinity indicator parameters in the POM period decreased due to the dilution by groundwater recharge during monsoon. A correlation matrix was generated to find a correlation among various groundwater quality parameters. Additionally, the Piper trilinear diagram was also plotted to illustrate the hydrogeochemical facies of the groundwater, and the interpretation of the diagram reveals that in the PRM period, 92.98% of the samples fall in zone-II, signifying the dominance of Na and Cl in the groundwater.

To evaluate the potability of groundwater and to classify the groundwater into different water quality classes, the GWQI was computed by applying a subjective approach to weigh the parameters. In addition to address the constraint and also to validate the assigned weight by employing a subjective approach, the entropy-weighted WQI (EGWQI) was calculated by employing an objective approach to weight the

parameters, in which the weight is allocated to individual parameters by mathematical calculations. According to the calculated value of GWQI and EGWQI, the groundwater of the study region was categorized into different classes of water quality. Moreover, the geographical dispersal of the potability of groundwater based on GWQI and EGWQI is illustrated through spatial maps generated in the GIS environment. The interpretation of the spatial maps of groundwater quality class based on GWQI depicts that 85.28% of the research region falls under the classes "Very poor and Unsuitable" in the PRM period; while, in the POM period, it decreases to 26.73%. Moreover, the interpretation of the spatial map of the groundwater quality class based on EGWQI represents that 73.01% of the area falls within the "Very poor and Unsuitable" classes in the PRM period, while in the POM period, it reduced to 12.09%.

To evaluate the appropriateness of groundwater for agriculture and to classify the groundwater into the different water quality classes, the entropy-weighted irrigation WQI (EIRWQI) was calculated. According to the calculated value of EIRWQI, the groundwater of the study region was categorized into different classes of water suitability for agriculture. Moreover, the geographical dispersal of the suitability of groundwater based on EIRWQI is illustrated through spatial maps generated in the GIS environment. The interpretation of the spatial maps of groundwater quality class based on EIRWQI depicts that 60.68% of the research region falls under the classes "Very poor and Unsuitable" in the PRM period, while in the POM period, it decreases to 16.66%. Furthermore, the findings of the GALDIT method to demarcate sweater intrusion vulnerable zone reveal that approximately 50% of the study area is categorized as a "High vulnerable zone", and the remaining 50% of the area can be categorized as a "Moderate vulnerable zone."

Acknowledgement

This research work has been made possible through the genuine guidance, encouragement, and support of many individuals to whom I would like to express my heartfelt gratitude. Firstly, I honestly express sincere thanks to my research supervisor, Dr. Jayeshkumar S. Patel, Principal of Vadodara Institute of Engineering, for his active involvement, motivating guidance, and continuous support throughout all stages of my work to bring this thesis to fruition. His unwavering guidance during the preliminary visits to the research area and interactions with farmers and local inhabitants allowed me to gain a deeper understanding of the issues and conduct thorough and meaningful work. I am deeply grateful for his generosity in sharing his extensive knowledge and expertise in the field of groundwater, which provided me with the skills and insight to apply theoretical concepts practically.

I am extremely thankful to my doctoral progress committee members, Dr. Rupesh P. Vasani, Director, SAL Institute of Engineering & Technology Research, Ahmedabad and Dr. Falguni P. Parekh, Associate professor, Water Resources Engineering and Management Institute, Samiala, Vadodara. This work would not have taken shape without their insightful suggestions and unwavering encouragement. With their continuous evaluation, I could get insight and motivation to work professionally to achieve the desired research objectives.

I am very thankful to the farmers and villagers of my research area for helping me to understand the current scenario and allowing me to collect the groundwater samples from their private borewells for two distinct seasons. I am also thankful to the officials of the West Central Region, Central Groundwater Board, Ahmedabad and Regional Data Centre, Gujarat Water Resource Development Corporation Ltd., Ahmedabad, for their kind cooperation during the data collection.

I would also like to express my deep gratitude to Dr. Manishbhai Shah, President, L.J. University, Ahmedabad and Shri Rohitbhai Patel, Academic Advisor, L.J. Institute of Engineering and Technology, LJU, Ahmedabad, for their unwavering trust in me and for consistently entrusting me with responsibilities. Without their continuous motivation and support, this work would not have come to fruition. I would also like to record my thanks to all my colleagues at the L.J. Institute of Engineering and Technology for their support, especially to Mr Jay Soni for encouraging me to join PhD and Ms Janki Adhvaryu for helping with GIS software.

This acknowledgement would be incomplete without mentioning my family's immense patience and unwavering support. No words, however carefully chosen, could fully express my gratitude toward my husband, Aalap, my son, Yatharth, and my mother-in-law, Nirupaben, who selflessly agreed to set aside their hobbies, needs, and personal time to support me in completing this work.

Finally, I would like to express my heartfelt gratitude to my loving parents for their constant encouragement, support, and selfless devotion throughout my educational journey. Their endless love and unwavering belief in my goals have consistently provided me with strength and motivation. My special thanks to my siblings Vidhi and Yash for their thorough support and encouragement in completing the work.

Last but not least, I would like to express my deep gratitude, appreciation, and satisfaction to all those who have contributed, both directly and indirectly, to the successful completion of my thesis. While some may not be specifically mentioned, their support remains in my heart and mind.

Bhavsar Zalak Aalap

Table of Contents

List of Abbreviation

Abbreviation	Meaning
PRM	Pre Monsoon
POM	Post Monsoon
GWQI	Groundwater Quality Index
EWQI	Entropy Weighted Water Quality Index
EGWQI	Entropy Weighted Groundwater Quality Index
EIRWQI	Entropy Weighted Irrigation Water Quality Index
PIG	Pollution Index of Groundwater
SPI	Synthetic Pollution Index
TDS	Total Dissolved Solids
EC	Electrical Conductivity
TH	Total Hardness
GIS	Geographic Information System
IDW	Inverse Distance Weighting
MCDM	Multicriteria Decision Making
EWM	Entropy Weight Method
AHP	Analytical Hierarchy Process
DEA	Data Envelopment Analysis
CCR	Charnes, Cooper, and Rhodes
SAR	Sodium Absorption Ratio
%Na	Percentage Sodium
RSC	Residual Sodium Carbonate
RSBC	Residual Sodium Bicarbonate
PS	Potential Salinity
KI	Kelly’s Index
MH	Magnesium Hazard
RA	Residual Alkalinity
PI	Permeability Index
SSP	Soluble Sodium Percentage
CAI-1	Chloroalkaline index-1
CAI-2	Chloroalkaline index-2

SI	Salinity Index
BIS	Bureau of Indian Standards
WHO	World Health Organization
SWI	Seawater Intrusion
HC	Hydraulic Conductivity
GI	GALDIT Index
GWRDC	Gujarat Water Resource Development Corporation Limited
CGWB	Central Groundwater Board

List of Symbols

Symbol	Meaning
Ca	Calcium
Mg	Magnesium
Na	Sodium
Cl	Chloride
SO_4	Sulfate
K	Potassium
F	Fluoride
NO_3	Nitrate
HCO_3	Bicarbonate
CO_3	Carbonate
$\delta^{18}O$	Oxygen Isotopes
δD	Deuterium

List of Figures

List of Tables

List of Appendices

Chapter - 1

Introduction

1.1.Background

Water is one of nature's most vital resources to support the human population's survival. Of the Earth's total freshwater resources, only 1.2% is found as surface water in lakes or rivers, 30.1% exists as groundwater, and the remaining 68.7% is locked in polar ice caps or glaciers, making it difficult to access (Wondimu Musie, 2023). Surface water has traditionally served as the primary water supply for humanity because of its accessibility and comparatively being less expensive. However, increasing demand from economic and population growth has put significant pressure on surface water supplies, leading to the exploration of groundwater as a viable alternative (Narayan et al., 2007). In the semi-arid and arid parts worldwide, groundwater is a crucial element of water requirements for various purposes. (Adimalla et al., 2018). A substantial part of India's population depends on groundwater, with approximately 30% of urban residents and about 90% of rural inhabitants relying on it for drinking and agriculture, making it a crucial resource for the country (Adimalla et al., 2020).

The quality of groundwater is equivalently significant to the quantity due to its usefulness for numerous purposes (Sarath Prasanth et al., 2012). The quality of groundwater deteriorates owing to various natural and anthropogenic processes such as subsurface hydrochemical processes, irregularities of precipitation, declined infiltration rate due to an increase in impervious land cover, degraded quality of recharging surface water, application of pesticides and fertilizers in agriculture, discharge of untreated industrial wastewater, depletion of groundwater level due to massive extraction of groundwater and rise of sea level because of climate change (Magesh et al., 2013; Sylus & Ramesh, 2015; Rawat et al., 2018; Barik & Pattanayak, 2019; Beyene et al., 2019; Kumari & Rai, 2020). Furthermore, the coastal area is confronting a substantial issue caused by increased groundwater salinity resulting from the migration of saline seawater in the freshwater resources, impacting groundwater dependent ecosystem (Mohanty & Rao, 2019; Baena-Ruiz & Pulido-Velazquez, 2021). The uncontrolled extraction of groundwater to meet the rising demand for several uses leads to a decrease in piezometer levels., which in turn become the primary cause of seawater intrusion in the coastal

aquifer of India (Maurya et al., 2019; P. Prusty, 2020). Seawater intrusion pollutes the valuable groundwater sources of the region, negatively impacting the health of individuals, plant life, and agricultural land. This, in turn, adversely affects the economic growth and living standards of the residents (Sahu, 2020).

1.2.Motivation of the Study

Gujarat has the longest coastline in India, measuring around 1,600 kilometres. It has intense agricultural and industrial activities that contribute to improve the economic growth of both the state and the country. The issue of groundwater salinity in coastal Gujarat as a result of extensive extraction by cultivators was initially identified in the late 1960s and 1970s. Twelve of the state's coastal districts have suffered from the effects of the salinity problem (R. Kumari et al., 2013). Many researchers have studied the imprint of seawater intrusion along the Saurashtra, Kutch, and South Gujarat coastal regions. However, no study has reported on the detailed hydrochemical analysis of groundwater to detect seawater intrusion vulnerability of the coastal aquifer of the Khambhat region.

(a)

(b)

Figure 1.1 (a) Photographs of Farms (b) Interaction with Villagers

Moreover, a preliminary field visit was conducted to interact with the inhabitants and to provide an overview of the region's current scenario. The key source of agriculture and potable water in the region is groundwater. Since all open wells of the region become salty, people extract groundwater for drinking and irrigation through the borewells. The fields irrigated with the groundwater in the region saw salt patches, indicating a higher concentration of salts in the water (Fig.1.1). In addition, villagers are facing health issues such as skin problems, hair fall, and kidney stones due to the consumption of salty water. The preliminary observations during the field visit indicate the requirement of the research to evaluate the quality of potable and agricultural water and to identify the susceptibility of the aquifer towards saltwater intrusion in the region that helps the local authority to plan mitigative measures that lead to groundwater sustainability along with the improvement in socioeconomic condition of the region.

1.3.Research Objectives

The major research objectives of the current work are:

- To determine the potability of groundwater by calculating the Groundwater Quality Index (GWQI) using the subjective method for criteria weighting for the PRM and POM seasons.
- To determine the potability of groundwater by calculating the Entropy Weighted Groundwater Quality Index (EGWQI) using the objective method for criteria weighting for the PRM and POM seasons.
- To determine the suitability of groundwater for agriculture by calculating Entropy Weighted Irrigation Water Quality Index (EIRWQI) using the objective method for criteria weighting for the PRM and POM seasons.
- To identify seawater intrusion vulnerable zones through the GALDIT method.

1.4. Scope of Work

The scope of the research is to assess groundwater quality in the coastal villages of Khambhat and Borsad Talukas of Anand district, Gujarat, for drinking and agricultural use. The first step involves groundwater sampling and laboratory testing of the samples for both the pre-monsoon (PRM) and post-monsoon (POM) seasons. To assess potability, Groundwater Quality Index (GWQI) and Entropy Weighted Groundwater

Quality Index (EGWQI) are computed by applying a weighted arithmetic technique, and two distinct methods are employed to allocate weight to the parameters. The next step involves categorizing the entire study region into different zones of groundwater quality based on the calculated values of GWQI and EGWQI by generating spatial maps using the IDW interpolation technique in GIS software. To assess the appropriateness of the groundwater for agriculture, the Entropy-weighted Irrigation Water Quality Index (EIRWQI) is calculated, and in a further step, a spatial map is generated in GIS software, illustrating the classes of the groundwater suitability according to the computed values of EIRWQI. The final step of the research includes applying the GALDIT method to identify seawater-vulnerable zones of the research region using GIS software.

This study presents a novel framework that combines a water quality indexing technique with a region-specific modification of the GALDIT model, enabling the integrated assessment of groundwater quality and seawater intrusion susceptibility. This dual-assessment strategy enhances the precision of risk identification and supports data-driven decision-making for sustainable water resource management in coastal regions. Moreover, for calculating the water quality index, the constraint of the subjective method in allocating weights to the parameters is addressed and validated by employing the Entropy, a mathematical formula-based method.

1.5.Description of Study Area

The current study area was selected after considering observations and conversations with residents during a preliminary field visit and after analyzing secondary data such as rainfall, water level, quality of the groundwater, etc., which are collected from the Central Groundwater Board and Groundwater Resources Development Corporation of Gujarat. The study area encompasses 62 villages, with 40 villages in Khambhat taluka and 22 in Borsad taluka of Anand district in Gujarat, India (Fig. 1.2). It is situated between North Latitudes 22° 13' 11" and 22° 25' 19" and East Longitudes 72° 31' 59" and 72° 46' 00" with the approximate length of forty kilometers and total area of 433.16 square kilometers along the Gulf of Khambhat (Bhavsar & Patel, 2023). The region has a semi-humid to humid climate, with the warmest month reaching 44 °C and the coldest month ranging from 9 to 15 °C due to its proximity to the coast. The average annual precipitation is 687mm, with an average of 40 wet days during the months of June to September of the year (Bhavsar & Patel, 2023). The average subsurface water depth of the region is 10 meters below ground, and the geology is accentuated by the alluvium,

mainly deposited by the Mahi River (Kumar et al., 2019). The economy of the region is mostly depending on agricultural activities owing to the highly fertile land (Bhavsar & Patel, 2023).

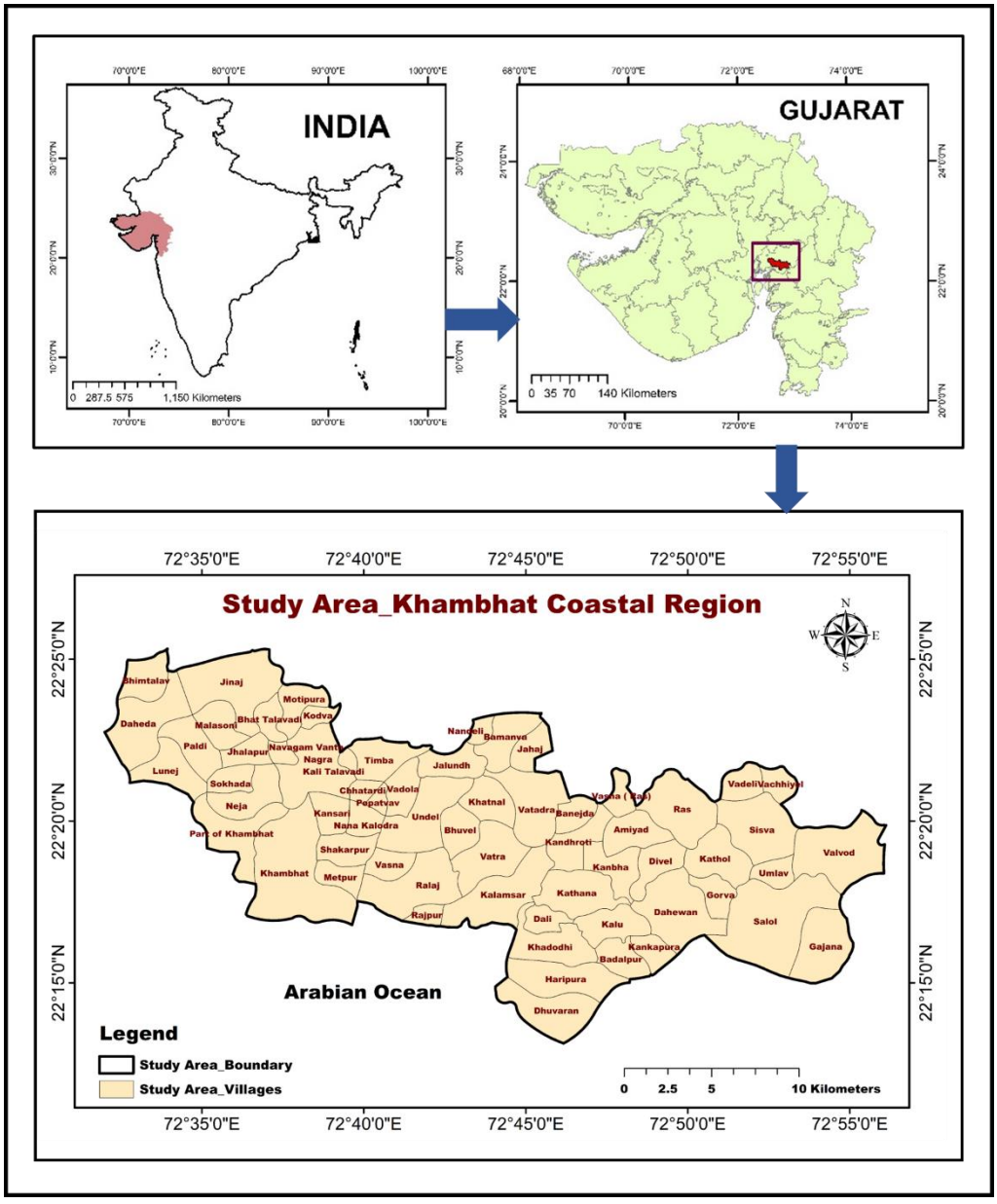

Figure 1.2 Study Area

1.6.Thesis Outline

The thesis contains a total of 7 chapters. The importance of groundwater, contamination of groundwater, seawater intrusion and its impact, study motivation, research objectives, and a description of the study area are discussed in the introductory chapter 1. Chapter 2 focuses on the literature review on groundwater quality assessment

for potability and irrigation along with the assessment of seawater intrusion. Chapter 3 dealt with the collection of groundwater samples, laboratory testing of the collected samples for the major hydrochemical parameters, generation of spatial maps showing the spatial dispersal of the amount of various hydrochemical parameters, and comparison of the laboratory results for both PRM and POM seasons. Chapter 4 encompasses the computation of the Groundwater Quality Index (GWQI) using the subjective method and entropy-weighted Groundwater Quality Index (EGWQI) employing the objective method for assigning weight to each parameter for two distinct seasons. Furthermore, according to calculated GWQI and EGWQI, groundwater quality suitability analysis for drinking is also discussed. Chapter 5 gives a detailed calculation of various irrigation indices and entropy-weighted Irrigation Water Quality Index (EIRWQI) for two distinct seasons. Moreover, the chapter also covers the groundwater suitability analysis for agriculture based on calculated EIRWQI. Chapter 6 discusses the assessment of seawater intrusion vulnerable zones using the GALDIT method. Chapter 7 finally presents conclusions of the work with recommendations and the scope of future research.

Chapter - 2

Literature Review

2.1 General

A literature review is essential for research since it offers an extensive overview of current findings, suggests limitations, and emphasizes areas requiring additional research. It illustrates the study, ensuring the research is relevant and develops upon previous research while preventing redundancy. This chapter discusses substantial literature studies on assessing groundwater quality for potability and agricultural use and examining seawater intrusion.

2.2 Groundwater Quality Assessment for Potability

(Verma et al. 2020) have evaluated groundwater quality in the Bokaro district of Jharkhand employing the water quality index method. As part of the hydrochemical analysis, one hundred-two groundwater samples were gathered for PRM and POM seasons and examined for twelve chemical parameters. The concentration of each of the parameters was compared to water quality standards of BIS and WHO to assess suitability for drinking. Furthermore, ten chemical parameters were selected to calculate WQI at each sampling location. A weight between 1 and 5 was assigned to each parameter using a subjective method for weighing criteria for calculating the index using a weighted arithmetic method. Finally, the index was categorized into five water suitability classes, from excellent quality to unsuitable. Moreover, a spatial map illustrating the appropriateness of water quality was generated by applying the geographic information system method, representing various zones of water quality classes in the study area. additionally, Ternary and Durov diagrams were plotted to recognize the Hydrogeological evolution of groundwater, hydrochemical facies, and ion exchange processes. The findings of the study depict that, in comparison to the dry season, water quality is considerably poorer during the wet season.

(Saikrishna et al. 2020) have studied the potable water quality of the Nalgonda district, Telangana, through WQI, correlation analysis, and linear regression analysis. The sampling of groundwater was carried out during the post-monsoon season. WQI

was calculated adopting the weighted arithmetic index approach, considering fourteen chemical criteria for a thorough evaluation of water quality. The research findings depict that 37% of the total samples fall into the class of very poor or unfit to drink. Moreover, the water quality class of the research area, from excellent quality to unsuitable for use, was illustrated through a spatial map. A correlation matrix was created for the water quality indicators, and the results indicate a strong correlation among EC, TDS, TH, Na, Mg, Ca, and Cl. The linear regression analysis shows that most of the parameters were correlated with each other.

(Subba Rao 2012) has calculated the pollution index of groundwater as an assessment tool for water potability in the Varaha River basin of Visakhapatnam. The index is a numerical measure that quantifies pollution levels and indicates the combined effect of each quality indicator on the overall water quality for potability. Thirty samples from open-dug wells were collected during PRM season for chemical analysis. Eleven pollution indicator parameters were used to calculate PIG, and each parameter was allocated a weight in the range of 1 to 5 depending on their significance in evaluating water quality. Based on the calculated value of PIG, the sampling locations were categorized into five pollution classes, from insignificant to very high pollution. An insignificant pollution zone has been detected in the upstream area, characterized by groundwater predominantly containing bicarbonate, while a highly polluted zone is identified in the downstream area, where groundwater is contaminated with chloride.

(Solangi et al. 2020) have evaluated and delineated the potable groundwater quality in the Sujawal district, a coastal region of Pakistan, by calculating the water quality index and the Synthetic pollution index and incorporating geospatial techniques. The collected ninety-four samples were examined for nine different physiochemical parameters. Applying the WQI and SPI models for several physicochemical parameters indicated the deterioration of groundwater quality in most of the research areas. The correlation matrix was generated for all nine parameters and depicted moderate to weak correlation among the parameters except TDS and EC, which are strongly correlated.

(Li et al. 2021) has investigated water potability in the southeast part of North China Plain (NCP) by calculating the water quality index using the entropy approach. The entropy technique exhibits significant objectivity and mitigates human influence in

weight computation. Groundwater sampling was carried out at 47 civilian wells for two distinct seasons, and the collected samples were examined for twelve chemical parameters. Moreover, GIS was used to produce a spatial map of each quality parameter. EWQI was calculated considering major chemical indicators including pH, TDS, TH, Na, Cl, SO_4, NO_3, and F), and based on calculated EWQI, the research area was classified into five water quality zones from excellent quality to unsuitable for drinking. The hydrochemical properties and genetic mechanisms of groundwater of the study region were examined utilizing conventional methods, including the Piper diagram, Gibb's plot, and ion ratio analysis. Gibb's plot and ion ratio observations show that rock weathering is the leading cause of groundwater's hydrochemical properties, along with evaporation, cation exchange, and anthropogenic inputs.

(Kumar and Augustine 2022) have employed an integrated approach, including hydrochemical analysis as well as an objective indexing EWQI, to examine the water quality of a total of thirty-two well samples in the Upper Odai sub-basin. Ultimately, water quality classes based on the calculated value of EWQI of the study region were represented through a spatial map generated using the IDW spatial interpolation technique in ArcGIS software. Moreover, the Piper diagram indicates that maximum samples were plotted in Na-Cl and Ca-Mg-Cl-SO_4 water types, and the presence of sodium and chloride ions shows the probability of saline water mixing.

(Adimalla 2021) has conducted research to assess drinking water quality in the Dubbak region of Telangana state. Groundwater samples were acquired for thirty sampling locations and analyzed for twelve hydrochemical parameters. An EWQI for each sampling location was calculated by applying the entropy method for weighing the parameters, and the results were compared with the pollution index of groundwater (PIG), which was calculated using the conventional subjective method for weighing the parameters. EWQI values were ranked in five water quality classes, indicating excellent water quality to extremely poor quality; similarly, PIG values were also ranked in five pollution classes, from insignificant to very high pollution. EWQI showed that 60% of groundwater samples from villages in the investigated region were marginally potable, and the rest were poor or extremely poor. On the other hand, PIG showed that 63% of the study area's samples had insignificant pollution, and the rest were marginally fit for drinking. Additionally, the spatial distribution of groundwater quality status according

to calculated EWQI and PIG was illustrated through spatial maps generated by applying GIS.

2.3 Groundwater Quality Assessment for Irrigation

(Rawat, Singh, and Gautam 2018) have conducted an investigation to appraise the appropriateness of the groundwater for agriculture in the Kanchipuram district of Tamil Nadu state of India. Over a period of nine years (2005-2013), researchers gathered borewell samples during the PRM and POM seasons. Various agricultural water indices (SAR, SSP, RA, KI, PI, CAI-1, CAI-2, PS, MH) were calculated to determine the appropriateness of the gathered samples and temporal variations of the individual indexes over the span of nine years are represented through the plot of well vs. value of the particular index at that location. According to the TDS analysis of the samples, all of the well water was adequate for irrigation before the monsoon; however, following the rain, the TDS value of some wells is affected by the rise in salt content. Furthermore, groundwater samples were categorized based on the calculated values of base-exchange index and meteoric index, and according to the calculated value of indices, the groundwater in the research area is categorized as Na-SO_4 type and of the deep meteoric percolation type, respectively. Gibb's diagram was plotted to observe the relationship between the composition of water and the geological characteristics of the aquifer, and the interpretation of the plot illustrates that the chemical weathering of the rock controls the chemistry of groundwater. Additionally, the Wilcox diagram was plotted to classify groundwater samples based on %Na and EC, and the analysis of the plot reveals that most samples are classified as excellent to permitted in both seasons. Moreover, the result of the Doneen plot, which is based on the permeability index, elucidates that most of the samples are in Class-1, suggesting the water is excellent for use.

(Barik and Pattanayak 2019) have conducted a study in Rourkela City of Odisha to examine groundwater quality for irrigating the city's green spaces. To assess the appropriateness of groundwater, 25 groundwater samples were collected during the PRM season, and quality indicator parameters pH and EC were considered. Furthermore, various indices such as SI, CI, TH, SAR, %Na, SSP, RSC, RSBC, PI, PS, CAI-1, CAI-2, KI, MH, and Mg/Ca ratio were computed using formulas provided by different researchers. To evaluate salinity threat, a plot of EC vs SAR, known as the USSL

diagram, was generated, indicating low to medium salinity threat. Additionally, the observations of Gibb's plot specify that the groundwater in the region is affected by the lithological composition of the underlying rock.

(Aravinthasamy et al. 2020) have investigated the irrigation risk of groundwater in the Dindigul and Tirupur districts of Tamil Nadu, India, implicating a combined approach of WQI and GIS. Groundwater sampling was carried out in the PRM season, and 61 samples were gathered. Laboratory testing of collected samples was carried out for ten water quality indicators as per the standard procedure. Furthermore, various irrigation indicator parameters such as SAR, %Na, KR, RSC, PI, and MH were computed to evaluate water for agriculture. Finally, the index was calculated by considering five parameters (EC, SAR, Na, Cl, and HCO_3), employing the weighted arithmetic method. The categorization of IWQI indicates that 57% of the groundwater samples fall into low to inadequate quality for agriculture. The spatial dispersal of the index was represented through a map generated employing the IDW technique in a GIS environment. The United States Soil Laboratory plot illustrates the synergistic effect of SAR and EC on crop development, categorizing irrigation water quality into 16 distinct zones. Almost half of the groundwater samples had water quality indicators of high salinity risk (C3) and low sodium risk (S1), which is inappropriate for soils with poor drainage. The Wilcox diagram depicts the synergistic impact of salinity and %Na, and the interpretation elucidates that 39% of the samples fall within the class of excellent to good quality. Additionally, the samples were also classified as per the Doneen classification, which is based on the value of PI, and the classification results denote that 92% of samples fall into the good category. Moreover, two mitigative measures were also suggested: applying Gypsum to increase soil permeability and artificial recharge for diluting salinity.

(Kavurmacı and Karakuş 2020) have calculated the water quality index by employing two distinct MCDM techniques: Data Envelopment Analysis and AHP for examining agricultural water. The research was conducted in Aksaray province of the Central Anatolian region of Turkey. The majority of water utilized for agriculture is sourced from ponds. Twenty water samples were gathered from the ponds to appraise water quality. In the initial phase of the AHP-supported water quality index formulation, 10 distinct options (irrigation ponds) and 13 sub-criteria categorized under three primary

criterion groups were recognized. The criteria are (i) physio-chemical parameters, (ii) chemical parameters, and (iii) appropriate parameters. The following stage involves the creation of n x n binary square comparison matrices. During the formulation of the comparison matrices, binary assessments of criteria and sub-criteria were conducted one-to-one based on their significance values. The scale proposed by Saaty (2008) was employed for bilateral mutual comparisons. Utilizing comparison matrices, the priority and weight vectors for each parameter in the hierarchy were established, resulting in the development of the IWQI. Data Envelopment Analysis (DEA) is a numerical methodology designed to assess the efficiency of Decision-making Units by utilizing several factors and varying units of measurement. The selection of input and output variables was established based on the assessments of ten distinct specialists in water quality. In the subsequent phase of the investigation, weight values were allocated to the identified inputs and outcomes. The assignment of weight values utilized the prioritization matrix employed in the AHP approach and the parameters' weight values. The weighted CCR model was selected in this study because of its ability to provide more precise findings for comparing the irrigation water quality of ponds. This study indicates that, despite some shortcomings in the fundamental DEA approach being neglected, the DEA technique has yielded more favorable outcomes than the AHP technique in assessing irrigation water quality. Additionally, the Wilcox diagram (Conductivity vs. %Na) was generated, and according to the diagram's interpretation, the majority of the samples have water classified as permissible to excellent quality.

(Batarseh et al. 2021) have carried out research to evaluate water quality for agriculture use in Abu Dhabi Emirate, employing the IWQI approach. The study included the collection and chemical examination of 145 groundwater samples for various physio-chemical indicators. The IWQI was determined using five agricultural water quality indicators: EC, SAR, concentration of sodium and chloride ions, and bicarbonate. The IWQI map was generated by overlaying thematic maps of five indicator parameters using geo-statistical analysis utilizing the Inverse Distance Weighted interpolation approach, an extension plugin included in the QGIS spatial analysis package. Overall, 96% of the examined wells exhibit a grade of high to severe restrictions for agricultural usage. Moreover, the Wilcox diagram, a plot of EC vs % Na, and the US salinity diagram, a plot of salinity (EC) vs SAR, were generated to assess water quality. The interpretation of the Wilcox diagram denotes that 88% of the accessed

wells fall in the " Unsuitable " category for agriculture. The USSL diagram indicates that most samples are situated in the C4S4 zone, characterized by the class associated with high salinity and high SAR, corroborating the findings of the Wilcox diagram. Additionally, for the further classification of the samples based on the effect of Na, Mg, Ca and HCO_3 on soil permeability, the Permeability index was calculated, and the PI Diagram was also developed. The interpretation of the PI diagram reveals that 81% of samples can be classified as Class-I, indicating that the samples are suitable for agriculture.

(Tejashvini et al. 2024) have performed an extensive evaluation of groundwater quality for irrigation purposes in the semi-arid area of Bangalore, Karnataka. The research highlighted the impact of urbanization and industrialization on groundwater quality along a rural–urban gradient. Thirty groundwater samples were collected in the pre-monsoon season and analyzed for several physicochemical characteristics, including Electrical Conductivity (EC), Sodium Adsorption Ratio (SAR), Residual Sodium Carbonate (RSC), and Total Hardness (TH), among others. The appropriateness for irrigation was assessed via metrics such as the Irrigation Water Quality Index (IWQI), Wilcox plot, and Gibbs diagram. The results indicated considerable geographical disparity, with rural regions often exhibiting superior water quality compared to metropolitan locations. Over 80% of urban samples were classified as having moderate irrigation restrictions due to elevated risks of salinity and sodium, whereas rural samples had lower restriction levels. The use of multivariate statistical techniques, including Principal Component Analysis (PCA), facilitated the identification of critical determinants that influence water quality. The study emphasized the necessity for consistent monitoring and suitable management measures, particularly in transitional and urban regions, to ensure sustainable agricultural utilization of groundwater.

2.4 Seawater Intrusion Assessment

(Satheeskumar et al. 2021) have investigated seawater intrusion in the Thoothukudi district of Tamil Nadu state, applying geochemical analysis. Forty groundwater samples were collected over two seasons and analyzed for major anions and cations: pH, Electric conductivity, tds, sodium, potassium, magnesium, calcium, bicarbonate, sulfate, phosphate, nitrate, and bromine. Samples exhibiting increased amounts of EC and TDS are obtained from the coastal region of the study region, signifying the impact of saline water ingress. A Piper diagram was plotted to recognize the geochemical facies of the groundwater. The

interpretation of the diagram denotes that the predominant water groups are the mixed Ca–Mg–Cl group and the Na–Cl group, which signifies the influence of seawater intrusion. Moreover, Gibb's plot was generated to find the impact of rock–water interaction, evaporation, and rainfall on groundwater. Observations of the plot illustrate that samples were shifted to the evaporation zone from the rock-water interaction zone, indicating an increase in the amount of sodium, chloride, and TDS due to seawater intrusion. The ratio of chloride and bromine delineated the regions affected by salinity within these study areas. Moreover, this study proposes an engineering solution, constructing a weir in Mukkani village to regulate the intrusion of seawater into surface water.

(Kumari, Kumar Singh, and Mukherjee n.d.) has assessed seawater intrusion in the coastal region of the Sabarmati River basin of Gujarat state through isotopic ($\delta^{18}O$ and δD) analysis and ionic ratios (Mg/Ca, Na/Cl, SO/Cl, K/Cl). Laboratory analysis was performed on twelve samples acquired from bore and tube wells for fourteen chemical parameters. The concentration of all chemical parameters was compared with the potable water standards suggested by BIS and WHO. Many parameters exhibit extensive variability in concentration, indicating multiple contamination sources, the impact of intricate hydrochemical processes, and considerable degradation of groundwater quality in the study area. Correlation analysis denotes that both EC and TDS are strongly correlated with Na, Cl, SO_4, Ca, and Mg; also, a very strong correlation between Na and Cl represents the influence of salinity. The calculated Na/Cl, K/Cl, and Mg/Ca ratios illustrate saline water ingress at many sampling locations. The standard equilibration method was employed to analyze isotopes $\delta^{18}O$ and δD, and plots of $\delta^{18}O$ versus Cl suggested saline water ingress at a few locations. Furthermore, to understand the hydrochemical process, the Piper trilinear diagram and the Scholler diagram were generated, and observation of both plots suggested the effect of seawater mixing. Moreover, A plot illustrating the concentration of electrical conductivity against the sodium absorption ratio was created to assess the groundwater's appropriateness for agricultural use and to identify potential salinity risks in the research area. The observation of the plot shows that most of the samples fall within the category of high salinity and low alkalinity, which are considered suitable water for irrigation.

(Dhakate, Ratnalu, and Sankaran 2020) have conducted research to evaluate seawater intrusion in the coastal stretches of the Udipi district of Karnataka state by applying hydrochemical and isotopic analysis. Groundwater sampling was conducted before the

monsoon, and 49 samples were chemically analyzed for 12 indicator parameters. Moreover, the spatial distribution of each parameter was illustrated by a spatial map generated using GIS software. Stable oxygen isotopes are important in determining groundwater age, identifying recharge source regions, assessing aquifer connectivity, elucidating groundwater-surface water interactions, inferring flow regimes, comprehending recharge-discharge mechanisms, mapping flow pathways, and estimating water residence time. A negative ratio of $\delta^{18}O$ at a few sampling locations indicates the mixing of saline water with groundwater. Furthermore, a total of six Bivariate plots, including Na vs Cl, TDS vs Cl, SO_4 vs Cl, Mg vs Cl, Ca vs Cl and Ca vs SO_4, were generated, and the bivariate plot of Na/Cl suggests seawater intrusion at the majority sampling locations. The brackish, mixed, and salty nature of the groundwater samples is suggested by the Piper plot, the Gibbs plot, and the TH vs. TDS plot. Additionally, seawater percentage values (SW%) of more than 5 at five sampling locations represent the mixing of brine with groundwater.

(Khan et al. 2021) have carried out a study to elucidate saline water intrusion and the geochemical factors influenced throughout the coastal regions of Tamil Nadu and Puducherry. In this context, 76 groundwater samples were gathered from various locations for two seasons and tested for ten water quality parameters. Various methodologies were employed to explicate the salinization process in the research region, including hydrochemical ionic alterations, hydrochemical facies evolution models, and seawater mixing indices. The interpretation of the HFE diagram denotes that approximately 20% of samples were influenced by saline water during both seasons. In contrast, Hydrochemical ionic changes illustrate that approximately 40% of samples were affected by seawater. Moreover, the seawater mixing index was calculated, which confirms saline water mixing.

(L.S. et al. 2013) have investigated scenarios of seawater intrusion in the Central Godavari region of Andhra Pradesh by employing two distinct approaches: Electrical Resistivity Tomography (ERT) studies and hydrochemical analysis. The electrical resistivity method involves energizing the subsurface by injecting a known quantity of current (I) and measuring the resulting voltage (V) at the ground surface. Electrical resistance [R] is computed by applying the equation (V/I), and the measured resistivities are obtained for each electrode arrangement while accounting for the geometrical component of the array. For the present study, a geotechnical investigation method known as the Wenner–Schlumberger array was employed to measure soil resistivity at 13 locations. SYSCAL

PRO-96, an IRIS instrument, was used to collect resistivity. Next, in order to create a 2D resistivity cross-section image, the apparent resistivity is converted to actual resistivity using the RES2D.INV inversion program. The resistivity survey findings revealed reduced resistivity in Kanavaram, near the Vasalatippa drain and Surasaniyanam, owing to the integration and intrusion of salty water into the freshwater during high tides from surface water. As a part of the geochemical examination, 42 groundwater samples were acquired for two distinct seasons and examined for ten chemical indicators. The elevated levels of sodium, chloride, sulfate, and total dissolved solids indicate that the identified salinity is derived from groundwater stored within marine clays rather than from the lateral intrusion of saltwater. Furthermore, to identify source salinity, ratios Na/Cl and SO_4/Cl were computed, and the findings suggest that the observed salinity is not due to the ingress of saline water.

(Kumar, Priju, and Prasad 2015) have applied geophysical method along with hydrochemical analysis to assess seawater intrusion in the Periyar river basin of Kerala state. Vertical Electrical Sounding utilizing the Schlumberger configuration was conducted at 15 sites, each reflecting distinct geomorphological setups, during the pre-monsoon period with the Aquameter CRM 500 model. The semi-quantitative analysis of the VES data indicates that most sounding curves are of the Q-type, signifying an increase in salinity with depth. The concentration of various cations and anions in 63 groundwater samples was measured as part of the hydrochemical analysis. In the western part of the study region, higher pH, EC, and TDS values were observed toward the seaward side. In contrast, increased sodium, chloride, and sulfate concentrations were observed in the northwest part of the region. Hill-Piper plots reveal that the predominant groundwater type is Na-Cl, followed by Mg-Cl in certain locations.

(Chang et al., 2019) have applied the GALDIT approach to investigate the saltwater intrusion status of Jeju Island in South Korea. Within the GALDIT indicators, the aquifer type, hydraulic conductivity, perpendicular distance from the shoreline, and aquifer thickness were considered static. In contrast, the groundwater level above sea level and existing salinity were considered time-dependent parameters indicative of aquifer stress. In order to enhance the evaluation process, this study substituted the standard GALDIT measure for electrical conductivity to depict the prevailing effects of SWI. During the evaluation, the relative importance of each variable is established by dividing the indicator

value range into four groups based on the site's given attributes. In addition, to allocate relative importance, the value range of the height of GWL above sea level was also modified to fit the Jeju model. The GALDIT study of Jeju Island indicates sustainable groundwater management with moderate to long-term vulnerability in the majority of the region.

(Chronidou et al. 2022) have introduced a revised iteration of the prevalent GALDIT approach, designated GALDIT-I, for evaluating groundwater susceptibility to salinization in coastal aquifers. In contrast to the original GALDIT approach, which focuses primarily on saltwater intrusion, GALDIT-I encompasses a broader range of salinization sources, including irrigation return flows, geogenic influences, and confined saline lenses. The technique applied to the Rhodope coastal aquifer in northern Greece utilizes adjusted parameter weights (using the Analytic Hierarchy Process), introduces new vulnerability classifications, and employs Total Dissolved Solids (TDS) in place of the Revelle index for impact evaluation. Validation with chloride concentrations demonstrated a robust correlation (Spearman's $r = 0.665$), demonstrating the method's efficacy in reflecting actual salinization trends. The enhanced vulnerability mapping delivered by GALDIT-I facilitates superior identification of high-risk areas and aids in the implementation of proactive groundwater management techniques. The research underscores the method's versatility and worldwide relevance for sustainable groundwater resource management.

2.5 Summary

The reviewed literature reveals the extensive use of several methodologies to assess groundwater quality for both potable and agricultural use, as well as to evaluate seawater intrusion in coastal areas. Techniques such as the Water Quality Index (WQI), Entropy Weighted Water Quality Index (EWQI), and Pollution Index of Groundwater (PIG) are extensively employed, augmented by spatial mapping and statistical analysis. In this context, subjective criteria weighing techniques offer benefits, including the integration of expert judgment, adaptability, and user-friendliness, especially in data-scarce situations. Nevertheless, they are susceptible to bias and inconsistency, which may compromise the repeatability and objectivity of findings. Conversely, objective approaches such as entropy weighting offer a data-driven and impartial approach, improving transparency and uniformity; nevertheless, they may neglect contextual or expert insights and are susceptible to outliers. The GALDIT model has been efficiently utilized in several studies for evaluating seawater intrusion, owing to its simplicity, spatial visualization capabilities, and

incorporation of essential hydrogeological characteristics. Although GALDIT serves as a valuable screening instrument, it has limitations, including subjectivity in weight assignment and its inability to account for temporal fluctuations or complex hydrogeochemical processes. An integrated strategy that combines subjective insights, objective data analysis, and GIS technologies is crucial for a thorough and reliable assessment of groundwater quality and seawater intrusion.

Chapter - 3

Groundwater Sampling and Groundwater Hydrochemistry

3.1 General

The chapter encompasses the method of collecting groundwater samples in the research area for both the PRM and POM seasons. Furthermore, the amount of major hydrochemical parameters in collected groundwater samples was determined by laboratory testing, which is also discussed in this chapter. The Piper diagram is represented and explained in depth to understand groundwater hydrochemistry. Additionally, spatial maps depicting the distribution of various hydrochemical parameters were created using the IDW interpolation method, which is the spatial analyst tool of ArcGIS 10.4.1 for both seasons. The chapter also illustrates this. Additionally, the correlation among the hydrochemical parameters using a correlation matrix is also discussed.

3.2 Sampling of Groundwater

It is imperative to conduct a chemical analysis of the groundwater to determine its quality for various applications. During the PRM season in May 2022, 57 groundwater samples were taken from the study region (Fig. 3.2), and 54 samples were collected for the POM season in October 2022 (Fig. 3.3). Fig. 3.1 illustrates a spatial map of locations of groundwater sampling. For the sampling, 1L polypropylene bottles were used, and before use, the bottles were immersed in a 1:1 hydrochloric acid solution for 24 hours and then cleaned with distilled water twice. After collecting the samples, the bottles were sealed firmly to protect them from the effects of air. All samples were then conveyed to the Gujarat State Fertilizer and Chemical Ltd. laboratory, Situated in Vadodara, Gujarat, India, for chemical analysis (Bhavsar & Patel, 2023). In the laboratory, groundwater samples were analyzed for a total of 13 hydrochemical parameters for groundwater quality, including pH, Total Dissolved Solids (TDS), Electrical Conductivity (EC), Calcium (Ca), Magnesium (Mg), Sodium (Na), Chloride (Cl), Sulfate (SO_4), Potassium (K), Fluoride (F), Nitrate (NO_3), Bicarbonate (HCO_3) and Carbonate (CO_3) for both seasons. The conventional methods provided by APHA

2012 for analyzing the samples. Tables 3.1 and 3.2 represent the statistical details of the chemical composition of hydrochemical parameters of the groundwater samples taken during the PRM and POM periods.

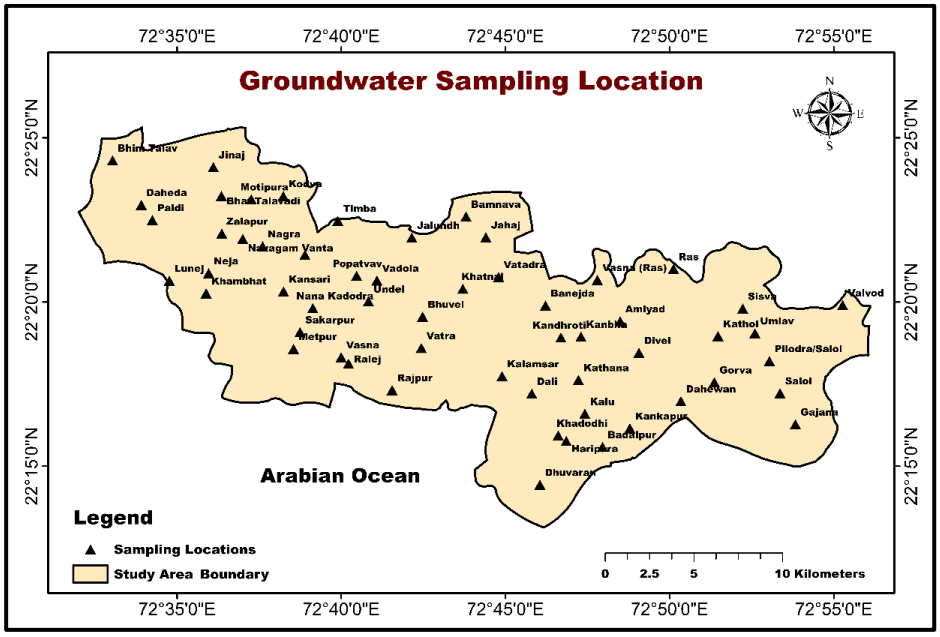

Figure 3.1 Groundwater sampling location Map

Figure 3.2 Groundwater sampling (PRM)

Figure 3.3 Groundwater sampling (POM)

Table 3.1 Statistical details of the chemical composition of hydrochemical parameters during the PRM season

Parameter	Minimum	Maximum	Median	Mean	Std. Dev
pH	7.12	8.96	7.81	7.90	0.38
TDS	1397	5951	3424	3438.68	1073.15
EC	1190	18500	3800	5134.21	3495.34
Ca	16	152	48	55.00	30.98
Mg	0	305	70	103.33	84.30
Na	15	1954	1005	904.56	327.59
Cl	178	3195	923	1193.47	761.69
SO_4	0	1301	304	414.63	411.42
K	0.73	109.31	5.05	9.80	15.91
F	0.17	1.02	0.55	0.63	0.26
NO_3	4.84	9.69	7.27	6.72	1.13
HCO_3	221	1244	567	601.68	219.65
CO_3	48	686	158	166.00	95.76

(The amount of all parameters is in mg/l excluding EC and pH; the Unit of EC is µƱ/cm, whereas pH is dimensionless)

Table 3.2 Statistical details of the chemical composition of hydrochemical parameters during the POM season

Parameter	Minimum	Maximum	Median	Mean	Std. Dev
pH	6.93	8.56	7.65	7.66	0.31
TDS	892	10935	2320	2852.04	1826.35
EC	750	15600	3100	4078.70	2918.35
Ca	15	168	55.5	66.41	41.68
Mg	12	154	28.5	39.37	32.96
Na	44	1775	354	475.02	364.83
Cl	142	3997	702	879.57	694.78
SO_4	0	1248	0	62.46	208.74
K	0.13	89.08	5.09	9.13	14.13
F	0.18	0.9	0.43	0.46	0.18
NO_3	2.42	50.86	7.27	7.35	6.25
HCO_3	421	4736	992.5	1177.46	827.93
CO_3	24	994	113	149.89	157.48

(The amount of all parameters is in mg/l excluding EC and pH; the Unit of EC is µƱ/cm, whereas pH is dimensionless)

3.3 Groundwater Hydrochemistry

3.3.1 pH

The pH of groundwater is a quantitative indicator of its acidity or alkalinity, measured in a range of 0 to 14, where 7 represents a neutral state. A pH value less than 7 denotes acidity, whereas a pH value more than 7 denotes alkalinity. It is influenced by several geological elements, including the composition of minerals and soil, natural processes such as the solubility of CO_2, the weathering of rocks, the pyrolysis of minerals, and human activities like industrial discharge, agriculture, and runoff (Singaraja et al., 2015). The pH value of the groundwater samples obtained in the PRM season ranges between 7.12 and 8.96, with an average of 7.90, while the value ranges between 6.93 and 8.56, with an average of 7.66 during the POM season. The samples are categorized into three categories: (Class- I) pH < 7.5, (Class- II) 7.5 ≤ pH ≤ 8.5, and (Class- III) pH > 8.5 for both seasons. Furthermore, Fig. 3.4 illustrates spatial maps showing the spatial dispersal of pH in the study region for both seasons. For both seasons, the majority of the samples can be categorized as Class-II, with a pH value from 7.5 to 8.5. According to the analysis, a total of 50 samples (87.72% samples) had pH values between 7.5 to 8.5 (Class-II) during the PRM season, and during the POM season, it decreased to 36 samples (66.67% samples). Moreover, spatial interpretation of the maps of pH shows that 95.07% and

82.84% of the research area are categorized as Class-II during the PRM and POM periods, respectively.

Table 3.3 Summary of Spatial Interpretation of pH Maps for both PRM and POM Seasons

Season	pH Range	Count of samples	% Samples	Area (sq. km)	Area (%)
PRM	pH < 7.5	6	10.53	15.39	3.55
	7.5 ≤ pH ≤ 8.5	50	87.72	411.79	95.07
	pH > 8.5	1	1.75	5.98	1.38
POM	pH < 7.5	16	29.63	74.1	17.11
	7.5 ≤ pH ≤ 8.5	36	66.67	358.82	82.84
	pH > 8.5	2	3.70	0.25	0.06

3.3.2 Total Dissolved Solids (TDS)

Total Dissolved Solids measure the cumulative concentration of organic and inorganic substances in groundwater, existing in molecular, ionized, or colloidal suspended forms. (Hem, 1985). The TDS is an essential water quality parameter, affecting its safety and appropriateness for many uses, such as drinking, irrigation, and industrial applications. The primary sources of TDS in groundwater are weathering rocks and saline water ingress. The concentration of TDS in groundwater is affected by irrigation, industrial discharge, and runoff. Groundwater total dissolved solids (TDS) originate from natural processes such as rock weathering and saltwater intrusion in coastal areas (Brindha & Michael Schneider, 2019). High concentrations of TDS are unsuitable for human consumption or agricultural use as they cause health problems, including skin diseases and kidney stones, lead to soil salinity, and negatively impact crop yields (Adimalla et al., 2020; Singh et al., 2020). The maximum TDS observed during the PRM season is 5951 mg/l, whereas in the POM season, it is 10935 mg/l. During the PRM period, the average TDS content in the groundwater samples was 3438.68 mg/l, while during the POM period, it was 2852.04 mg/l. All PRM season samples have a TDS content over 1000 mg/l, signifying water salinity. The collected groundwater samples are categorized into three categories: (Class- I) TDS < 3000; 33.33% and 77.78% samples fall in class-I during PRM season POM season respectively, (Class- II) 3000 ≤ TDS ≤ 4500; 49.12% and 14.81% samples fall in Class-II during PRM season POM season

respectively and (Class- III) TDS > 4500; 17.54% and 7.41% samples fall in Class-I during PRM season POM season respectively (Table 3.4).

Table 3.4 Summary of Spatial Interpretation of TDS Maps for both PRM and POM Seasons

Season	TDS Range (mg/l)	Count of samples	% Samples	Area (sq. km)	Area (%)
PRM	TDS < 3000	19	33.33	114.16	26.36
	3000 ≤ TDS ≤ 4500	28	49.12	297.62	68.71
	TDS > 4500	10	17.54	21.37	4.93
POM	TDS < 3000	42	77.78	309.19	71.38
	3000 ≤ TDS ≤ 4500	8	14.81	100.48	23.20
	TDS > 4500	4	7.41	23.49	5.42

3.3.3 Electrical Conductivity (EC)

Electrical conductivity determines the ability of water to conduct an electric current, which signifies the existence of total dissolved solids (Sarath Prasanth et al., 2012). The higher value of EC depicts water salinity, rendering water unfit for drinking and agricultural use. The Highest EC value of the groundwater samples collected in the PRM season is 18500 µ℧/cm, with an average value of 5134.21 µ℧/cm, whereas in the POM season, the highest value of EC is 15600 µ℧/cm, with a mean value of 4078.70 µ℧/cm. Groundwater samples are classified into three classes based on the value of EC: EC < 3000 (Class-I), 3000 ≤ EC ≤ 5000 (Class-II), and EC > 5000 (Class-III). Furthermore, analytical data represent that 73.68 % of samples (42 samples) have measured values of EC more than 3000 µ℧/cm (Class-II & III), which covers 90.62% of the study region in the period of PRM (Table 3.5), while during the POM season, 55.56% samples (30 samples) have measured value of EC more than 3000 µ℧/cm (Class-II & III), encompasses 70.02% of the study area (Fig. 3.6).

Table 3.5 Summary of Spatial Interpretation of EC Maps for both PRM and POM Seasons

Season	EC Range (µʊ/cm)	Count of samples	% Samples	Area (sq. km)	Area (%)
PRM	EC < 3000	15	26.32	40.62	9.38
	3000 ≤ EC ≤ 5000	19	33.33	211.38	48.80
	EC > 5000	23	40.35	181.16	41.82
POM	EC < 3000	24	44.44	129.876	29.98
	3000 ≤ EC ≤ 5000	20	37.04	226.45	52.28
	EC > 5000	10	18.52	76.83	17.74

3.3.4 Calcium (Ca)

Calcium in groundwater predominantly originates from the natural decomposition of calcium-rich rocks and minerals, such as limestone, gypsum, and dolomite. (Khan et al., 2021). Calcium is crucial for the growth and functioning of human skeletal structures, including bones and teeth. It also plays a significant role in maintaining soil health by impacting soil pH and structure. It aids in the neutralization of soil acidity, hence enhancing the accessibility of other nutrients to plants. The maximum concentration of calcium observed during the PRM season is 152 mg/l, whereas in the POM season is 168 mg/l. The mean value of the amount of calcium in the groundwater samples is 55.0 mg/l and 66.41 mg/l in the PRM and POM periods, respectively. The samples are grouped into three classes: (Class- I) Ca < 75, (Class- II) 75 ≤ Ca ≤ 100, and (Class- III) Ca > 100 for both seasons. A total of 49 samples (85.96%) collected in the PRM period and 36 samples (66.67%) in the POM period are categorized as Class-I, having an amount of calcium less than 75 mg/l (Table 3.6) and spatial interpretation of the calcium map (Fig. 3.7) shows that 88.15 % of the study region fall in Class-I category during the PRM season whereas, during the POM season, the Class-I study area is reduced to 69.43%, which indicates increase in the concentration of Ca during the POM season than the PRM season.

3.3.5 Magnesium (Mg)

The occurrence of magnesium in groundwater results from the natural process of weathering magnesium-rich rocks and soil activities, such as the breakdown of organic matter and the movement of soil elements through leaching**.** Magnesium is vital for human health since it contributes to muscle functioning, neuron transmission, blood sugar regulation, and bone health. It also helps in improving soil

fertility, which leads to healthy plant development and increased agricultural yields. The Highest concentration of Mg in the samples acquired in the PRM season is 305.0 mg/l with a mean of 103.33; during the POM season, the highest concentration is 154 mg/l with a mean of 39.37 mg/l. It indicates that the amount of magnesium is decreased during the POM season due to rainwater infiltration into the ground during the monsoon season, hence diluting dissolved minerals of the groundwater. The samples are divided into three classes: (Class- I) Mg < 100, (Class- II) 100 ≤ Mg ≤ 200, and (Class- III) Mg > 200 for both seasons (Table 3.7). The analysis of the data shows that 70.18% of samples (40 samples) and 61.92 % of the research region fall under the Class-I category in the PRM season. It is observed that during the POM season, the count of samples that fall within Class-I is increased to 50 (92.59%), and the percentage of study regions that fall in Class-I is also increased to 94.87%.

Table 3.6 Summary of Spatial Interpretation of Calcium (Ca) Maps for both PRM and POM Seasons

Season	Ca Range (mg/l)	Count of samples	% Samples	Area (sq. km)	Area (%)
PRM	Ca < 75	49	85.96	381.85	88.15
	75 ≤ Ca ≤ 100	3	5.26	40.05	9.25
	Ca > 100	5	8.77	11.26	2.60
POM	Ca < 75	36	66.67	300.73	69.43
	75 ≤ Ca ≤ 100	6	11.11	89.7	20.71
	Ca > 100	12	22.22	42.72	9.86

Table 3.7 Summary of Spatial Interpretation of Magnesium (Mg) Maps for both PRM and POM Seasons

Season	Mg Range (mg/l)	Count of samples	% Samples	Area (sq. km)	Area (%)
PRM	Mg < 100	40	70.18	268.23	61.92
	100 ≤ Mg ≤ 200	9	15.79	143.03	33.02
	Mg > 200	8	14.04	21.9	5.06
POM	Mg < 100	50	92.59	410.96	94.87
	100 ≤ Mg ≤ 200	4	7.41	22.12	5.11
	Mg > 200	0	0.00	0	0.00

3.3.6 Sodium (Na)

The primary source of sodium in groundwater is the weathering of sodium-rich mineral formations, including feldspars, clay minerals, and evaporites such as halite and mirabilite. (Todd & Mays, 2005). However, sodium dissolved in the groundwater in the coastal region through sea spray and ancient marine deposits. Additionally, a higher amount of sodium in the groundwater of coastal areas is observed as a result of saline water ingress into groundwater (Gopinath et al., 2019; Balasubramanian et al., 2022). The amount of sodium in the samples obtained in the PRM season ranges between 15 mg/l to 1954 mg/l, with a mean of 904.56 mg/l, while the value ranges from 44 mg/l to 1775 mg/l, with a mean of 475.02 mg/l in the POM season. The collected groundwater samples are categorized into three categories: (Class- I) Na < 500; 12.28% and 62.96% samples fall under Class-I during PRM season POM season respectively, (Class- II) 500 ≤ Na ≤ 1000; 33.33% and 24.07% samples fall in Class-II during PRM season POM season respectively and (Class-III) Na > 1000; 54.39% and 12.96% samples fall within Class-III in PRM season and POM periods, respectively (Table 3.8). Furthermore, from the analysis of the spatial map of sodium, it is detected that most of the research area falls within Class-II, with sodium concentration between 500 – 1000 mg/l during the PRM Season. In contrast, in the POM season, most study areas fall within Class-I with a sodium concentration of less than 500 mg/l, indicating groundwater dilution due to rainwater penetration (Fig. 3.9).

Table 3.8 Summary of Spatial Interpretation of Sodium (Na) Maps for both PRM and POM Seasons

Season	Na Range (mg/l)	Count of samples	% Samples	Area (sq. km)	Area (%)
PRM	Na < 500	7	12.28	10.67	2.46
	500 ≤ Na ≤ 1000	19	33.33	305.55	70.54
	Na > 1000	31	54.39	116.94	27.00
POM	Na < 500	34	62.96	273.03	63.03
	500 ≤ Na ≤ 1000	13	24.07	150.85	34.83
	Na > 1000	7	12.96	9.275	2.14

3.3.7 Chloride (Cl)

Chloride is naturally present in groundwater due to the dissolution of minerals containing chloride, such as halite (rock salt) and sylvite. Human consumption of high-concentration Cl water leads to health problems such as hypertension and cardiovascular issues. At the same time, the high concentration of Cl also affects the salinity of the soil, which adversely affects crop yield. The Highest concentration of Cl during the PRM season is 3195 mg/l, with a mean value of 1193.47 mg/l, while during the POM season, the highest concentration is 3997 mg/l, with a mean value of 879.57 mg/l. According to Cl concentration, the samples are classified into three categories: Cl < 1000 (Class-I), 1000 ≤ Cl ≤ 2000 (Class-II), and Cl > 2000 (Class-III). Furthermore, analytical data show that 47.37% of samples (27 samples) have measured values of Cl more than 1000 mg/l (Class-II & III), which covers 54.07% of the study region during the PRM season (Table 3.9), while during the POM season, 18.52% samples (10 samples) have measured value of chloride more than 1000 mg/l (Class-II & III), encompasses 18.84% of the research area (Fig. 3.10). During the PRM period, the high amount of chloride in the groundwater specifies that the groundwater is affected by seawater intrusion (Lakshmanan et al., 2013; Chandrasekar et al., 2014; Omprakash & Gadikar, 2018).

Table 3.9 Summary of Spatial Interpretation of Chloride (Cl) Maps for both PRM and POM Seasons

Season	Cl Range (mg/l)	Count of samples	% Samples	Area (sq. km)	Area (%)
PRM	Cl < 1000	30	52.63	198.98	45.94
	1000 ≤ Cl ≤ 2000	18	31.58	207.119	47.82
	Cl > 2000	9	15.79	27.06	6.25
POM	Cl < 1000	44	81.48	351.51	81.15
	1000 ≤ Cl ≤ 2000	7	12.96	71.31	16.46
	Cl > 2000	3	5.56	10.33	2.38

3.3.8 Sulfate (SO_4)

Sulfate in groundwater is naturally derived by dissolving sulfate minerals, such as gypsum and anhydrite, present in sedimentary rock formations (Kanagaraj et al., 2018). High amounts of sulfate in potable water might induce gastrointestinal discomfort in individuals. Additionally, Excessive sulfate in agriculture can cause

soil acidification and impact plant development, potentially resulting in decreased crop yields and modified soil microbial activity. The mean sulfate concentration in the groundwater samples collected in the PRM is 414.63 mg/l; in the POM season, it is 62.46 mg/l. The observed maximum amount of sulfate in the PRM period is 1301.0 mg/l, whereas 1248.0 mg/l in the POM period. The collected groundwater samples are categorized into three categories: (Class- I) $SO_4 < 400$; 56.14% and 94.44% samples fall within Class-I in PRM season and POM season respectively, (Class- II) $400 \leq SO_4 \leq 800$; 24.56% and 3.70% samples fall within Class-II during PRM season POM season respectively and (Class- III) $SO_4 > 800$; 19.30% and 1.85% samples fall in Class-III during PRM season POM season respectively (Table 3.10) and spatial interpretation of sulfate map (Fig. 3.11) shows that 54.29% of the study region fall in Class-I category during the PRM season whereas, during the POM season, the Class-I study area is increased to 97.55%, indicating a decline in the concentration of sulfate in POM season than PRM season.

Table 3.10 Summary of Spatial Interpretation of Sulfate (SO_4) Maps for both PRM and POM Seasons

Season	SO_4 Range (mg/l)	Count of samples	% Samples	Area (sq. km)	Area (%)
PRM	$SO_4 < 400$	32	56.14	235.18	54.29
	$400 \leq SO_4 \leq 800$	14	24.56	171.05	39.49
	$SO_4 > 800$	11	19.30	26.94	6.22
POM	$SO_4 < 400$	51	94.44	422.54	97.55
	$400 \leq SO_4 \leq 800$	2	3.70	9.11	2.10
	$SO_4 > 800$	1	1.85	1.5	0.35

3.3.9 Potassium (K)

The primary source of potassium in groundwater is weathering potassium-rich rocks, such as feldspar and mica. Agricultural runoff and fertilizer leaching cause a rise in the potassium level in the groundwater (Kanagaraj et al., 2018). Potassium is vital for human well-being; it contributes to maintaining cell functioning, nerve transmission, and muscle contraction. However, excessive consumption of potassium can result in hyperkalemia, which can lead to heart and muscle complications. Moreover, Potassium is an essential mineral in agriculture that promotes plant development, increases crop output, and improves resistance to

diseases. However, an imbalance of potassium can negatively affect soil chemistry and decrease agricultural productivity. The potassium concentration in the groundwater samples that are collected during the PRM season ranges between 0.73 to 109.31 mg/l, with an average value of 9.8 mg/l, while the value ranges between 0.13 to 89.08 mg/l, with a mean value of 9.13 mg/l during the POM season. The collected groundwater samples are grouped into three categories: (Class- I) $K < 15$, (Class- II) $15 \leq K \leq 20$, and (Class- III) $K > 20$ for both seasons. The potassium concentration falls within the Class-I category, with 85.96% samples in the PRM period and 87.04% in the POM periods (Table 3.11). Furthermore, the interpretation of the spatial map of potassium shows that the Class-I category encompasses most areas of the study region, 83.06% and 88.36 % of the research area in the PRM and POM periods, respectively (Fig. 3.12). Moreover, the data analysis denotes no major change in the amount of potassium during both seasons.

Table 3.11 Summary of Spatial Interpretation of Potassium (K) Maps for both PRM and POM Seasons

Season	K Range (mg/l)	Count of samples	% Samples	Area (sq. km)	Area (%)
PRM	$K < 15$	49	85.96	359.79	83.06
	$15 \leq K \leq 20$	3	5.26	70.412	16.26
	$K > 20$	5	8.77	2.95	0.68
POM	$K < 15$	47	87.04	382.74	88.36
	$15 \geq K \leq 20$	2	3.70	48.41	11.18
	$K > 20$	5	9.26	2	0.46

3.3.10 Fluoride (F)

Fluoride in groundwater is mostly attributed to the dissolution of fluoride-containing minerals, such as fluorite, apatite, and micas (Todd & Mays, 2005). Fluoride is advantageous in moderate quantities for maintaining optimal dental health since it aids in cavity prevention. However, excessive ingestion of fluoride can result in dental and skeletal fluorosis, which can cause harm to tooth enamel and bone diseases. In agriculture, high fluoride concentrations inhibit plant photosynthesis, decreasing crop yield. During the PRM, groundwater samples have an average fluoride concentration of 0.63 mg/l; however, it decreases to 0.46 mg/l during the POM. The highest fluoride concentration in the PRM season is 1.02 mg/l

and 0.9 mg/l in the POM season. The samples are grouped into three categories: (Class- I) F < 0.5; 33.33% and 64.81% samples fall in Class-I during PRM and POM season, respectively, (Class- II) 0.5 ≤ F ≤ 0.75; 31.58% and 25.93% samples categorized as Class-II during PRM and POM season respectively and (Class- III) F > 0.75; 35.09% and 9.26% samples fall in Class-III in PRM and POM period respectively (Table 3.12). Spatial interpretation of Fluoride maps denotes that 74.17% of the research area falls within Classes I and II in the PRM period. In comparison, Classes I and II cover 98.52% of the study area during the POM period (Fig. 3.13).

Table 3.12 Summary of Spatial Interpretation of Fluoride (F) Maps for both PRM and POM Seasons

Season	F Range (mg/l)	Count of samples	% Samples	Area (sq. km)	Area (%)
PRM	F < 0.5	19	33.33	170.11	39.27
	0.5 ≤ F ≤ 0.75	18	31.58	151.18	34.90
	F > 0.75	20	35.09	111.87	25.83
POM	F < 0.5	35	64.81	303.17	69.99
	0.5 ≤ F ≤ 0.75	14	25.93	123.6	28.53
	F > 0.75	5	9.26	6.39	1.48

3.3.11 Nitrate (NO_3)

The primary origins of nitrate in groundwater are the decay of organic materials and the microbial decomposition of nitrogen molecules in soil. The anthropogenic contributors to the rise of nitrate concentration in the groundwater include fertilizers in agriculture, discharge from wastewater, and septic systems. Excessive levels of nitrates in potable water can adversely affect the health of the community, such as methemoglobinemia or "blue baby syndrome" in infants, as well as being associated with cancers and thyroid disorders in adults. The mean nitrate concentration in the groundwater samples collected in the PRM is 6.72 mg/l; in the POM season, it is 7.35 mg/l. The highest nitrate concentration during the PRM and POM season is 9.69 mg/l and 50.86 mg/l, respectively. The acquired samples are divided into three categories: (Class- I) NO_3 < 6.5; 24.56% and 44.44% samples fall within Class-I during PRM and POM period, respectively, (Class- II) 6.5 ≤ NO_3 ≤ 8.0; 73.68% and 37.04% samples fall into Class-II in PRM season POM season respectively and (Class- III) NO_3 > 8.0; 1.75% and 18.52% samples fall under Class-III in PRM and POM periods,

respectively (Table 3.13). Spatial interpretation of Nitrate (NO_3) maps denotes that 99.34% of the study area falls within Classes I and II in the PRM season. In comparison, Class-I and Class-II categories cover 77.04% of the study area during the POM season (Fig. 3.14).

Table 3.13 Summary of Spatial Interpretation of Nitrate (NO_3) Maps for both PRM and POM Seasons

Season	NO_3 Range (mg/l)	Count of samples	% Samples	Area (sq. km)	Area (%)
PRM	$NO_3 < 6.5$	14	24.56	147.76	34.11
	$6.5 \leq NO_3 \leq 8.0$	42	73.68	282.57	65.23
	$NO_3 > 8.0$	1	1.75	2.83	0.65
POM	$NO_3 < 6.5$	24	44.44	189.59	43.77
	$6.5 \leq NO_3 \leq 8.0$	20	37.04	144.12	33.27
	$NO_3 > 8.0$	10	18.52	99.46	22.96

3.3.12 Bicarbonate (HCO_3)

The existence of bicarbonate in groundwater is mostly due to the dissolution of carbonate minerals, including limestone and dolomite, as water penetrates these geological formations. Moreover, it can arise from the chemical reaction between carbon dioxide in soil and water, resulting in the production of carbonic acid, which in turn breaks down into bicarbonate ions. Excessive levels of bicarbonate in potable water can result in alkalosis in humans, manifesting as symptoms such as muscle fasciculations and mental impairment. Furthermore, High concentrations of bicarbonate in agriculture can result in soil alkalinity, which can negatively impact the availability of nutrients and impede plant growth. Groundwater samples taken during the PRM period have a mean HCO_3 level of 601.68 mg/l, with a maximum level of 1244.0 mg/l. During the POM period, on the other hand, the HCO_3 concentration is highest at 4736.0 mg/l with a mean of 1177.46 mg/l. The collected groundwater samples are divided into three classes: (Class- I) $HCO_3 < 450$, (Class-II) $450 \leq HCO_3 \leq 850$, and (Class- III) $HCO_3 > 850$ for both seasons (Table 3.14). The data analysis shows that 68.42% of samples (39 samples) and 86.67 % of the research region fall into the Class-II category during the PRM season. On the other hand, it is observed that during the POM season, the count of samples that fall into Class-II decreased to 16 (29.63%), Class-III increased to 37 (68.52%). Spatial

interpretation of the HCO_3 map depicts that 86.67% of the study region falls into Class-II, which is decreased to 7.0% during the POM season.

Table 3.14 Summary of Spatial Interpretation of Bicarbonate (HCO_3) Maps for both PRM and POM Seasons

Season	HCO_3 Range (mg/l)	Count of samples	% Samples	Area (sq. km)	Area (%)
PRM	$HCO_3 < 450$	11	19.30	31.17	7.20
	$450 \leq HCO_3 \leq 850$	39	68.42	375.44	86.67
	$HCO_3 > 850$	7	12.28	26.55	6.13
POM	$HCO_3 < 450$	1	1.85	0.16	0.04
	$450 \leq HCO_3 \leq 850$	16	29.63	30.33	7.00
	$HCO_3 > 850$	37	68.52	402.68	92.96

3.3.13 Carbonate (CO_3)

Carbonate minerals, such as limestone and dolomite, are the main contributors to the presence of carbonate in groundwater through their dissolution. This phenomenon occurs when water, which is often mildly acidic due to dissolved carbon dioxide, infiltrates through formations of carbonate rock. As it does so, it dissolves the minerals present in the rock and releases carbonate ions into the groundwater. High amounts of carbonate in potable water can result in adverse health effects, including gastrointestinal disruptions and the development of renal calculi in humans. Moreover, Excessive carbonate in agriculture can lead to soil alkalinity, which can impede plant growth by reducing the availability of vital nutrients. The average carbonate concentration in the groundwater samples acquired in the PRM is 166.0 mg/l; in the POM, it is 149.89 mg/l. The highest carbonate concentrations during the PRM and POM periods are 686.0 mg/l and 994.0 mg/l, respectively. The collected groundwater samples are divided into three categories: (Class- I) $CO_3 < 150$; 49.12% and 62.96% samples fall under Class-I during PRM season and POM season, respectively, (Class- II) $150 \leq CO_3 \leq 300$; 45.61% and 27.78% samples fall under Class-II during PRM season POM season respectively, and (Class- III) $CO_3 > 300$; 5.26% and 9.26% samples fall in Class-III during PRM season POM season respectively (Table 3.15). Spatial interpretation of Carbonate (CO_3) maps denotes that 97.63% of the research area falls within Classes I and II in the PRM period. In contrast, Classes I and II cover 97.07% of the research region during the POM season (Fig. 3.16).

Table 3.15 Summary of Spatial Interpretation of Carbonate (CO_3) Maps for both PRM and POM Seasons

Season	CO_3 Range (mg/l)	Count of samples	% Samples	Area (sq. km)	Area (%)
PRM	$CO_3 < 150$	28	49.12	175.37	40.49
	$150 \leq CO_3 \leq 300$	26	45.61	247.49	57.14
	$CO_3 > 300$	3	5.26	10.3	2.38
POM	$CO_3 < 150$	34	62.96	251.11	57.97
	$150 \leq CO_3 \leq 300$	15	27.78	169.38	39.10
	$CO_3 > 300$	5	9.26	12.67	2.93

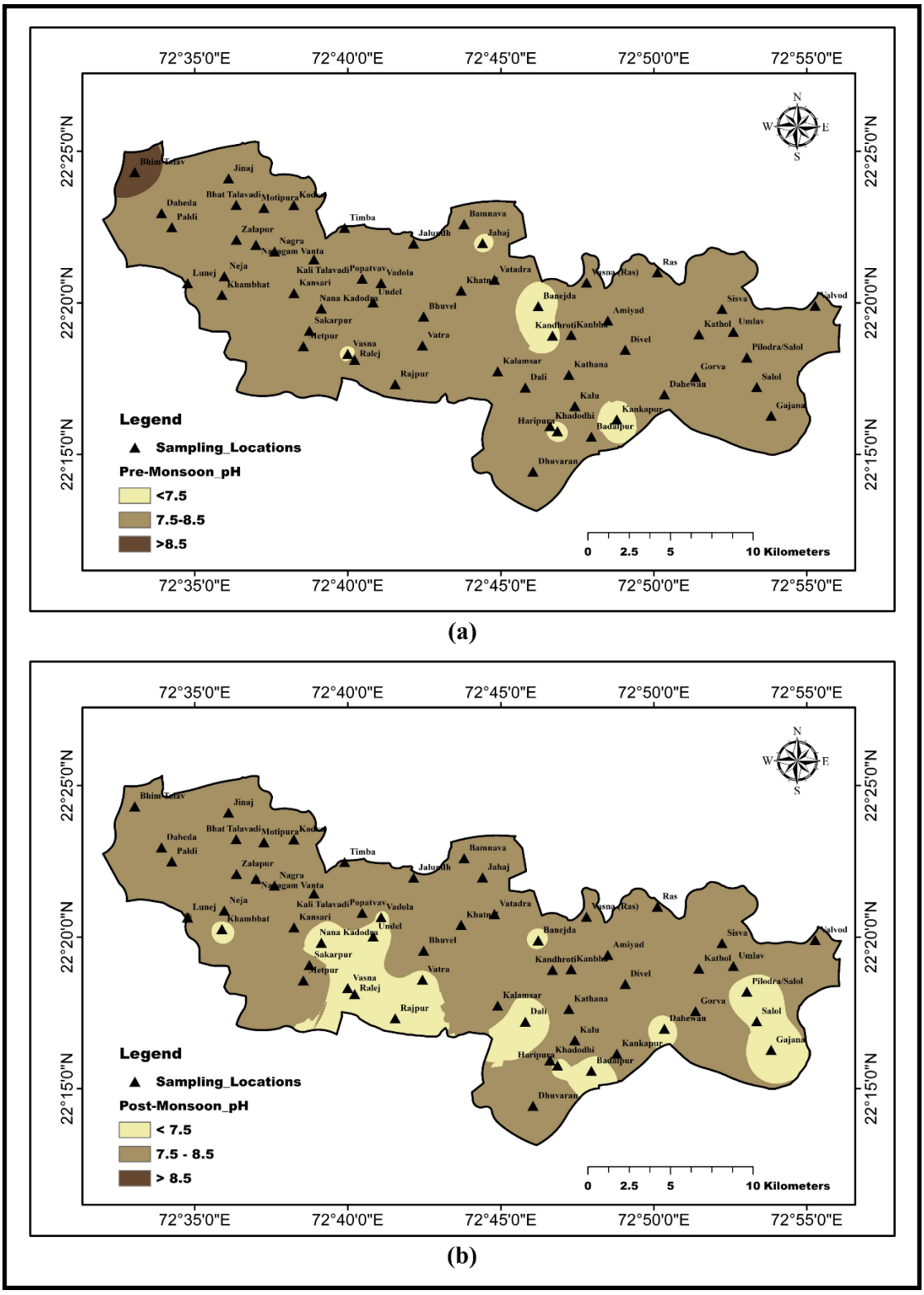

Figure 3.4 (a) Spatial Map of pH for the PRM Season (b) Spatial Map of pH for the POM Season

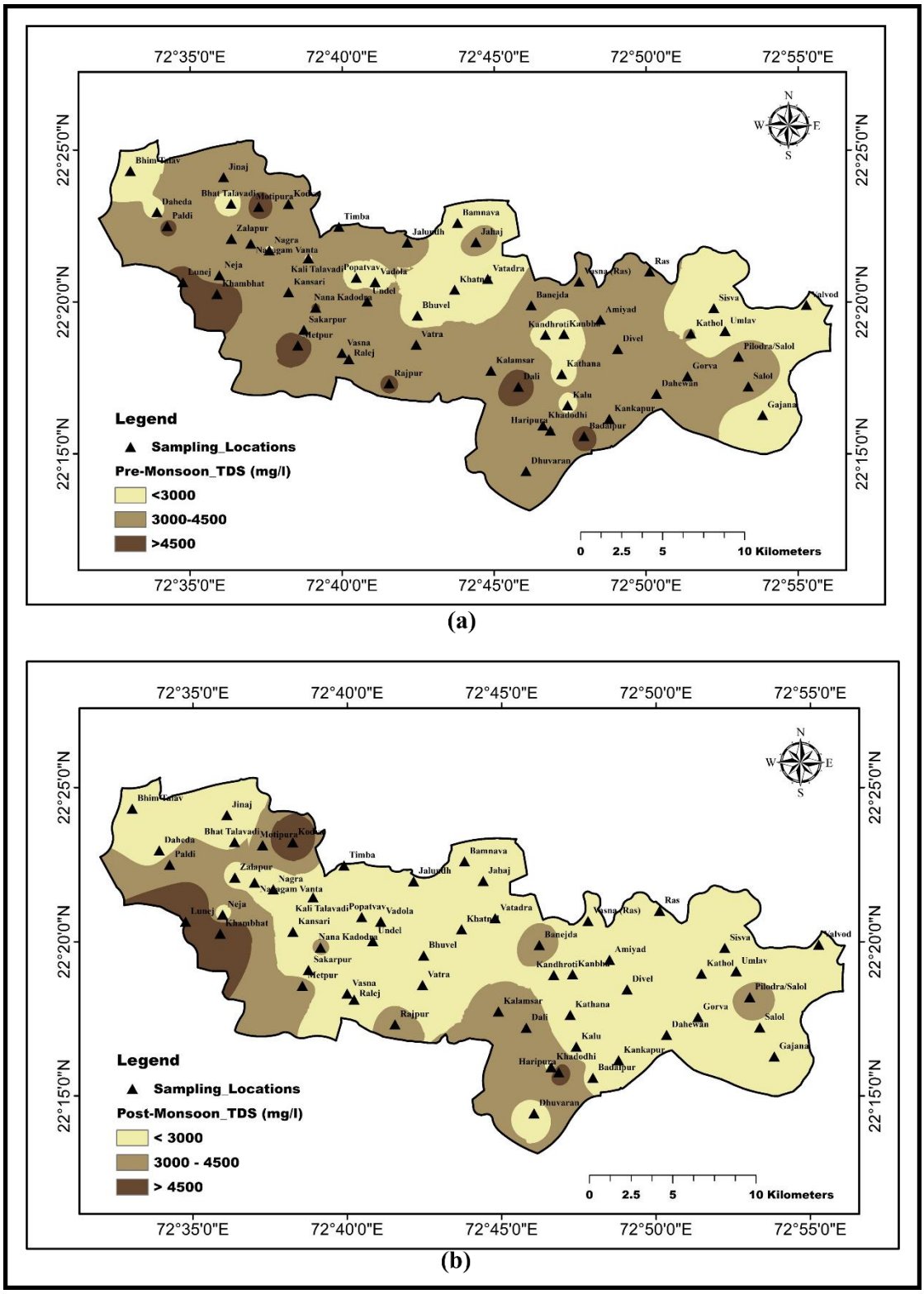

Figure 3.5 (a) Spatial Map of TDS for the PRM Season (b) Spatial Map of TDS for the POM Season

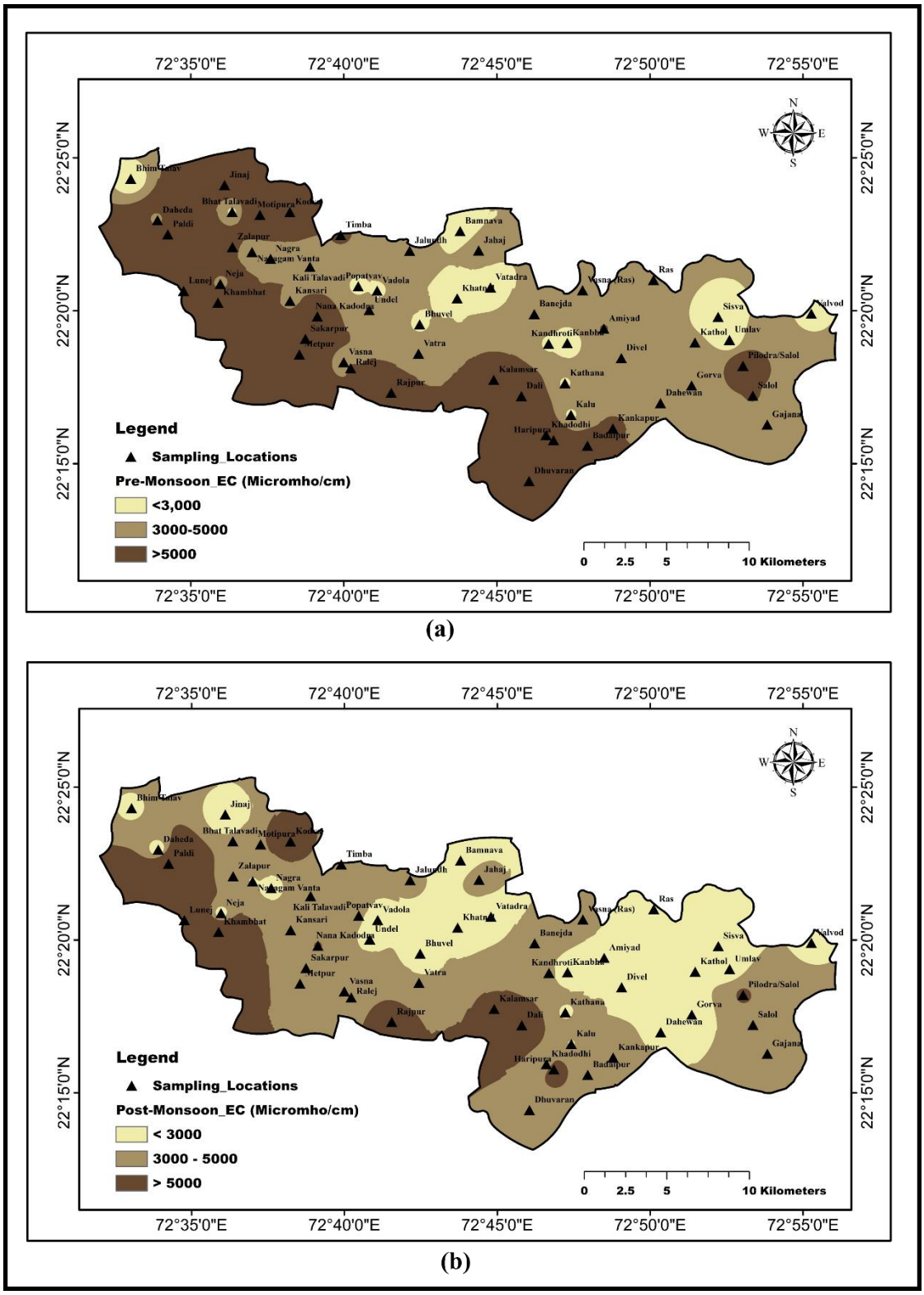

Figure 3.6 (a) Spatial Map of EC for the PRM Season (b) Spatial Map of EC for the POM Season

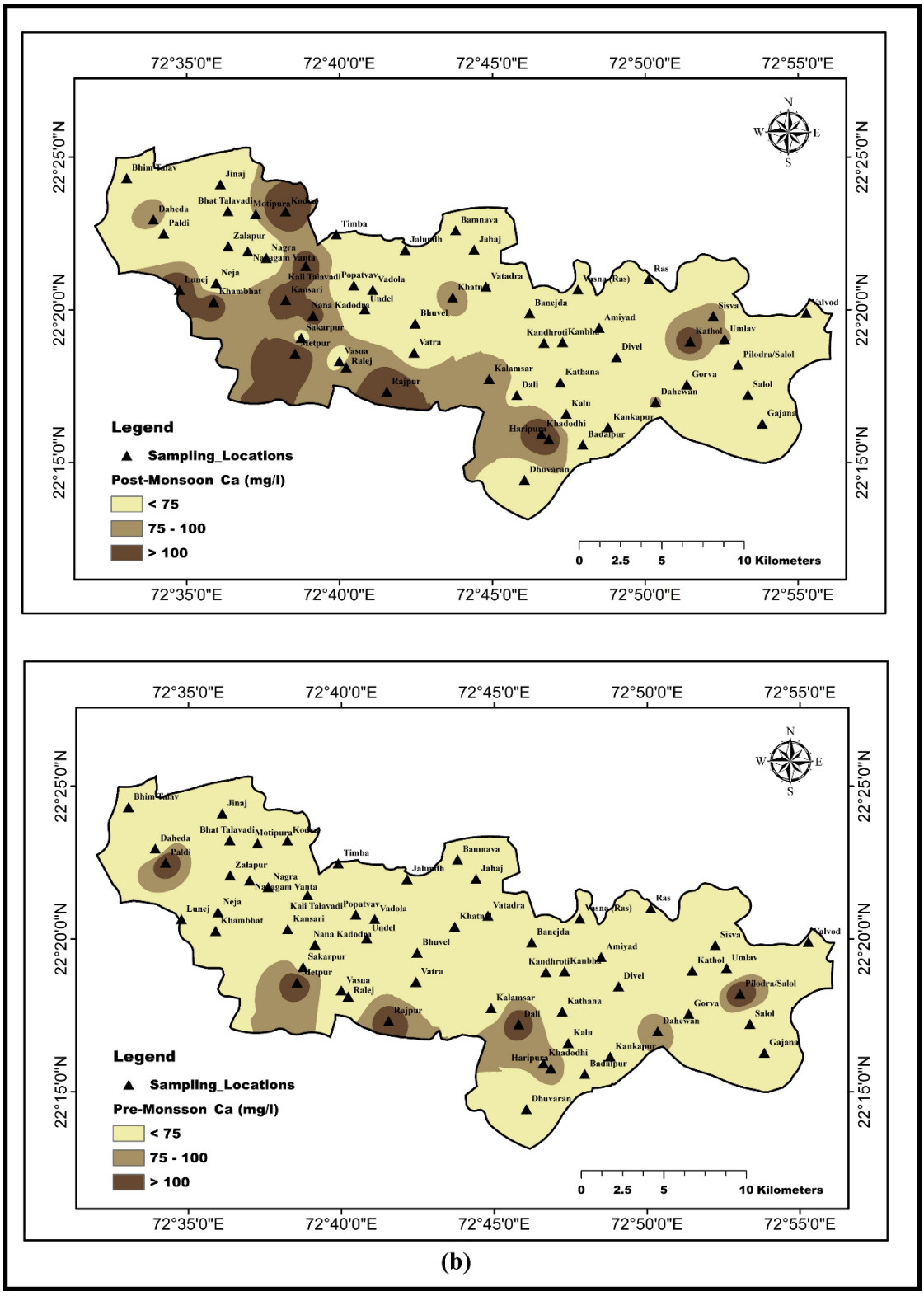

(b)

Figure 3.7 (a) Spatial Map of Calcium (Ca) for the PRM Season (b) Spatial Map of Calcium (Ca) for the POM Season

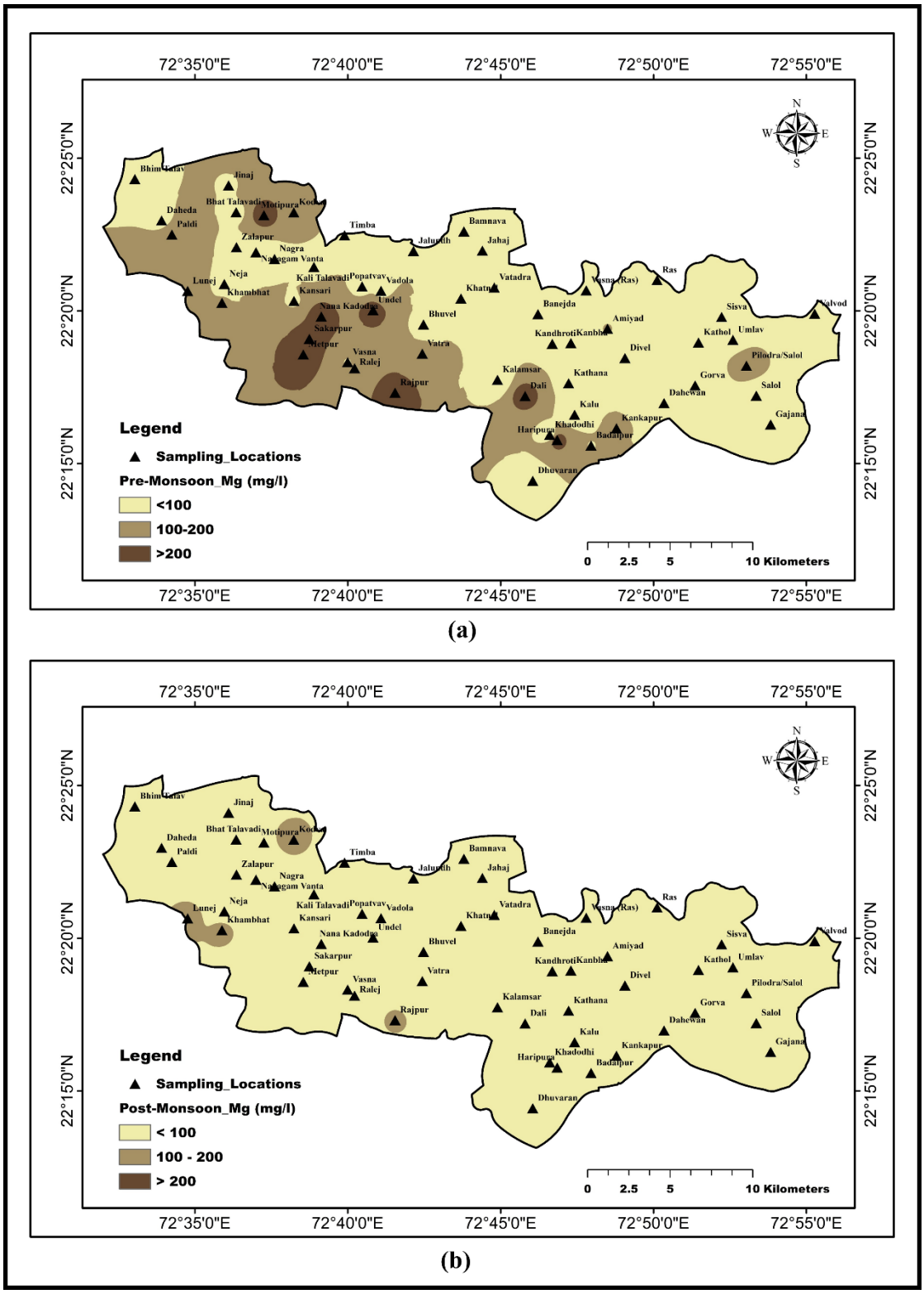

Figure 3.8 (a) Spatial Map of Magnesium (Mg) for the PRM Season (b) Spatial Map of Magnesium (Mg) for the POM Season

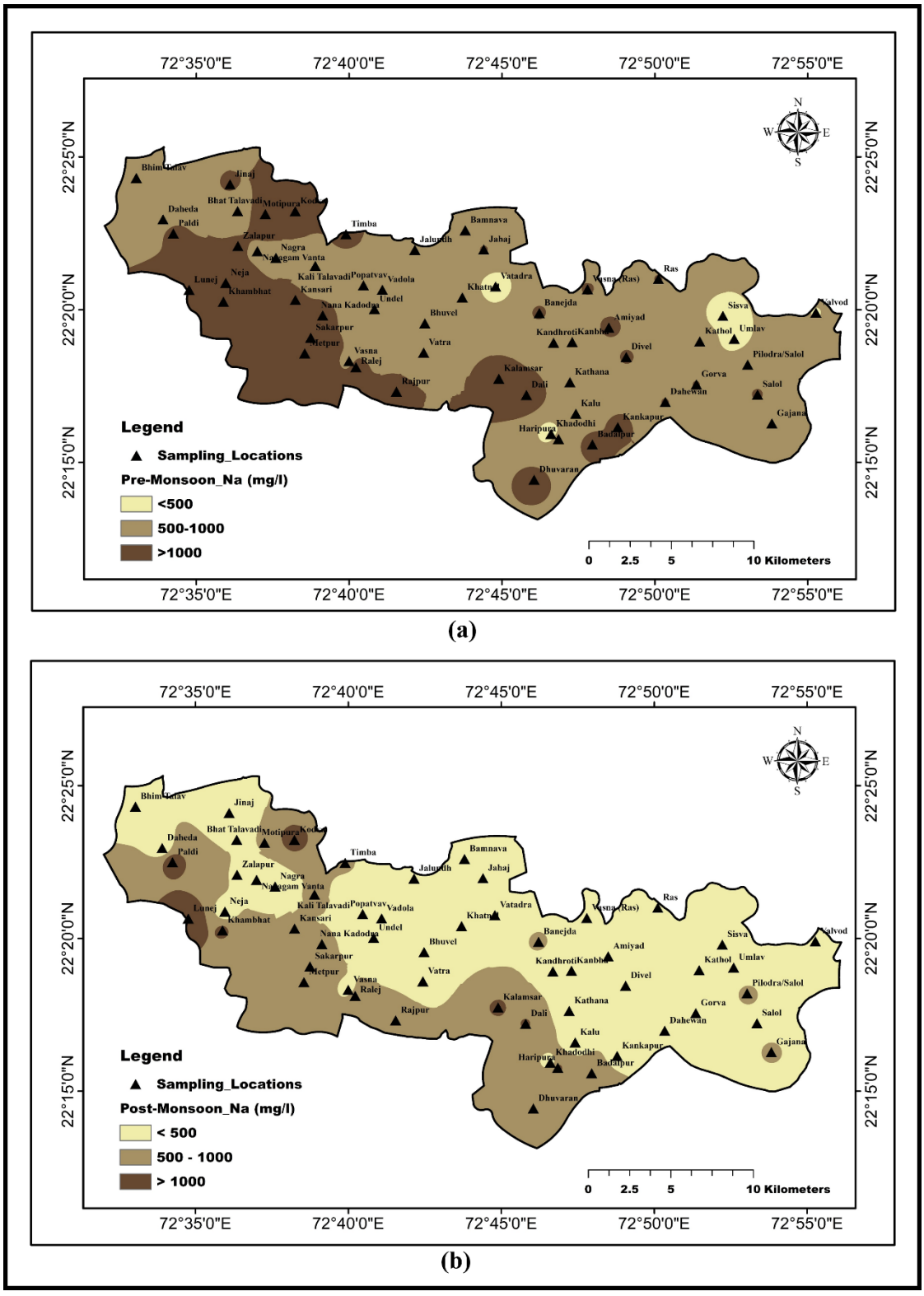

Figure 3.9 (a) Spatial Map of Sodium (Na) for the PRM Season (b) Spatial Map of Sodium (Na) for the POM Season

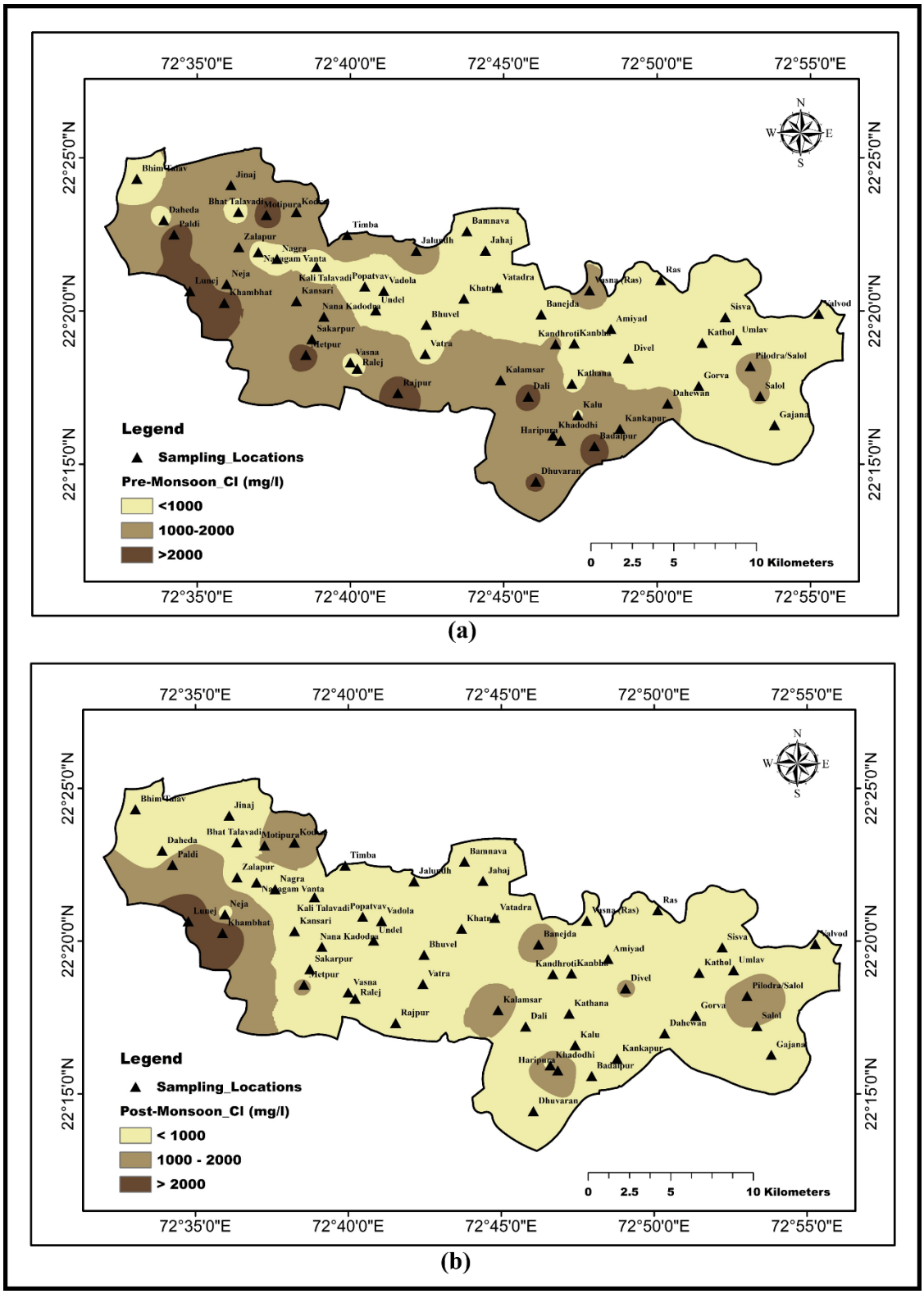

Figure 3.10 (a) Spatial Map of Chloride (Cl) for the PRM Season (b) Spatial Map of Chloride (Cl) for the POM Season

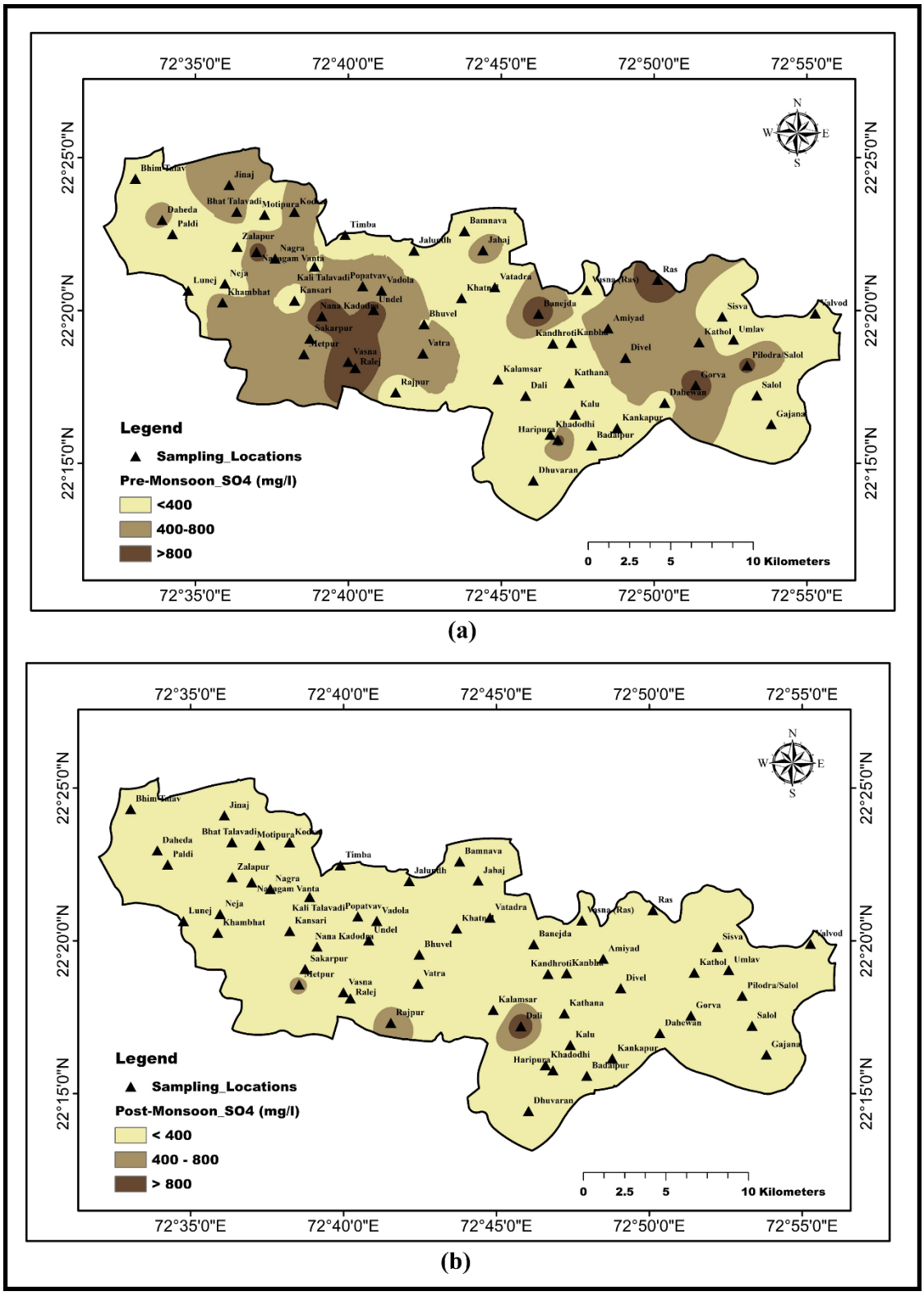

Figure 3.11 (a) Spatial Map of Sulfate (SO_4) for the PRM Season (b) Spatial Map of Sulfate (SO_4) for the POM Season

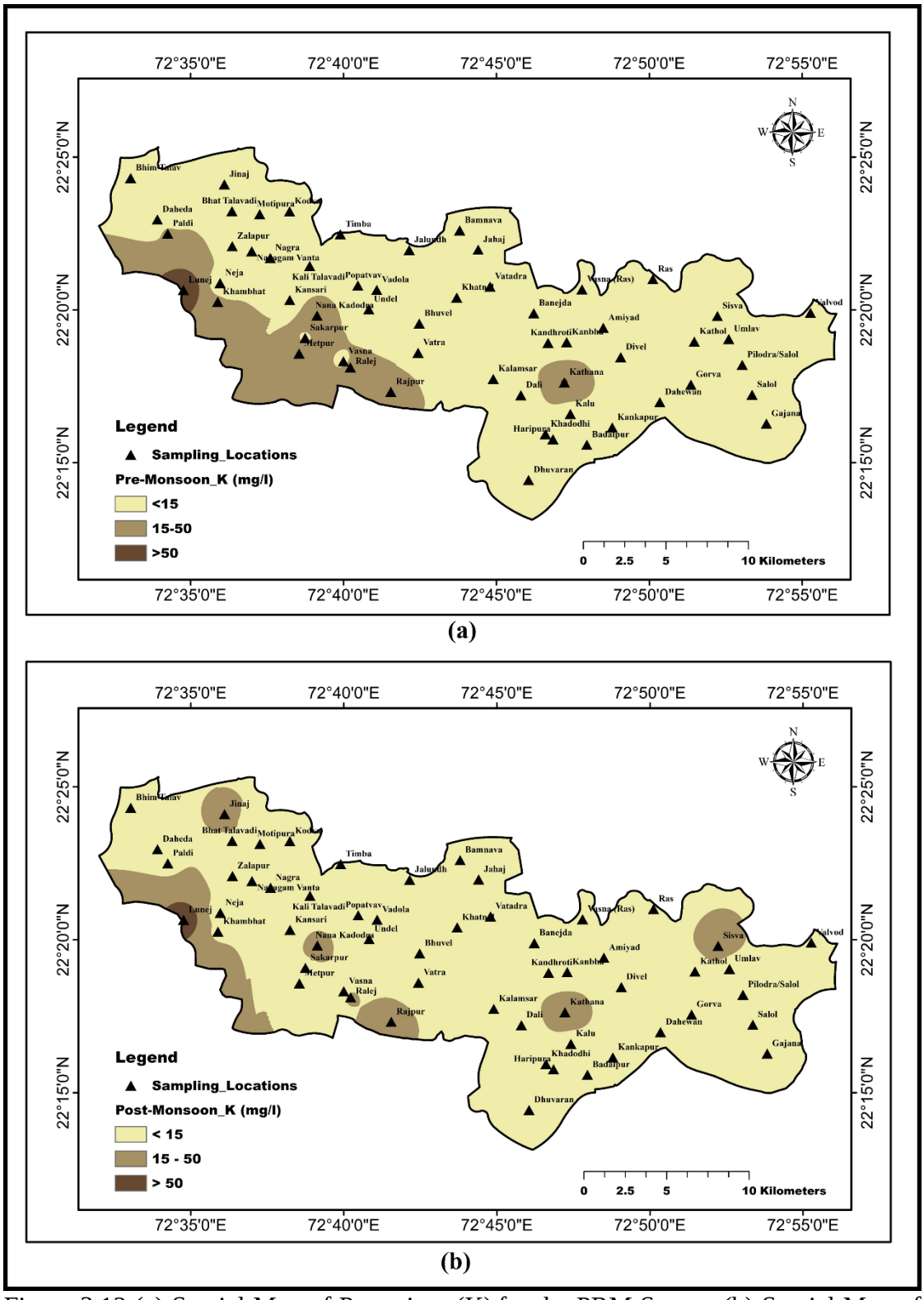

(a)

(b)

Figure 3.12 (a) Spatial Map of Potassium (K) for the PRM Season (b) Spatial Map of Potassium (K) for the POM Season

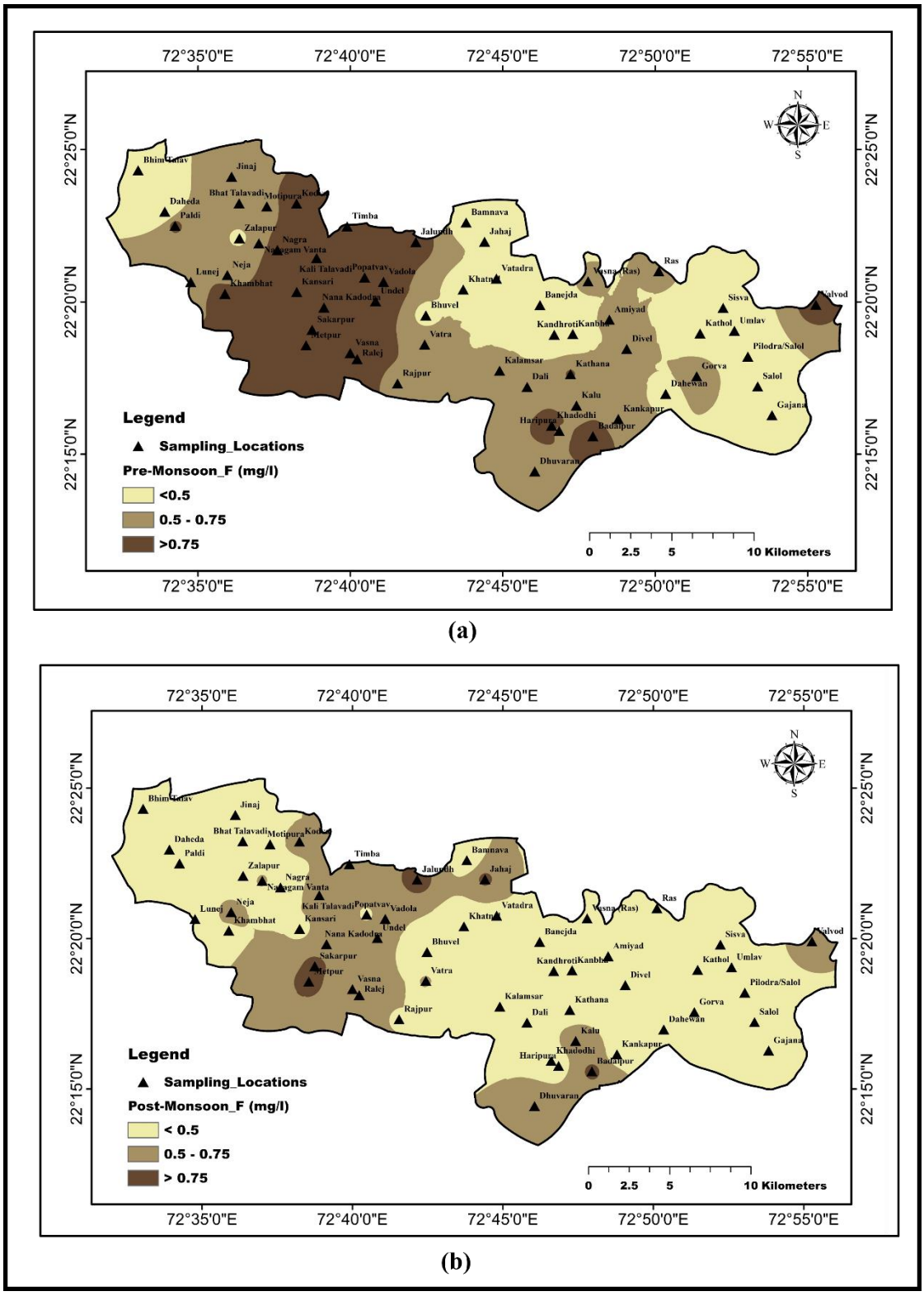

(a)

(b)

Figure 3.13 (a) Spatial Map of Fluoride (F) for the PRM Season (b) Spatial Map of Fluoride (F) for the POM Season

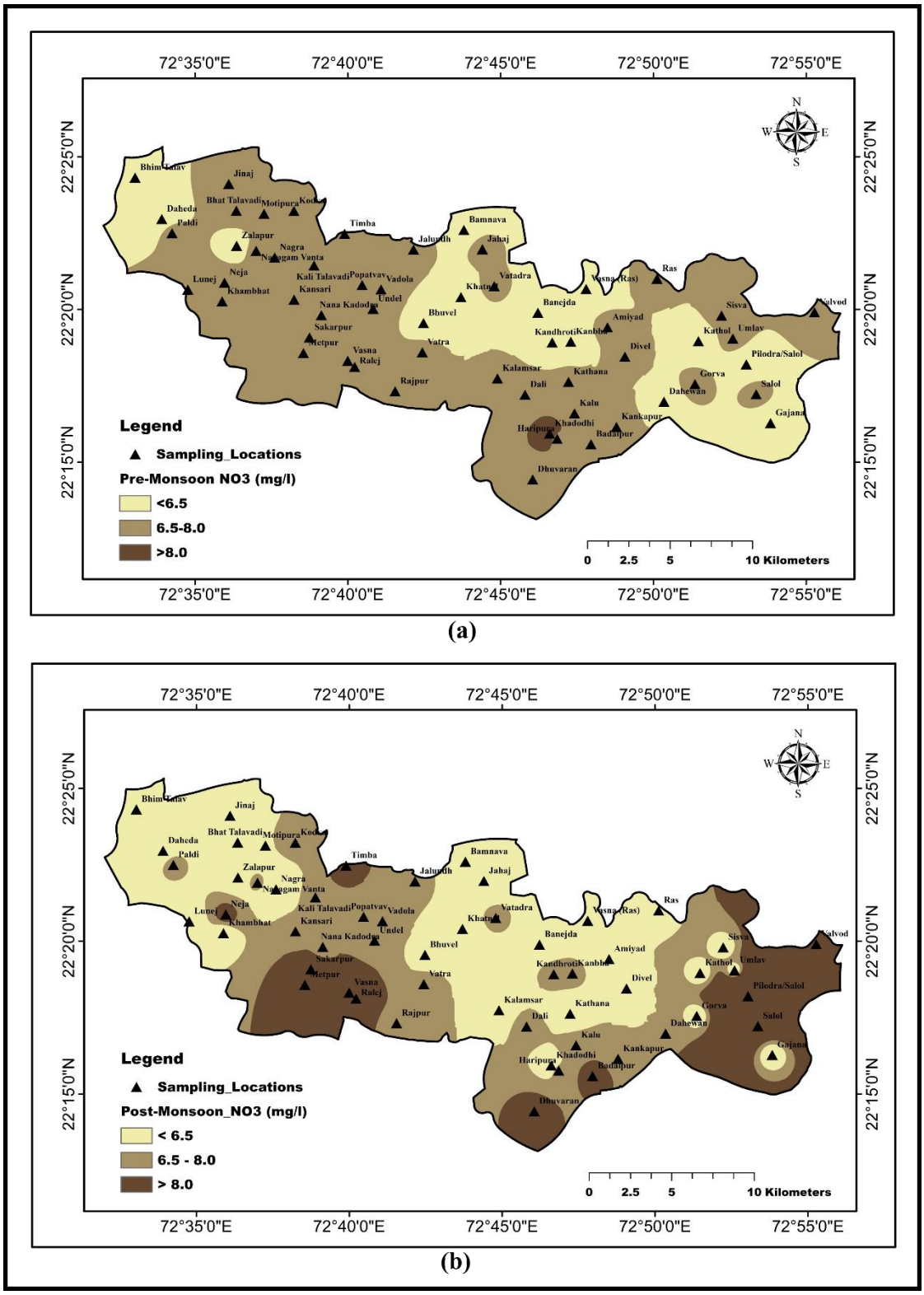

Figure 3.14 (a) Spatial Map of Nitrate (NO_3) for the PRM Season (b) Spatial Map of Nitrate (NO_3) for the POM Season

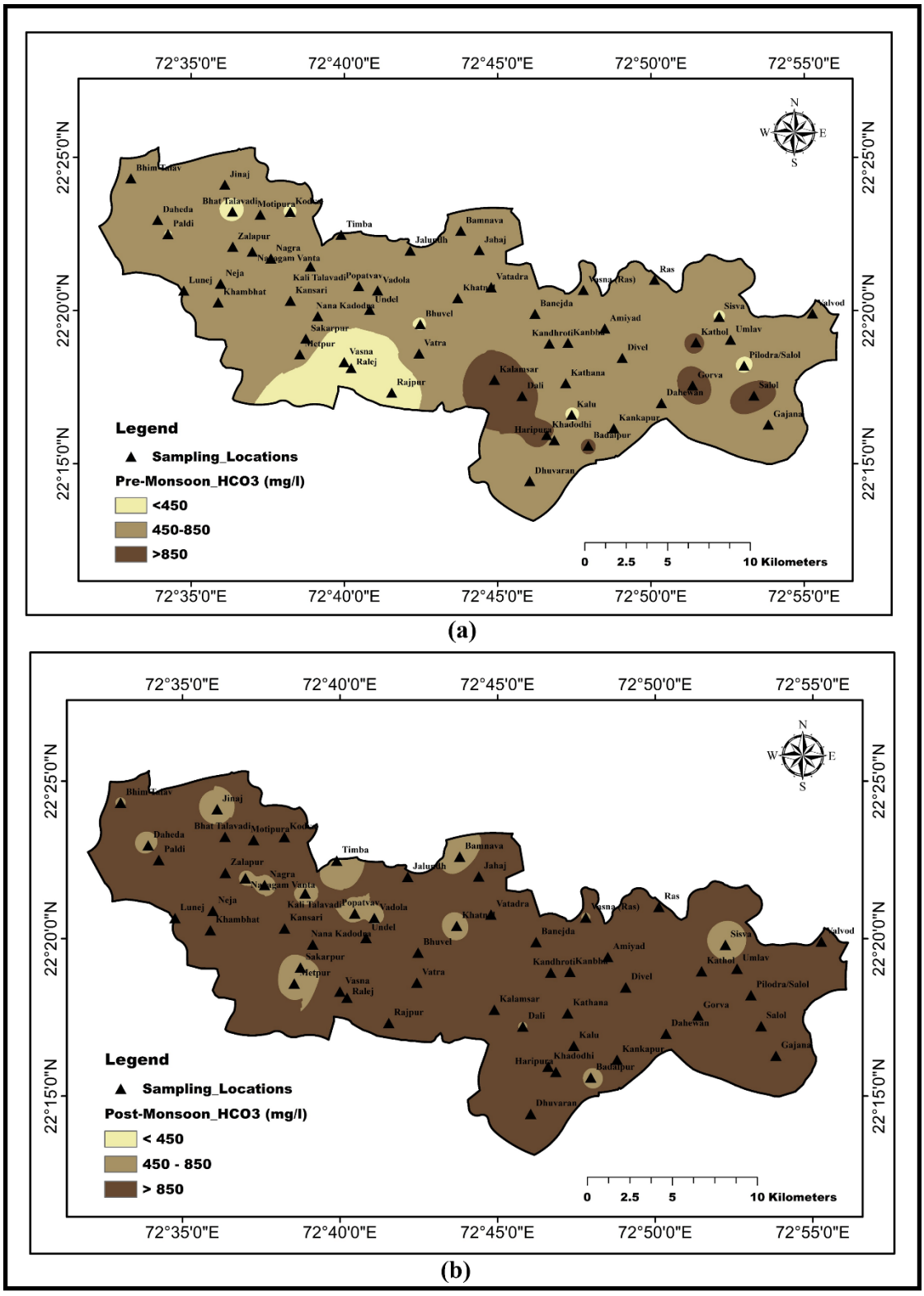

Figure 3.15 (a) Spatial Map of Bicarbonate (HCO_3) for the PRM Season (b) Spatial Map of Bicarbonate (HCO_3) for the POM Season

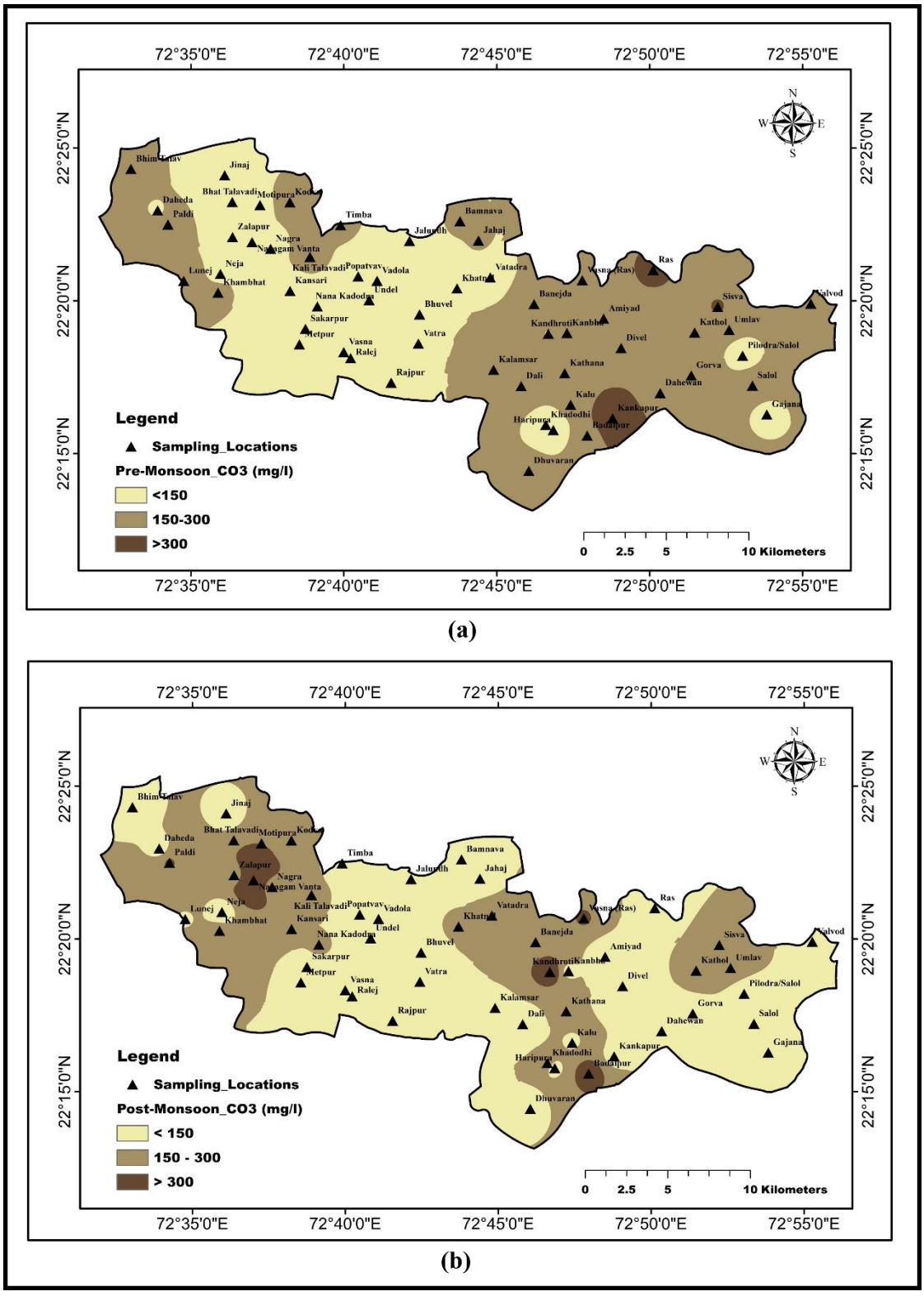

(a)

(b)

Figure 3.16 (a) Spatial Map of Carbonate (CO_3) for the PRM Season (b) Spatial Map of Carbonate (CO_3) for the POM Season

3.3.14 Hydrogeochemical facies

The geochemistry of groundwater can be graphically understood by plotting the amount of major cations (Ca, Mg, Na and K) and anions (HCO_3, CO_3, SO_4, and Cl) on the Piper trilinear diagram (Arthur M. Piper, 1944). Piper trilinear diagrams are efficient tools for illustrating the hydrogeochemical facies as they demonstrate the associations between the significant dissolved compounds in the groundwater sample (Chandrasekar et al., 2014; Singaraja et al., 2015; Mostaza-Colado et al., 2018). The diagram comprises three plots: (i) Left ternary plot, which delineates the proportion of cations; (ii) Right ternary plot, which delineates the proportion of anions; and (iii) one diamond-shaped plot, representing hydrogeochemical facies. The diamond-shaped plot can be categorized into six distinct water type zones: "Zone-1: Ca-HCO_3 water type, Zone-2: Na-Cl water type, Zone-3: Mixed Ca-Na-HCO_3 water type, Zone-4: Mixed Ca-Mg-Cl water type, Zone-5: Ca-Cl water type, and Zone-6: Na-HCO_3 water type" (Chandrasekar et al., 2014).

Fig. 3.17 and Fig. 3.18 show the Piper trilinear diagram for the PRM and POM periods, respectively. For the PRM period, the left ternary plot shows the iconic supremacy of Na + K over Ca and Mg cations, While the right ternary plot indicates the dominance of Cl over SO_4 and HCO_3 anions. Furthermore, the left ternary plot of the POM season demonstrates the supremacy of Na + K over Ca and Mg cations, while HCO_3 dominates SO_4 and Cl anions according to the right ternary plot. Most of the groundwater samples (92.98%) acquired in the PRM period fall under the Zone-2 category (Na-Cl water type) of the diamond-shaped plot, indicating sodium and chloride are dominant in the groundwater. Out of the four remaining samples, three samples represent the Zone-3 category (Mixed Ca-Na-HCO_3 type), and only 1 sample shows the Zone-4 category (Mixed Ca-Mg-Cl type). On the other hand, according to the POM diamond-shaped plot, 46.29% of samples (25 samples) fall within the Na-Cl water type (Zone-2); 44.44% (24 samples) fall under the Zone-3 category (Mixed Ca-Na-HCO_3 type), and 9.26% (5 samples) fall under the Zone-1 category (Ca-HCO_3 type). A significant fraction of the groundwater exhibits a Na–Cl water type, which commonly confirms significant impacts from seawater (Thilagavathi et al., 2012; Singaraja et al., 2015).

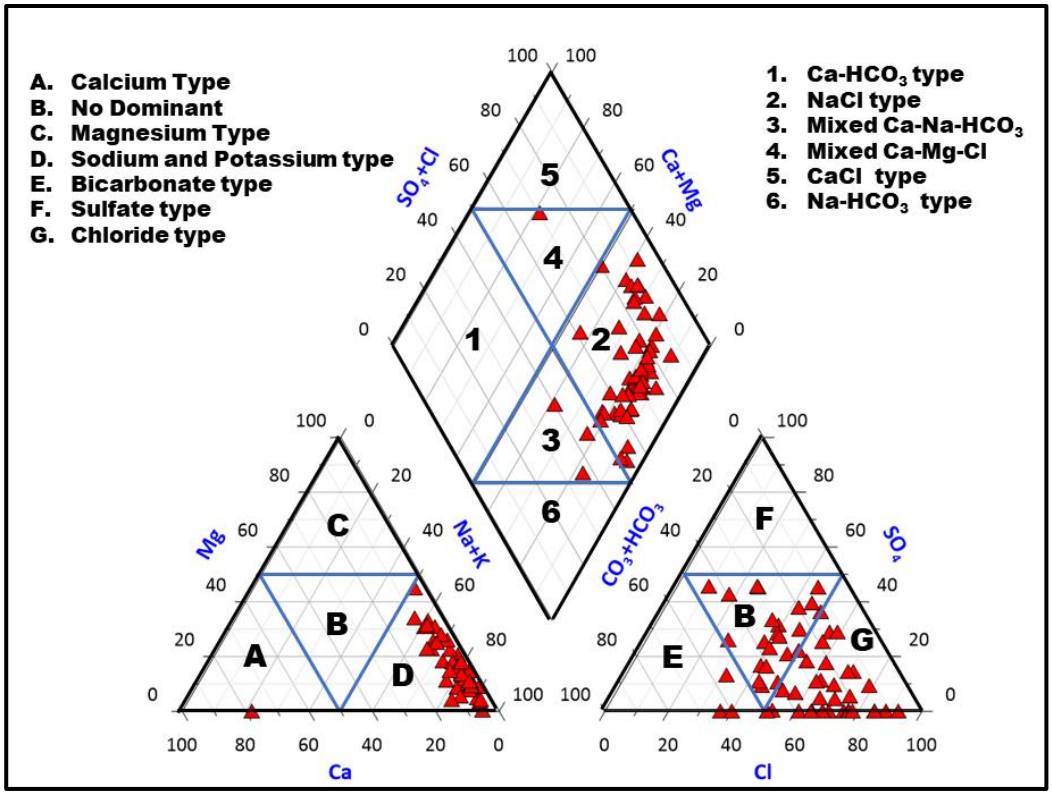

Figure 3.17 Piper trilinear diagram for the PRM Season

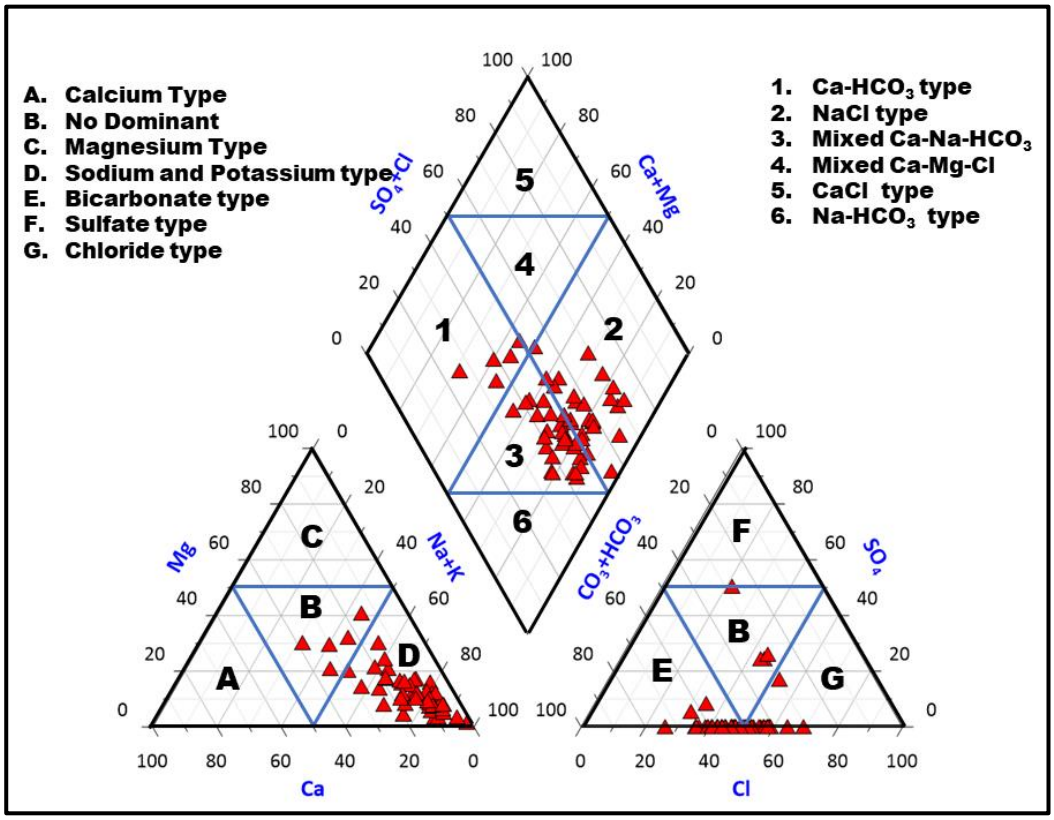

Figure 3.18 Piper trilinear diagram for the POM Season

3.4 Correlation Analysis

The geochemistry of the groundwater often involves the application of statistical techniques (Singaraja et al., 2015; Gopinath et al., 2019; Maurya et al., 2019; M. Kumari & Rai, 2020). A correlation matrix was generated to determine the most substantial hydrochemical parameters for assessing the appropriateness of groundwater for various uses and to identify the correlation among them (Table 3.16 and Table 3.17). The matrix is an adequate statistical analysis technique in which correlation among the different parameters can be identified using correlation coefficient (r). The correlation coefficient is interpreted based on the coefficient interval. The relationship between two parameters represents a very high positive or negative correlation for the value of r greater than or equal to ±0.9, whereas the value of r falls within the range ± 0.7 to ±0.9, which denotes a high positive or negative correlation between the parameters. In contrast, the relationships between the two parameters are considered negligible for the r-value less than or equal to ±0.3. The value of r ranges from ±0.5 to ±0.7, indicating moderate positive or negative correlation, while a low positive or negative correlation is considered for the value of r ranges between ±0.5 to ±0.7 (Hinkle, D. E., Wiersma, W., Jurs, 2003).

According to the resultant matrix, TDS shows a very high to high positive correlation with Na, Cl, EC, and Mg during the PRM season and with Cl, HCO_3, EC, Na, and Mg during the POM season, denoting these ions are dominant contributors to the TDS of the groundwater. The research shows high positive correlations between EC and Cl (PRM: r = 0.82, POM: r = 0.79) during both seasons, indicating these ions result from the same source. The laboratory results of the hydrochemical parameters from the previous studies can confirm the above observation. During the hydrochemical investigation, it was observed that the concentration of these parameters was high near the coast, suggesting that the region is affected by the salinity ingress.

Table 3.16 Correlation matrix of various hydrochemical parameters during PRM Season

Parameter	EC	CO3	HCO3	NO3	F	K	SO4	Cl	Na	Mg	Ca	TDS	pH
pH	-0.17	-0.06	-0.03	-0.19	-0.17	-0.07	-0.16	-0.25	-0.21	-0.29	-0.37	-0.35	1.00
TDS	0.81	0.03	0.09	0.29	0.38	0.28	0.17	0.81	0.88	0.66	0.56	1.00	
Ca	0.61	-0.11	-0.17	0.14	0.17	0.18	0.04	0.57	0.34	0.60	1.00		
Mg	0.60	-0.21	-0.32	0.15	0.28	0.29	0.21	0.61	0.45	1.00			
Na	0.62	0.12	0.03	0.11	0.28	0.15	0.21	0.62	1.00				
Cl	0.83	-0.11	-0.03	0.25	0.32	0.41	-0.34	1.00					
SO4	-0.06	-0.10	-0.23	0.05	0.19	-0.09	1.00						
K	0.49	-0.11	-0.23	0.18	0.17	1.00							
F	0.31	-0.25	-0.02	0.68	1.00								
NO3	0.29	-0.02	0.21	1.00									
HCO3	-0.04	0.23	1.00										
CO3	-0.02	1.00											
EC	1.00												

Table 3.17 Correlation matrix of various hydrochemical parameters during POM Season

Parameter	EC	CO3	HCO3	NO3	F	K	SO4	Cl	Na	Mg	Ca	TDS	pH
pH	-0.10	0.39	0.03	-0.28	-0.25	0.22	-0.40	0.06	-0.15	0.02	-0.17	-0.01	1.00
TDS	0.86	0.12	0.94	0.07	-0.02	0.48	0.07	0.96	0.84	0.69	0.47	1.00	
Ca	0.37	-0.04	0.36	-0.15	0.10	0.27	0.22	0.38	0.50	0.66	1.00		
Mg	0.54	0.02	0.67	-0.12	0.10	0.40	0.14	0.60	0.55	1.00			
Na	0.91	0.04	0.66	0.08	0.05	0.40	0.33	0.74	1.00				
Cl	0.79	0.09	0.92	0.12	-0.09	0.48	-0.11	1.00					
SO4	0.28	-0.14	-0.15	0.05	0.11	0.01	1.00						
K	0.48	-0.04	0.45	-0.09	-0.03	1.00							
F	-0.02	0.04	-0.03	0.18	1.00								
NO3	0.08	-0.07	0.02	1.00									
HCO3	0.72	0.01	1.00										
CO3	0.07	1.00											
EC	1.00												

Chapter - 4

Groundwater Quality Assessment for Potability

4.1 General

The assessment of water quality is the process of examining the state and properties of water to ascertain its suitability for intended usage, which involves analyzing different physical, chemical, and biological parameters. To aid in assessing water quality, different standards are developed at national and regional levels (Beyene et al., 2019). (BIS, 2012) and (WHO, 2017) have set acceptable limits for concentrations of drinking water quality indicator parameters since water quality directly impacts human health. Exceeding acceptable limits in drinking water may adversely impact human health (Beyene et al., 2019; Rao et al., 2021).

To assess the appropriateness of the water from the analysis of several parameters is a robust task (Mukate et al., 2019; Solangi et al., 2020). To simplify this complex operation, it is necessary to consolidate several parameters into a single compound value that effectively summarizes water quality in an easily comprehensible way while maintaining its scientific integrity (Mukate et al., 2019). Consequently, conventional techniques like individual parameter evaluation of water quality were supplanted by the water quality index (WQI), first formulated by Horton in 1965 (Gao et al., 2020).

The water quality index incorporates data on the concentration of various water quality indicator parameters to develop an integrated index that succinctly and intuitively quantifies water quality (Zhe et al., 2021). Parameters are often weighted based on their perceived significance to overall water quality (Vasanthavigar et al., 2010; Verma et al., 2020). The weight allocated to each indicator quantifies the significance of each indicator, and hence, the rationale behind the weights directly influences the validity of the WQI outcomes (Mukate et al., 2019). The method to allocate weight to the indicator parameters can be categorized as (i) Subjective methods such as AHP, SMART, ROC, Delphi, etc., in which weight is allocated based on the opinion of experts or decision-makers and (ii) Objective methods such as Entropy, Standard deviation, CRITIC, etc., in which mathematical or statistical calculations are employed to allocate weight to the parameters (Alessio Ishizaka, 2013).

The chapter covers the groundwater quality index calculation using two methods to allocate weight to each quality indicator parameter for the PRM and POM seasons, along with the results. Furthermore, spatial maps representing different classes of quality of groundwater for potability according to computed groundwater quality indices were generated through the geospatial analyst tool IDW (Inverse Distance Weighted) interpolation through ArcGIS 10.4.1 for both seasons are also illustrated in this chapter.

4.2 Groundwater Quality Index (GWQI) Calculation

The subjective method of assigning weight to each quality parameter was employed to compute the GWQI of each sampling location for the PRM and POM seasons. The calculation involves the below given five steps:

(1) Eleven groundwater quality parameters were selected to generate the index: pH, TDS, Ca, Mg, Na, Cl, SO_4, K, F, NO_3, and HCO_3.

(2) Depending on their influence on the appropriateness of water for human consumption, a weight on a scale of 1 to 5 was allocated to each indicator parameter (Table 4.1). Parameters such as TDS, Chloride, Fluoride, and Nitrate were assigned the highest weight of "5", indicating their significant influence. Parameters such as bicarbonate were assigned the lowest weight of "1," indicating their minimal influence. Additionally, the parameters pH, Sodium, and Sulfate were designated a weight of "4". The parameters Calcium and Magnesium are assigned a weight of 3, while the parameter Potassium is assigned a weight of 2 (Bhavsar & Patel, 2023).

(3) Each indicator parameter's proportional weight (PWi) is calculated by applying Eq.1, which is given in Table 4.1.

$$PW_i = \frac{W_i}{\sum_{i=1}^{n} W_i} \quad \text{.....(Eq.1)}$$

where, PW_i is the proportional weight of i^{th} parameter, W_i is the allocated weight of the i^{th} parameter, and n is the count of parameters.

Table 4.1 Water Quality Standards for potability, allocated weight, and proportional weight of groundwater quality indicator parameters (Bhavsar & Patel, 2023)

Groundwater quality Parameters	**Permissible value of indicator parameters (B_i)** (In mg/l except pH)	**Allocated Weight (AW_i)**	**Proportional Weight (PW_i)**
pH	7.5 - 8.5	4	0.10
TDS	500	5	0.12
Ca	75	3	0.07
Mg	30	3	0.07
Na	200	4	0.10
Cl	250	5	0.12
SO_4	200	4	0.10
K	12	2	0.05
F	1	5	0.12
NO_3	45	5	0.12
HCO_3	300	1	0.02
Σ Sum		41	1.00

(4) The percentage quality grade (QG_i) of each indicator parameter is computed by dividing the amount of each indicator parameter by its permissible value and multiplying it by 100 (Eq.2)

$$QG_i = \frac{A_i}{B_i} \times 100 \quad \text{.....(Eq.2)}$$

where, QG_i is the percentage quality grade of i^{th} parameter, A_i is the amount of i^{th} parameter and B_i is the permissible value of i^{th} parameter.

(5) The sub-quality index ($SGWQI_i$) of each indicator parameter is determined by taking the product of proportional weight (PW_i) and the percentage quality grade (QG_i) by applying Eq.3.

$$SGWQI_i = QG_i \times PW_i \quad \text{.....(Eq.3)}$$

Ultimately, the final GWQI of individual sampling locations is computed by taking the sum of the SGWQI value of all eleven parameters (Eq.4)

$$GWQI = \sum_{i=1}^{n} SGWQI \quad \text{.....(Eq.4)}$$

According to the calculated GWQI value of each sampling location, the groundwater samples are divided into five distinct classes of quality: Excellent water quality: GWQI≤50, Good water quality: 50<GWQI≤100, Poor water quality: 100<GWQI≤200, Very poor water quality: 200<GWQI≤300, and Unsuitable to use: GWQI > 300 (Ismail et al., 2020; Saikrishna et al., 2020; Bhavsar & Patel, 2023)

4.3 Groundwater potability analysis based on calculated GWQI

For the PRM season, GWQI was computed for 57 sampling locations, while the index was calculated for 54 locations for the POM season. The GWQI and associated water quality class of each sampling location are graphically represented in Fig. 4.1. The GWQI value of groundwater samples collected during the PRM season ranges between 93.45 to 479.57, with an average value of 265.66, while the value ranges between 70.03 to 687.18, with a mean of 185.22 in the POM period.

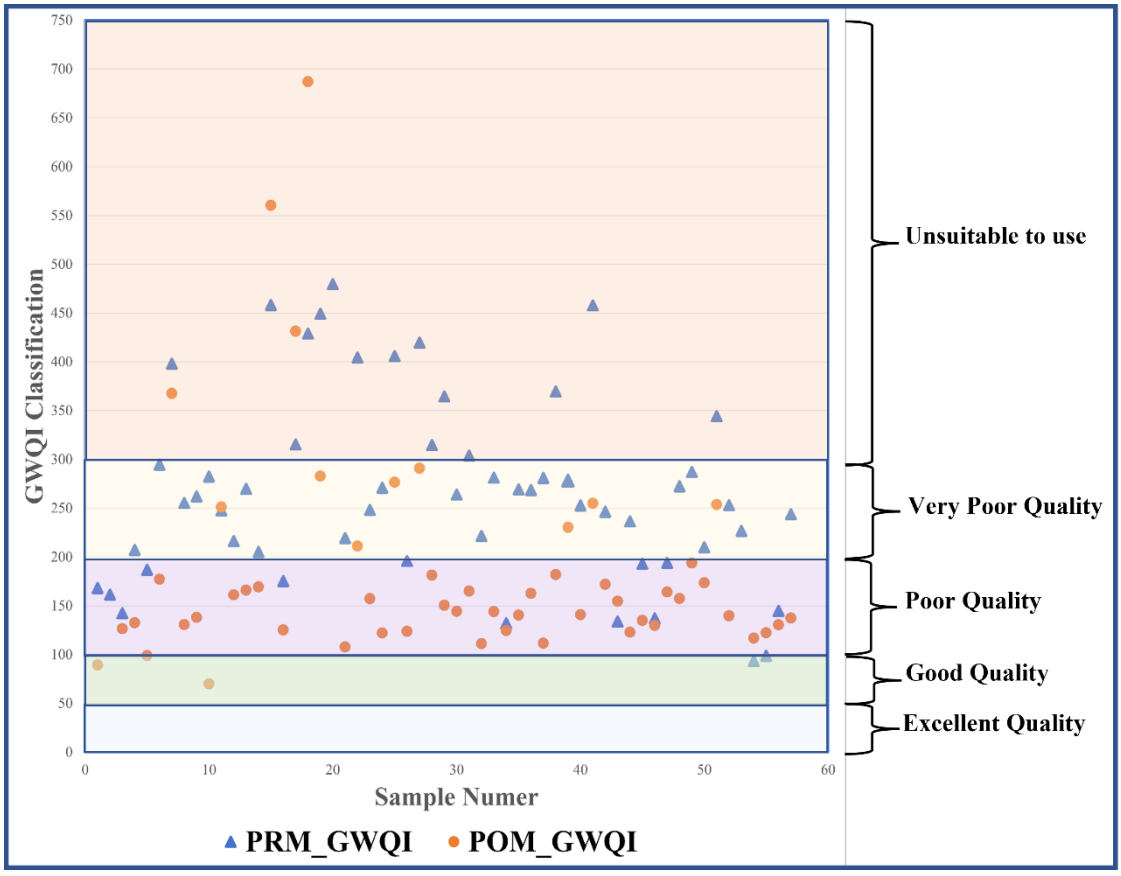

Figure 4.1 Graphical representation of GWQI value and associated water quality class for PRM and POM seasons

GWQI values of 26.32% of acquired samples (15 samples) during the PRM season and 7.41% (4 samples) during the POM season are greater than 300, signifying that the groundwater is not potable. During the PRM season, the water quality of 28 samples (49.12% samples) is classified as very poor, whereas 12 samples (21.05% samples) are classified as poor quality, signifying the quality of groundwater of the research region during the PRM season is inappropriate for the consumption. However, Due to the groundwater recharge, the count of samples categorized as very poor quality is reduced to 8 (14.81% samples) during the POM season, while 72.22% samples (39 samples) fall under the poor quality water for drinking. It is observed that only 3.51% of samples (2 samples) and 5.56% of samples (3 samples) during the PRM and POM season, respectively, can be categorized as good quality water. Throughout the PRM and POM seasons, not a single sample from the study area has water considered excellent quality. (Table 4.2).

Table 4.2 Details of groundwater quality according to GWQI for potability

Season	Range of GWQI	Quality Class	Samples count	% Samples
PRM	GWQI ≤ 50	Excellent Quality	0	0.00
	50 < GWQI ≤ 100	Good Quality	2	3.51
	100 < GWQI ≤ 200	Poor Quality	12	21.05
	200 < GWQI ≤ 300	Very Poor Quality	28	49.12
	GWQI > 300	Unsuitable to use	15	26.32
POM	GWQI ≤ 50	Excellent Quality	0	0.00
	50 < GWQI ≤ 100	Good Quality	3	5.56
	100 < GWQI ≤ 200	Poor Quality	39	72.22
	200 < GWQI ≤ 300	Very Poor Quality	8	14.81
	GWQI > 300	Unsuitable to use	4	7.41

4.4 Entropy Weighted Groundwater Quality Index (EGWQI) calculation

To calculate the Entropy Weighted Groundwater Quality Index (EGWQI) of each sampling location for the PRM and POM seasons, the objective method to assign weight to each quality parameter was applied. In the current research, the entropy method (EWM) was employed to allocate weight to individual parameters. In order to evaluate the WQI, weight is a crucial element. In contrast to the subjective assignment approach, EWM guarantees that weights are both unique and objective by eliminating the

influence of subjective decision-making experience (Odu, 2019; Adimalla et al., 2020; Kumar & Augustine, 2022). The calculation involves below given six steps:

(1) eleven groundwater quality parameters were selected to generate the index: pH, TDS, Ca, Mg, Na, Cl, SO_4, K, F, NO_3, and HCO_3.

(2) Generate a matrix of groundwater quality by applying the below given matrix:

$$P=\begin{bmatrix} p_{11} & p_{12} & \cdots & p_{1y} \\ p_{21} & p_{22} & \cdots & p_{2y} \\ \vdots & \vdots & \ddots & \vdots \\ p_{x1} & p_{x2} & \cdots & p_{xy} \end{bmatrix}$$

where, x (i=1,2,3,…,x) is the number of groundwater samples; y (j=1,2,3,…,y) is the number of indicator parameters of each groundwater sample.

(3) Employing a method known as "generating quotient after range pretreatment", to compute standardized values (R_{ij}) by first evaluating Q_{ij} applying Eq.5 and then determining R_{ij} applying Eq. 6 to generate the final standardized matrix. (Subba Rao et al., 2020) :

$$\text{(a) } Q_{ij} = \frac{(P_{ij})_{highest} - (P_{ij})}{(P_{ij})_{highest} - (P_{ij})_{least}} \quad \text{.....(Eq.5)}$$

where,$(P_{ij})_{least}$ and $(P_{ij})_{highest}$ is the least and greatest value of individual indicator parameters in the samples.

$$Q=\begin{bmatrix} q_{11} & q_{12} & \cdots & q_{1y} \\ q_{21} & q_{22} & \cdots & q_{2y} \\ \vdots & \vdots & \ddots & \vdots \\ q_{x1} & q_{x2} & \cdots & q_{xy} \end{bmatrix}$$

where, Q is a standardized matrix.

$$\text{(b) } R_{ij} = \frac{Q_{ij}}{\sum_{i=1}^{m} Q_{ij}} \quad \text{.....(Eq.6)}$$

$$R=\begin{bmatrix} r_{11} & r_{12} & \cdots & r_{1y} \\ r_{21} & r_{22} & \cdots & r_{2y} \\ \vdots & \vdots & \ddots & \vdots \\ r_{x1} & r_{x2} & \cdots & r_{xy} \end{bmatrix}$$

where, R is the final standardized matrix.

(4) Compute the entropy (E_j) applying Eq. 7 and then determine the entropy weight (W_j) of individual indicator parameters applying Eq. 8 (Bao et al., 2020):

$E_j = \frac{1}{\ln(m)} \sum_{i=1}^{m} R_{ij} * \ln(R_{ij})$ (When $R_{ij} = 0$, $R_{ij} * \ln(R_{ij})$ is defined to be 0...……(Eq.7)

$W_j = \frac{(1-E_j)}{\sum_{i=1}^{m}(1-E_j)}$ ……..(Eq.8)

(5) Estimate the quality grade (Q_j) of the individual indicator parameter (Adimalla, 2021)

$$Q_j = \frac{A_j}{Bj}$$

……(Eq.9)

$Q_{pH} = \frac{A_{pH} - 7}{8.5 - 7}$ $A_{pH} > 7$

$Q_{pH} = \frac{7 - A_{pH}}{8.5 - 7}$ $A_{pH} < 7$

where, A_j denotes the amount of indicator parameter j in mg/l; B_j denotes the permissible value of j^{th} indicator parameter

(6) Calculate the weighted groundwater quality index (EGWQI) by computing the sub-quality index of each parameter ($SEGWQI_j$), which is a product of quality grade and entropy weight. Ultimately, the final EGWQI of the location is determined by adding the value of the sub-quality index of all eleven parameters. (C. Li et al., 2021). The following equations are applied:

$SEGWQI_j = Q_j * W_j$ ……..(Eq.10)

$EGWQI = \sum_{j=1}^{m} SGWQI$ ……(Eq.11)

Ultimately, the groundwater quality of each sampling location is classified into five categories according to the calculated value of EGWQI at that location: Excellent quality: EGWQI≤1.0, Good quality: 1.0<EGWQI≤1.5, Poor quality: 1.5<EGWQI≤2.0, Very poor quality: 2.0<EGWQI≤2.5 and Unsuitable to use: EGWQI > 2.5 (Subba Rao, 2012)

4.5 Groundwater potability analysis based on calculated EGWQI

For the PRM season, EGWQI was computed for 57 sampling locations, while the index was calculated for 54 locations for the POM season. The EGWQI and associated water quality class of each sampling location are graphically represented in Fig. 4.2. The EGWQI value of groundwater samples acquired in the PRM period ranges between 0.80 and 4.13, with a mean of 2.35, while the value ranges from 0.72 and 5.91, with a mean of 1.60 in the POM period.

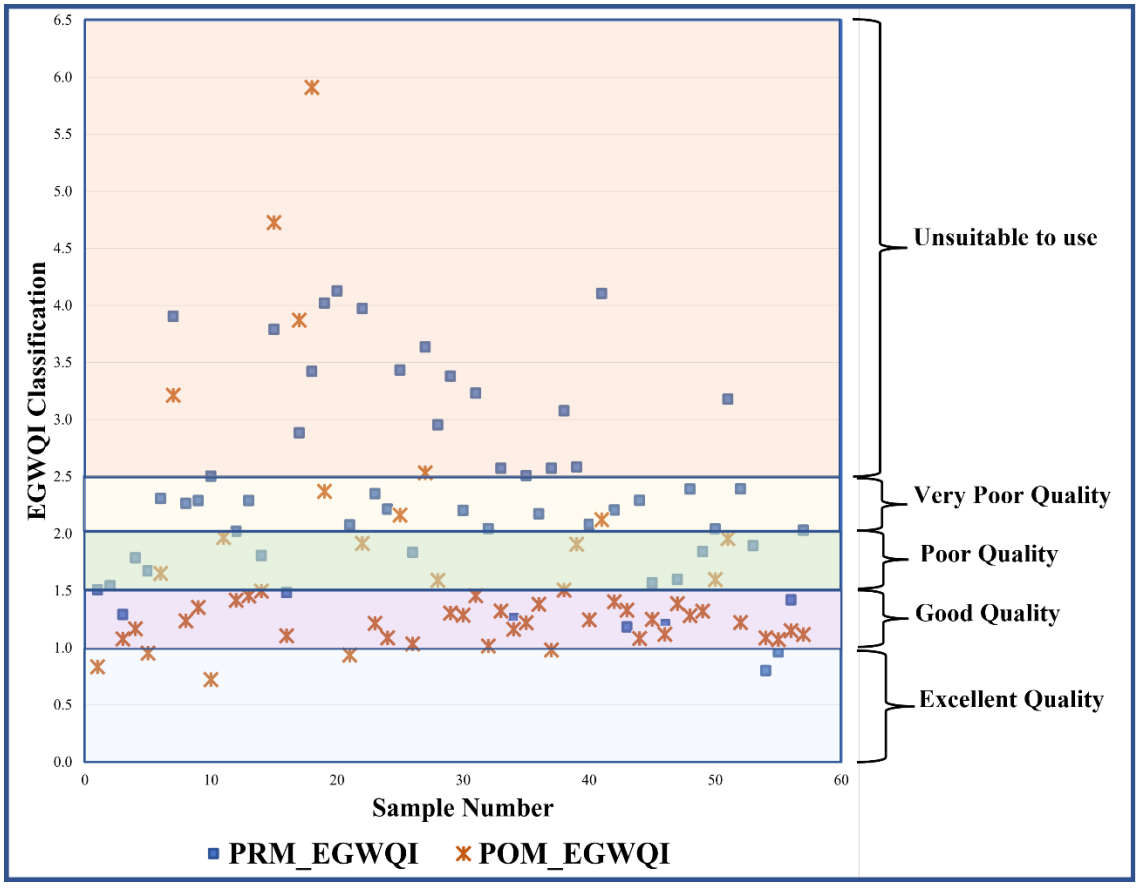

Figure 4.2 Graphical representation of EGWQI value and associated water quality class for PRM and POM seasons

EGWQI values of 35.09% of samples (20 samples) in the PRM period and 9.26% (5 samples) in the POM period are greater than 2.5, signifying the groundwater is not potable. In the PRM period, 18 samples (31.58% samples) are classified as having very poor water quality. In contrast, 11 samples (19.30%) are classified as poor quality, indicating that the study region's groundwater quality in the PRM period is inappropriate for consumption. However, Due to the groundwater recharge, the count of samples categorized as very poor quality is reduced to 3 (5.56% samples) in the POM period, while 14.81% samples (8 samples) fall under the poor-quality water for drinking. It is observed that 10.53% of samples (6 samples) in the PRM and 61.11% of samples (33 samples) in the POM period can be categorized as good-quality water. Furthermore, 3.51% of samples (2 samples) in the PRM and 9.26% of samples (5 samples) in the POM period fall under the class of excellent water quality (Table 4.3).

Table 4.3 Details of groundwater quality according to EGWQI for potability

Season	EGWQI Range	Groundwater quality class	Samples count	% Samples
PRM	EGWQI ≤ 1.0	Excellent Quality	2	3.51
	1.0 < EGWQI ≤ 1.5	Good Quality	6	10.53
	1.5 < EGWQI ≤ 2.0	Poor Quality	11	19.30
	2.0 < EGWQI ≤ 2.5	Very Poor Quality	18	31.58
	EGWQI > 2.5	Unsuitable to use	20	35.09
POM	EGWQI ≤ 1.0	Excellent Quality	5	9.26
	1.0 < EGWQI ≤ 1.5	Good Quality	33	61.11
	1.5 < EGWQI ≤ 2.0	Poor Quality	8	14.81
	2.0 < EGWQI ≤ 2.5	Very Poor Quality	3	5.56
	EGWQI > 2.5	Unsuitable to use	5	9.26

4.6 Geospatial analysis

Water quality monitoring data inherently includes temporal and spatial features, and Geographic Information Systems (GIS) serves as an exceptional platform for the visualization and analysis of such data. Due to resource constraints, it is not possible to evaluate the quality of water at every single location of the study region. Therefore, some interpolation using current data is required to create a spatial water quality map for analyzing trends (H. Li et al., 2019). Many researchers extensively used a variety of spatial interpolation methods, both geostatistical and non-geostatistical, to generate spatial water quality map (Magesh et al., 2013; Verma et al., 2020; Kumar & Augustine, 2022; Naz et al., 2024). To create a geographical map illustrating the geographic distribution of GWQI and EGWQI value at each sampling location for both PRM and POM seasons (Fig. 4.3 and Fig. 4.4), the current study used non-geostatistical interpolation technique known as "Inverse Distance Weighted (IDW)" in ArcGIS 10.4.1 software (Bhavsar & Patel, 2023). Moreover, Tables 4.4 and 4.5 denote the Summary of Spatial Interpretation of groundwater quality class according to GWQI Maps and EGWQI Maps for both PRM and POM Seasons.

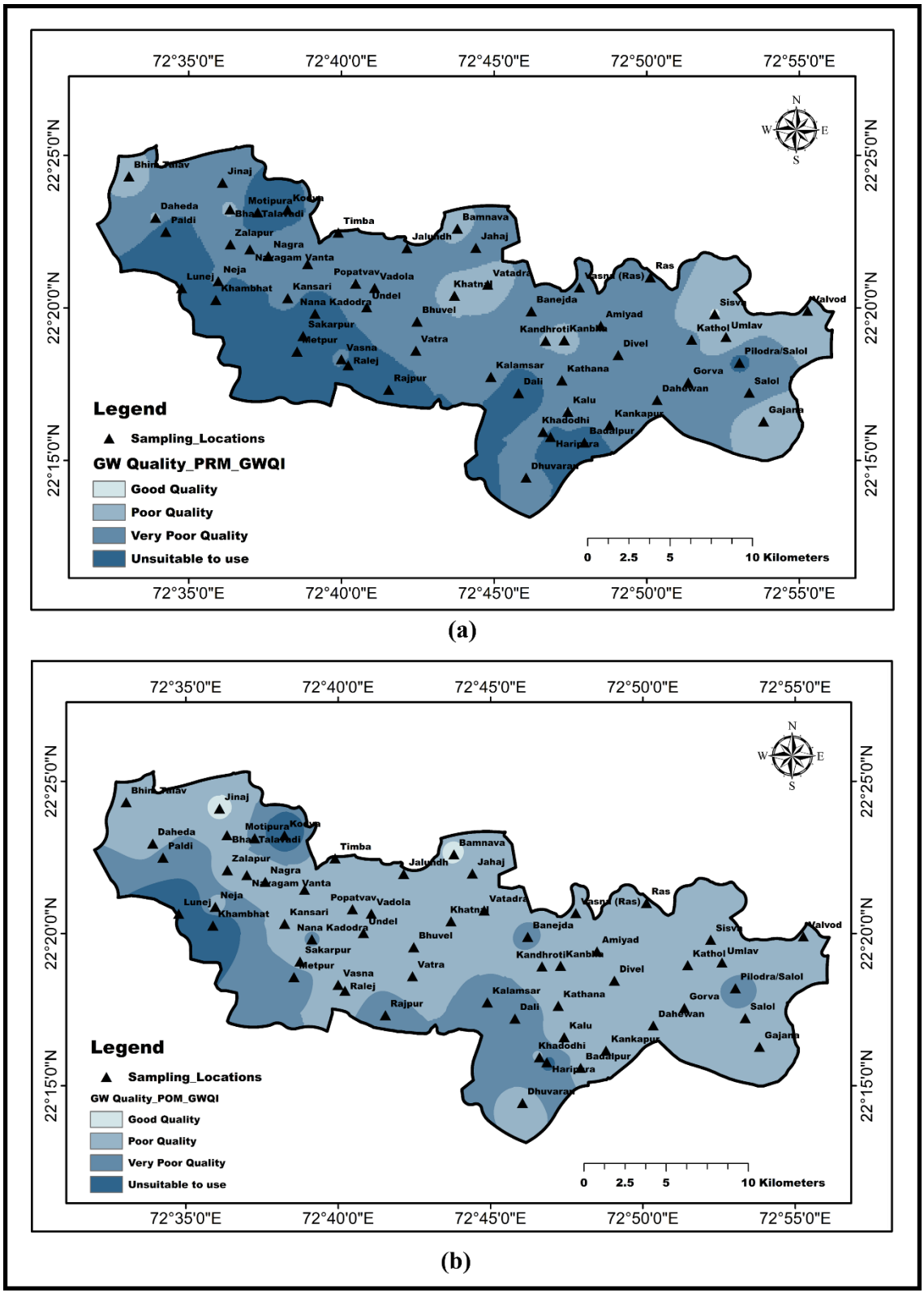

(a)

(b)

Figure 4.3 (a) Spatial Map groundwater quality class according to GWQI for the PRM season (b) Spatial Map groundwater quality class according to GWQI for the POM season

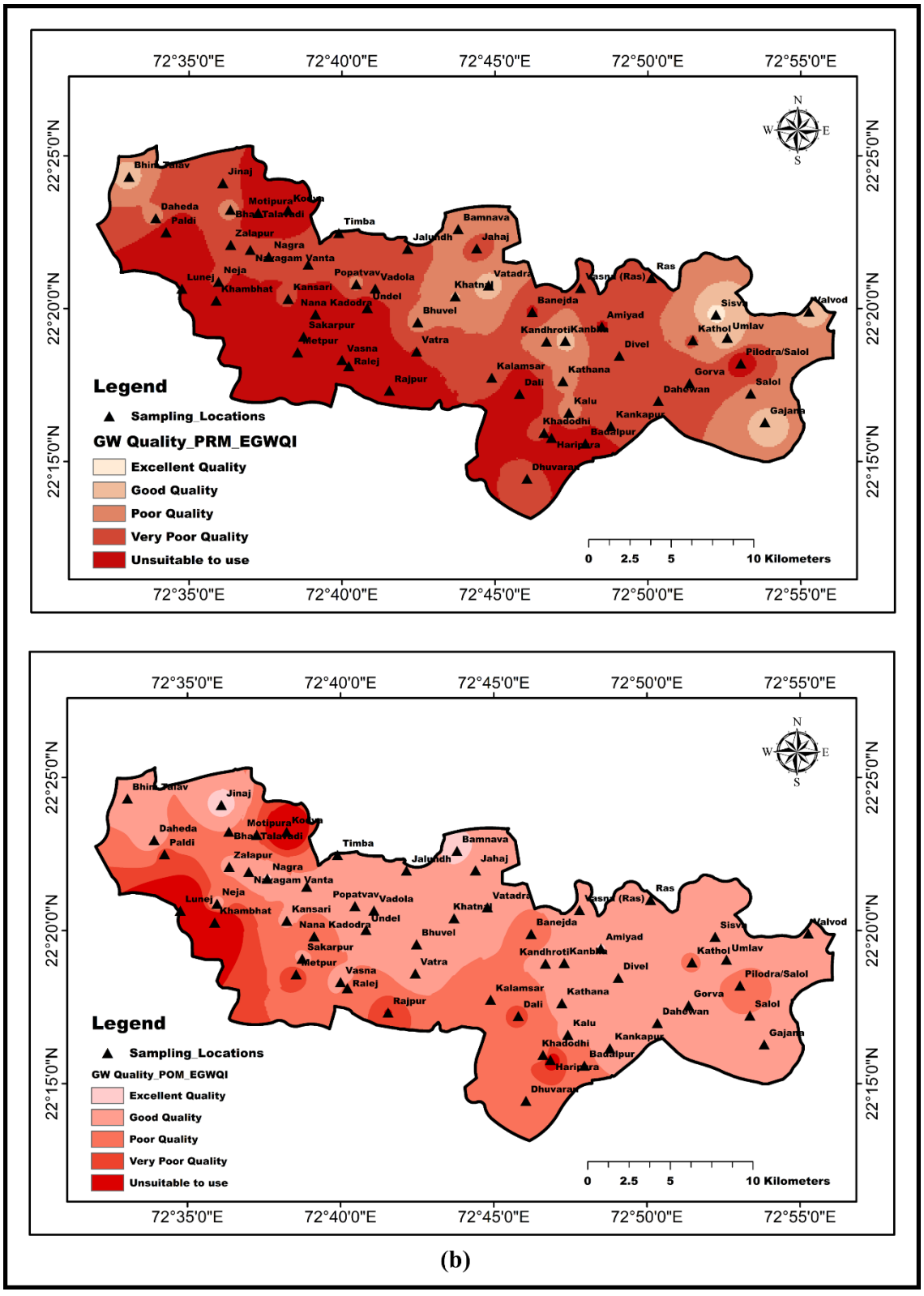

Figure 4.4 (a) Spatial Map groundwater quality class according to EGWQI for the PRM season (b) Spatial Map groundwater quality class according to EGWQI for the POM season

Table 4.4 Summary of Spatial Interpretation of Groundwater Quality Class according to GWQI Maps for both PRM and POM Seasons

Season	GWQI Range	Groundwater quality class	Area (Sq.km)	% Area
PRM	GWQI ≤ 50	Excellent Quality	0	0
	50 < GWQI ≤ 100	Good Quality	0.23	0.05
	100 < GWQI ≤ 200	Poor Quality	64.62	14.92
	200 < GWQI ≤ 300	Very Poor Quality	256.78	59.28
	GWQI > 300	Unsuitable to use	111.53	25.75
POM	GWQI ≤ 50	Excellent Quality	0	0
	50 < GWQI ≤ 100	Good Quality	2.83	0.65
	100 < GWQI ≤ 200	Poor Quality	314.55	72.62
	200 < GWQI ≤ 300	Very Poor Quality	96.79	22.35
	GWQI > 300	Unsuitable to use	18.98	4.38

Table 4.5 Summary of Spatial Interpretation of Groundwater Quality Class according to EGWQI Maps for both PRM and POM Seasons

Season	EGWQI Range	Groundwater quality class	Area (Sq.km)	% Area
PRM	EGWQI ≤ 1.0	Excellent Quality	0.90	0.21
	1.0 < EGWQI ≤ 1.5	Good Quality	19.31	4.46
	1.5 < EGWQI ≤ 2.0	Poor Quality	96.70	22.32
	2.0 < EGWQI ≤ 2.5	Very Poor Quality	176.31	40.70
	EGWQI > 2.5	Unsuitable to use	139.94	32.31
POM	EGWQI ≤ 1.0	Excellent Quality	5.24	1.21
	1.0 < EGWQI ≤ 1.5	Good Quality	248.30	57.33
	1.5 < EGWQI ≤ 2.0	Poor Quality	127.20	29.37
	2.0 < EGWQI ≤ 2.5	Very Poor Quality	30.86	7.13
	EGWQI > 2.5	Unsuitable to use	21.50	4.96

Chapter - 5

Groundwater Quality Assessment for Agriculture

5.1 General

The quality of groundwater for agriculture may fluctuate substantially based on the type and amount of dissolved salts. Groundwater contains small but significant amounts of dissolved salts. These salts derive from the erosion and disintegration of rocks and soil, encompassing the progressive dissolving of minerals like lime and gypsum. As water percolates through the soil, the salts get dissolved in it. When such water is used for irrigation, it stays in it until either the water evaporates or the crop absorbs it. (Ayers, R.S. 1994). The appropriateness of water for agriculture is influenced not only by the overall salt concentration but also by the specific kind of salt present. As the overall salt concentration rises, several soil and agricultural issues arise, necessitating the assessment of the water quality to sustain acceptable crop production (Rawat, Singh, and Gautam 2018).

Various anions and cations, such as Na, Cl, Ca, Mg, K, CO_3, HCO_3, etc., define the quality of water (Karakuş and Yıldız 2020). To measure the appropriateness of groundwater for agriculture, various agricultural indices such as SAR, %Na, RSC, RSBC, PS, KI, MH, and Mg/Ca ratio are frequently used (Gautam et al., 2016; Aravinthasamy et al., 2020; Singh et al., 2020). A primary restriction in water quality studies is the multitude of potentially measurable indicator parameters, together with the time and expense associated with data collection, processing, and interpretation. To address these difficulties, an effective water quality index based on water quality indicator parameters is necessary to be developed to facilitate the classification of the water quality for the intended use (Karakuş and Yıldız 2020). Water quality indices (WQIs) facilitate integrating extensive information produced by water monitoring programs into a singular value representing water quality (El Behairy et al. 2021). The weight assigned to individual indicator parameters defines the validity of the calculated WQI as it computes the significance of the parameter (Zhe, Xigang, and Feng 2021). The entropy technique is used widely to mitigate issues of complexity, bias, and

arbitrary weight selection, whereby weights are allocated to parameters statistically (Islam et al., 2020; Dash & Kalamdhad, 2021; C. Li et al., 2021; Rao et al., 2021).

The chapter encompasses the computation of various indices to examine the suitability of the groundwater for agriculture, along with the results. Furthermore, the irrigation groundwater quality index (EIRWQI) was determined by applying the entropy method to assign weight to individual quality parameters for the PRM and POM seasons, which is also discussed. Additionally, spatial maps representing different classes of groundwater quality suitability for agriculture depending on calculated groundwater quality indices were generated using the spatial analyst tool IDW (Inverse Distance Weighted) interpolation through ArcGIS 10.4.1 for both seasons, which are also illustrated in this chapter.

5.2 Irrigation Water Quality Indices

For assessing appropriateness of the groundwater for irrigation, a total of seven agriculture water quality indices, i.e.,1) Sodium Absorption Ration, 2) Percentage Sodium, 3) Residual Sodium Carbonate, 4) Residual Sodium Bicarbonate, 5) Potential Salinity,6) Kelly's Index and 7) Magnesium hazard was calculated for total 57 sampling location during the PRM season and 54 sampling locations during the POM seasons. Table 5.1 and Table 5.2 present the statistical details of the computed irrigation indices for two distinct seasons.

Table 5.1 Statistical details of various irrigation indices during the PRM season

Parameter	Minimum	Maximum	Median	Mean	Std. Dev
SAR	0.48	43.44	17.86	18.21	7.28
% Na	21.84	94.63	81.97	77.69	12.02
RSC	-24.05	25.73	6.94	4.15	10.96
RSBC	-2.19	18.48	7.26	7.12	4.15
PS	10.01	90.13	33.15	37.98	20.42
KI	0.18	17.56	4.54	4.59	2.89
MH	0.00	91.60	73.46	69.84	18.08

Table 5.2 Statistical details of various irrigation indices during the POM season

Parameter	Minimum	Maximum	Median	Mean	Std. Dev
SAR	1.19	61.27	10.98	12.04	9.23
% Na	31.51	97.02	75.87	72.59	14.00
RSC	-0.30	63.41	14.71	17.74	12.76
RSBC	4.16	70.69	13.59	15.98	12.97
PS	4.01	112.76	19.93	25.46	19.48
KI	0.37	32.42	3.11	3.97	4.51
MH	19.31	73.87	50.03	48.96	12.32

5.2.1 Sodium Absorption Ratio (SAR)

Groundwater with excessive amounts of sodium is inappropriate for agricultural use. Sodium-rich water interacts with the soil, reducing permeability and eventually affecting crop yield (Adagba, Kankara., and Idris 2022). SAR measures sodium concentration associated with the total concentration of Mg and Ca in the water. It is widely used to assess the appropriateness of water for agriculture (Rawat et al., 2018). The SAR for each sampling location for the two distinct seasons was calculated using an equation developed by Todd & Mays, 2005 and concentrations of all cations were taken in meq/l. The Highest value of SAR during the PRM season is 43.44, with an average of 18.21, while during the POM season, the highest value of SAR is 61.27, with a mean value of 12.04. The groundwater samples are categorized into four classes according to the calculated SAR value: SAR $\leq$ 6 (Class-I), 6 < SAR $\leq$ 12 (Class-II), 12 < SAR $\leq$ 20 (Class-III), and SAR > 20 (Class-IV) (Spandana, Suresh, and Prathima n.d.). Furthermore, analytical data represent that 85.96% of samples (49 samples) have measured values of SAR more than 12 (Class-III & IV), which covers 96.86% of the research region during the PRM season (Table 5.3), while during the POM season, 44.44% samples (24 samples) have measured value of SAR more than 12 (Class-III & IV), encompasses 46.98% of the study area (Fig. 5.1).

$$SAR = \frac{Na^+}{\sqrt{(Ca^+ + Mg^+)/2}} \quad \text{.....(Eq. 1)}$$

5.2.2 Percentage Sodium (%Na)

The %Na indicates the ratio of sodium to the total amount of cations in the water, often expressed as a percentage. (Richard 1954). It is a frequently used indicator for assessing the appropriateness of agriculture. Excessive amounts of sodium in the water

may lead to absorption by clay particles, resulting in the displacement of magnesium and calcium ions, diminished soil permeability, and impaired internal drainage (Barik and Pattanayak, 2019; Kumari and Rai, 2020). %Na was calculated employing the equation given by (Wilcox, 1955). The amount of all anions is in meq/l.

$$\%Na = \frac{[Na^{+}+K^{+}]}{[Ca^{+}+Mg^{+}+Na^{+}+K^{+}]}\ X\ 100 \quad \text{.....(Eq.2)}$$

Table 5.3 Summary of Spatial Interpretation of SAR Maps for both PRM and POM Seasons

Season	SAR Range	Count of samples	% Samples	Area (Sq.km)	Area (%)
PRM	SAR ≤ 6	3	5.26	0.87	0.20
	6 < SAR ≤ 12	5	8.77	12.72	2.94
	12 < SAR ≤ 20	30	52.63	303.48	70.06
	SAR > 20	19	33.33	116.08	26.80
POM	SAR ≤ 6	12	22.22	20.99	4.85
	6 < SAR ≤ 12	18	33.33	208.67	48.17
	12 < SAR ≤ 20	18	33.33	178.17	41.13
	SAR > 20	6	11.11	25.33	5.85

Table 5.4 Summary of Spatial Interpretation of %Na Maps for both PRM and POM Seasons

Season	%Na Range	Count of samples	% Samples	Area (Sq.km)	Area (%)
PRM	%Na ≤ 40	1	1.75	0.55	0.13
	40 < %Na ≤ 60	2	3.51	5.5	1.27
	60 < %Na ≤ 80	20	35.09	254.79	58.82
	%Na > 80	34	59.65	172.32	39.78
POM	%Na ≤ 40	1	1.85	1.65	0.38
	40 < %Na ≤ 60	9	16.67	32.11	7.41
	60 < %Na ≤ 80	24	44.44	352.69	81.42
	%Na > 80	20	37.04	46.71	10.78

Groundwater %Na values during the PRM season vary from 21.84 to 94.63 (mean 77.69), but during the POM season, they range from 31.51 to 97.02 (mean 72.59). The collected groundwater samples are classified into four suitability classes: (Class- I) %Na ≤ 40, (Class- II) 40 < %Na ≤ 60, (Class- III) 60 < %Na ≤ 80, and (Class- IV) %Na > 80

for both seasons (Adimalla, Li, and Venkatayogi 2018). Furthermore, (Fig. 5.2) illustrates spatial maps showing the spatial distribution of %Na value in the study region for both seasons. Most collected samples during both seasons had %Na values greater than 60 (class III and class IV). According to the analysis, a total of 54 samples (94.74% samples) have %Na values greater than 60 (Class-III & Class-IV) during the PRM season, and during the POM season, a total of 44 samples (81.48% samples) fall under Classes III and IV. Moreover, spatial interpretation of the maps of %Na shows that 98.60% and 92.21% of the study region are classified as Classes III and IV during the PRM and POM periods, respectively (Fig. 5.2).

5.2.3 Residual Sodium Carbonate (RSC)

Residual Sodium Carbonate is one of the indices applied to assess the potential threat of sodium deposits in soils irrigated with water containing high concentrations of bicarbonate and carbonate ions. Excessive RSC values suggest that water may exacerbate soil sodicity since carbonate ions precipitate Ca and Mg, resulting in sodium being the predominant cation (Edet, 2017). RSC was calculated for all sampling locations of the research region for both PRM and POM seasons using the formula given by (Eaton, 1950). Usually, RSC is measured in milliequivalent/liter. So, the amount of all parameters is taken in meq/l in Eq.3.

$$RSC = [CO_3^{2-} + HCO_3^{2-}] - [Ca^{2+} + Mg^{2+}] \quad \text{.....(Eq.3)}$$

Table 5.5 Summary of Spatial Interpretation of RSC Maps for both PRM and POM Seasons

Season	RSC Range	Count of samples	% Samples	Area (Sq.km)	Area (%)
PRM	RSC ≤ 1.25	17	29.82	122.82	28.36
	1.25 < RSC ≤ 2.5	1	1.75	17.42	4.02
	RSC > 2.5	39	68.42	292.92	67.62
POM	RSC ≤ 1.25	1	1.85	0.05	0.01
	1.25 < RSC ≤ 2.5	0	0.00	0.43	0.10
	RSC > 2.5	53	98.15	432.68	99.89

The minimum RSC in the groundwater samples acquired in the PRM is -24.05 meq/l; in the POM season, it is -0.30 meq/l. The maximum value of RSC during the PRM and POM season is 25.73 meq/l and 63.41 meq/l, respectively. The collected groundwater

samples are classified into three suitability categories: (Class- I) RSC ≤ 1.25, (Class- II) 1.25 < RSC ≤ 2.5, and (Class- III) RSC > 2.5 for both seasons (Rawat et al. 2018). A total of 39 samples (68.42% samples) and 53 samples (98.15% samples) fall in the Class-III category during the PRM season and POM season, respectively (Table 5.5) and spatial interpretation of the RSC map (Fig. 5.3) shows that 67.62% of the study region fall in Class-III category during the PRM season whereas, during the POM season, the Class-III study area is increased to 99.89%, which indicates increase value of RSC in the POM season than the PRM season.

5.2.4 Residual Sodium Bicarbonate (RSBC)

Residual Sodium Bicarbonate is another index that determines groundwater suitability for agriculture. It evaluates the impact of bicarbonate ions in irrigation water on soil health. (Salil Kumar Gupta, Suresh Kumar Gupta 1987) had developed an equation to calculate RSBC. RSBC is calculated for each sampling location in meq/l. In the PRM period, the average RSBC value of the acquired samples is 7.12 meq/l, but in the POM period, it is 15.98 meq/l. During the PRM season, the maximum value is 18.48 meq/l, whereas during the POM season, it is 70.69 meq/l.

$$RSBC = [HCO_3^- + Ca^{2+}] \quad \text{.....(Eq.4)}$$

Table 5.6 Summary of Spatial Interpretation of RSBC Maps for both PRM and POM Seasons

Season	RSBC Range	Count of samples	% Samples	Area (Sq.km)	Area (%)
PRM	RSBC ≤ 5	15	26.32	81.08	18.71
	5 < RSBC ≤ 10	31	54.39	309.39	71.43
	RSBC > 10	11	19.30	42.69	9.86
POM	RSBC ≤ 5	2	3.70	0.3	0.07
	5 < RSBC ≤ 10	14	25.93	34.02	7.85
	RSBC > 10	38	70.37	398.84	92.08

The collected groundwater samples are divided into three categories (Adagba et al. 2022): (Class- I) RSBC ≤ 5; 26.32% in the PRM and 3.70% samples in the POM fall under Class-I, (Class- II) 5 < RSBC ≤ 10; 54.39% in the PRM and 25.93% samples in the POM fall under Class-II and (Class- III) RSBC > 10.0; 19.30% in the PRM and 70.37% samples in the POM fall under Class-III (Table 5.6). Spatial interpretation of

RSBC maps denotes that 9.86% of the study area falls within Class-III in the PRM season. In comparison, the Class-III category covers 92.08% of the study area during the POM season (Fig. 5.4).

5.2.5 Potential Salinity (PS)

Potential Salinity is an index widely used to assess the long-term salinity risk of irrigation water, considering the salts that may build up in the soil post-irrigation. The calculation is based on the chloride and sulfate concentrations, emphasizing salts that persist in the soil while the water evaporates or is absorbed by plants. Excessive PS values indicate an increased risk of soil salinization over time. For the study region, the PS value is calculated using the equation given by (Doneen, 1964). During the PRM season, the PS value of the groundwater samples ranges between 10.01 and 90.13 meq/l, while the value ranges between 4.01 and 112.76 meq/l in the POM season. The groundwater samples are grouped into two classes: (Class- I) PS ≤ 10 and (Class- II) PS > 10 for both seasons (Subbarao et al., 2018). The PS value falls within the Class-II category, with 100% samples in the PRM and 94.44% in the POM period (Table 5.7). Furthermore, the interpretation of the spatial map of potassium shows that the Class-II category encompasses most areas of the study region, 100% and 99.31 % of the research area in the PRM and POM seasons, respectively (Fig. 5.5).

$$PS = [Cl^- + \frac{1}{2}SO_4^{2-}] \quad \text{.....(Eq.5)}$$

Table 5.7 Summary of Spatial Interpretation of PS Maps for both PRM and POM Seasons

Season	PS Range	Count of samples	% Samples	Area (Sq.km)	Area (%)
PRM	PS ≤ 10	0	0.00	0	0
	PS > 10	57	100.00	433.16	100
POM	PS ≤ 10	3	5.56	2.99	0.69
	PS > 10	51	94.44	430.17	99.31

5.2.6 Kelley's Index (KI)

Kelley's Index refers to the ratio of sodium ions to the aggregate concentration of calcium and magnesium in the groundwater. Kelly's ratio greater than one signifies high sodium in the water (Kelley, 1941). Using such water for agriculture leads to the deposition of salt in the soil, which may influence soil permeability and structure

(Adagba et al., 2022). Consequently, water with Kelly's ratio below one is appropriate for agriculture (Barik and Pattanayak, 2019). Kelley's index was calculated by employing the formula given by (Kelley, 1941) for all sampling locations for both seasons. The amount of all parameters was taken in meq/l. With a mean of 4.59, the greatest KI value during the PRM season is 17.56, while during the POM season, it is 32.42, with a mean of 3.97.

$$KI = \frac{Na^{+}}{Ca^{2+} + Mg^{2+}} \quad \text{.....(Eq. 6)}$$

On the basis of KI Value, groundwater samples are divided into two classes: Class- I) KI ≤ 1 and (Class- II) KI > 1 for both seasons. Furthermore, analytical data represent that 98.25% of samples (56 samples) have measured values of KI more than 1 (Class-II), which covers 99.92% of the research region during the PRM season (Table 5.8), while during the POM season, 90.74% samples (49 samples) have measured value of KI more than 1 (Class-II), encompasses 99.56% of the study area (Fig. 5.6).

Table 5.8 Summary of Spatial Interpretation of KI Maps for both PRM and POM Seasons

Season	KI Range	Count of samples	% Samples	Area (Sq.km)	Area (%)
PRM	KI ≤ 1	1	1.75	0.34	0.08
	KI > 1	56	98.25	432.82	99.92
POM	KI ≤ 1	5	9.26	1.89	0.44
	KI > 1	49	90.74	431.27	99.56

5.2.7 Magnesium Hazard (MH)

Excessive magnesium concentrations in soil are anticipated to cause alkalisation of soil, which adversely impacts crop output (Barik and Pattanayak 2019). The Magnesium hazard value is suggested for assessing irrigation water, and it is computed as a percentage using the equation given by (Paliwal, 1972), with all ion concentrations represented in meq/l. MH value is computed for all PRM and POM periods sampling locations. The MH values in acquired samples in the PRM period vary from 0.0 to 91.60, with a mean of 69.84, whereas in the POM period, the values range from 19.31 to 73.87, with a mean of 48.96. The groundwater samples are divided into two classes (Beyene, Aberra, and Fufa 2019): (Class- I) MH ≤ 50%; 10.53% and 48.15% samples fall within Class-I in PRM season and POM season, respectively, and (Class- II) MH > 50%;

89.47% samples in the PRM and 51.85% samples in the POM fall within Class-II (Table 5.9). Spatial interpretation of the MH map (Fig. 5.7) shows that 94.99% of the study area is encompassed by Class-II in the PRM period, whereas, in the POM period, the Class-II study area decreased to 42.47%, indicating a decline in the amount of magnesium during the POM season as compared to PRM season.

$$MH = \frac{Mg^{2+}}{Ca^{2+} + Mg^{2+}} X\ 100 \quad \text{.....(Eq.7)}$$

Table 5.9 Summary of Spatial Interpretation of MH Maps for both PRM and POM Seasons

Season	MH Range	Count of samples	% Samples	Area (Sq.km)	Area (%)
PRM	MH ≤ 50	6	10.53	21.70	5.01
	MH > 50	51	89.47	411.46	94.99
POM	MH ≤ 50	26	48.15	249.21	57.53
	MH > 50	28	51.85	183.95	42.47

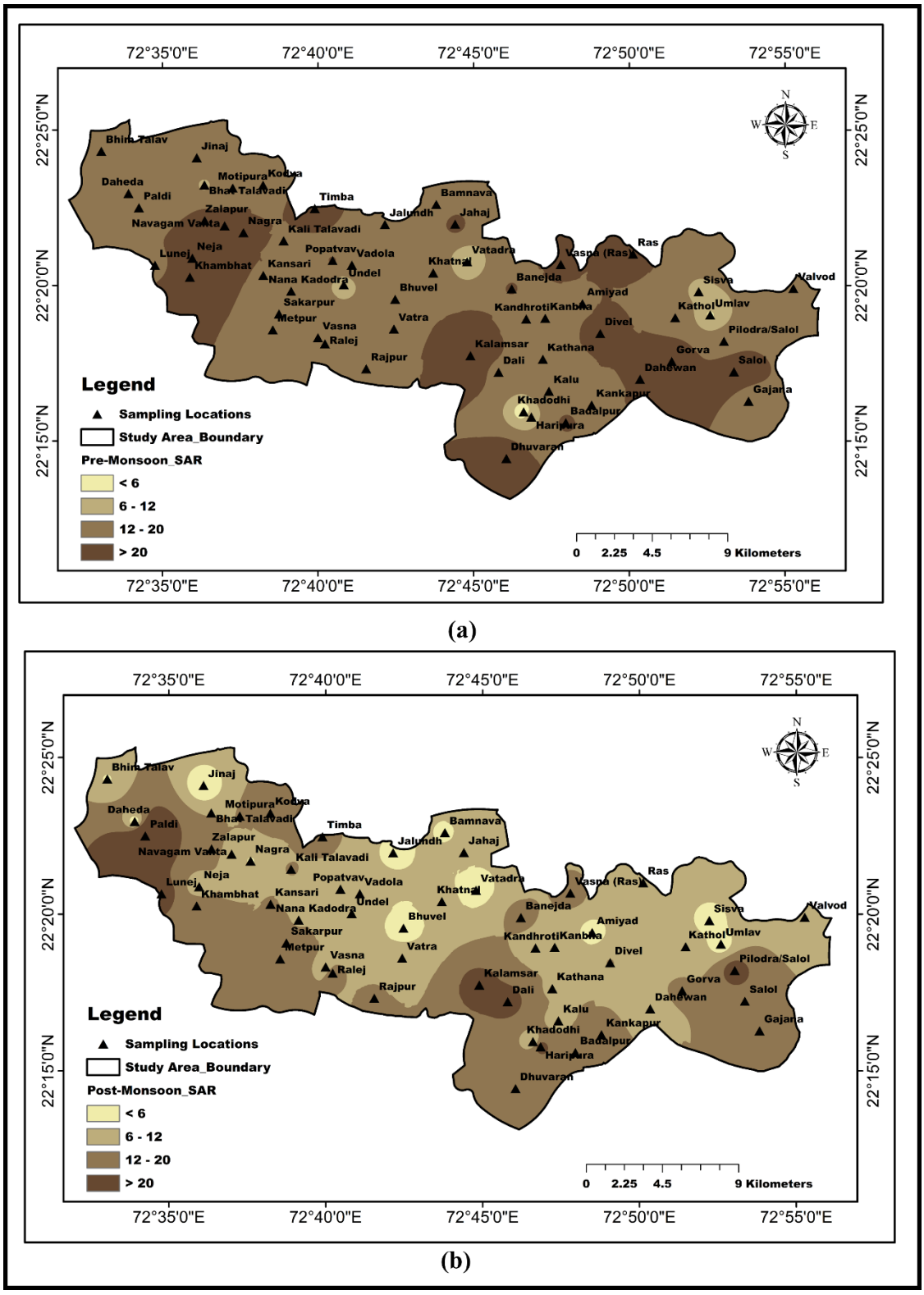

Figure 5.1 (a) Spatial Map of SAR for the PRM Season (b) Spatial Map of SAR for the POM Season

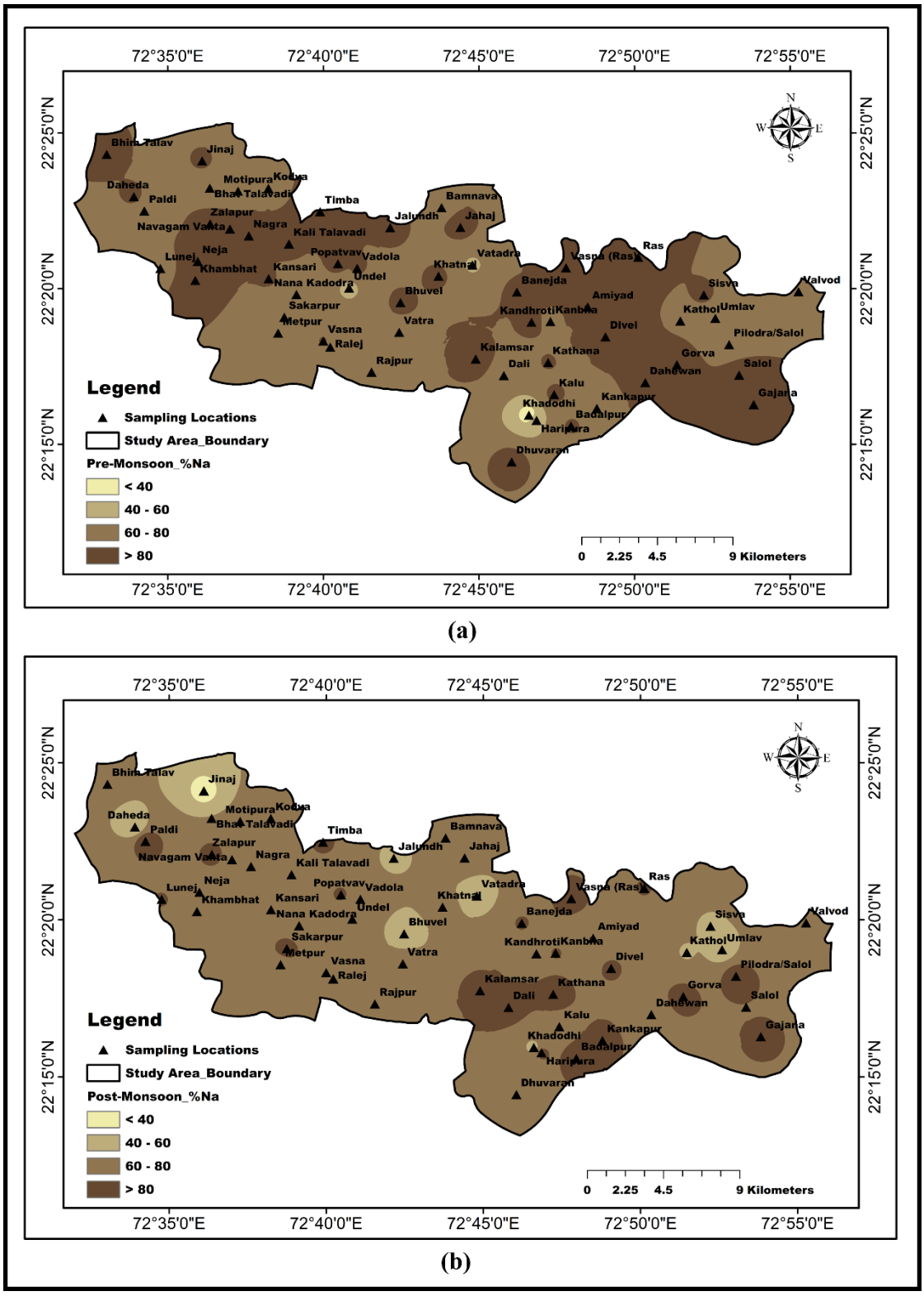

Figure 5.2 (a) Spatial Map of %Na for the PRM Season (b) Spatial Map of %Na for the POM Season

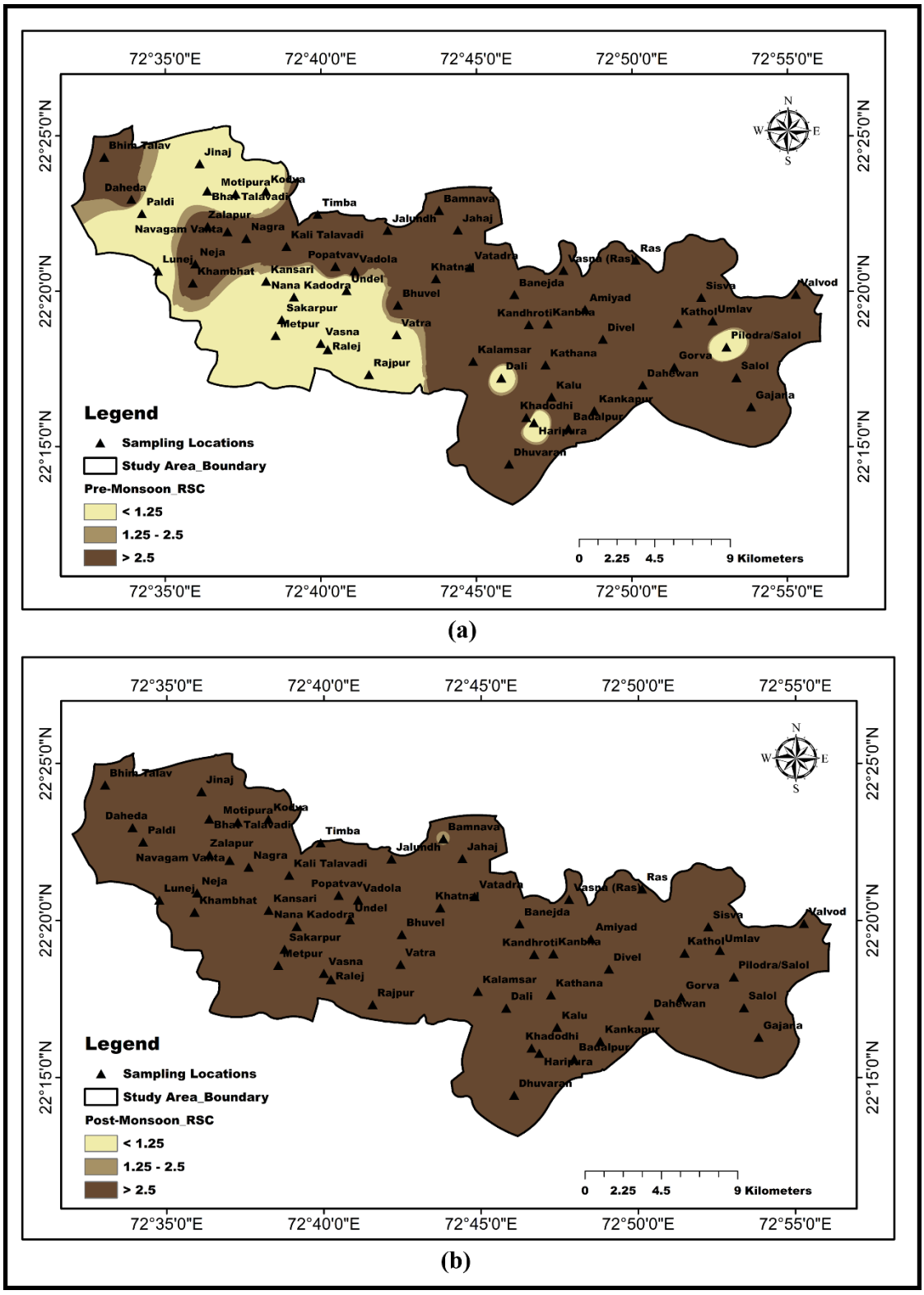

Figure 5.3 (a) Spatial Map of RSC for the PRM Season (b) Spatial Map of RSC for the POM Season

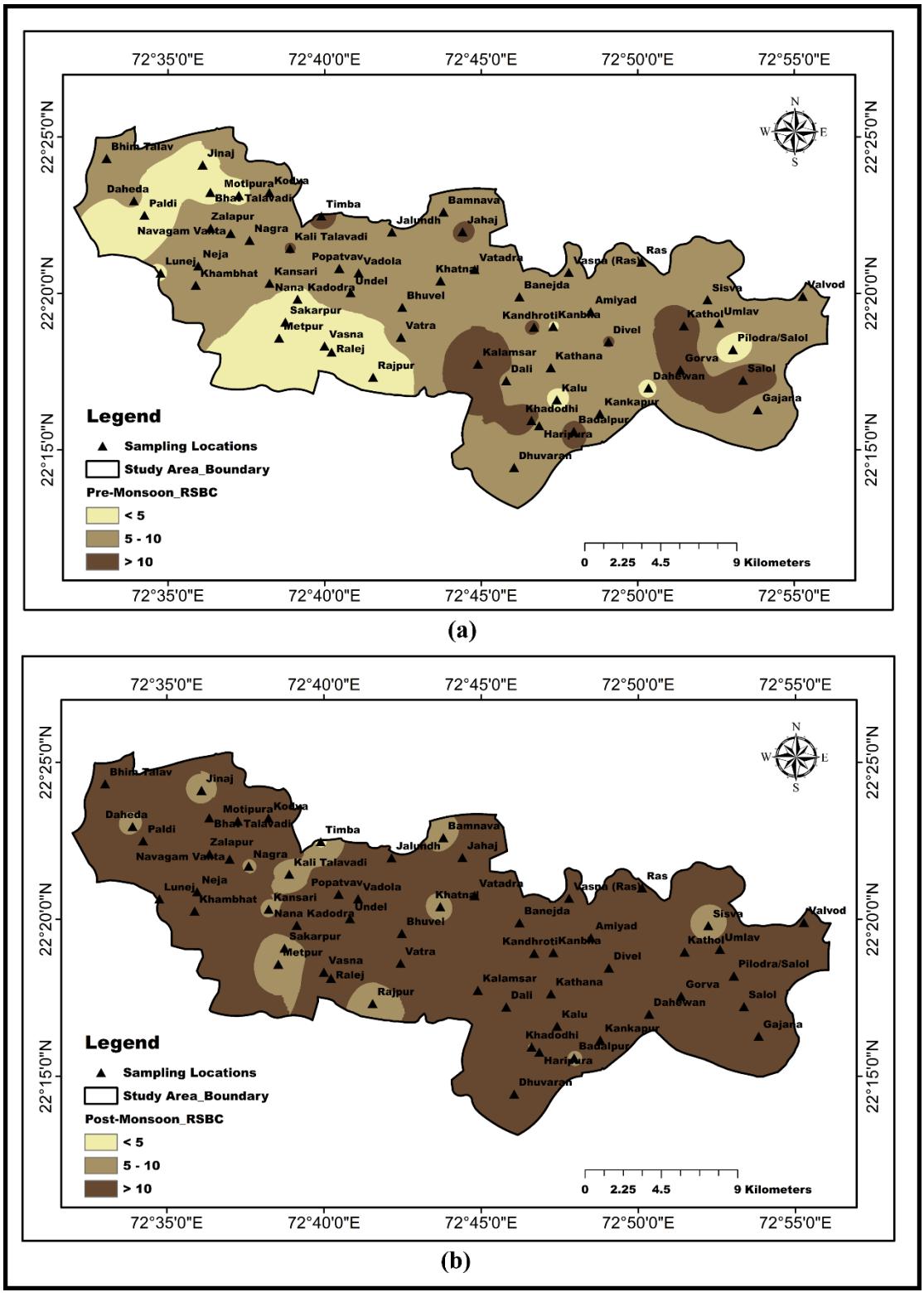

Figure 5.4 (a) Spatial Map of RSBC for the PRM Season (b) Spatial Map of RSBC for the POM Season

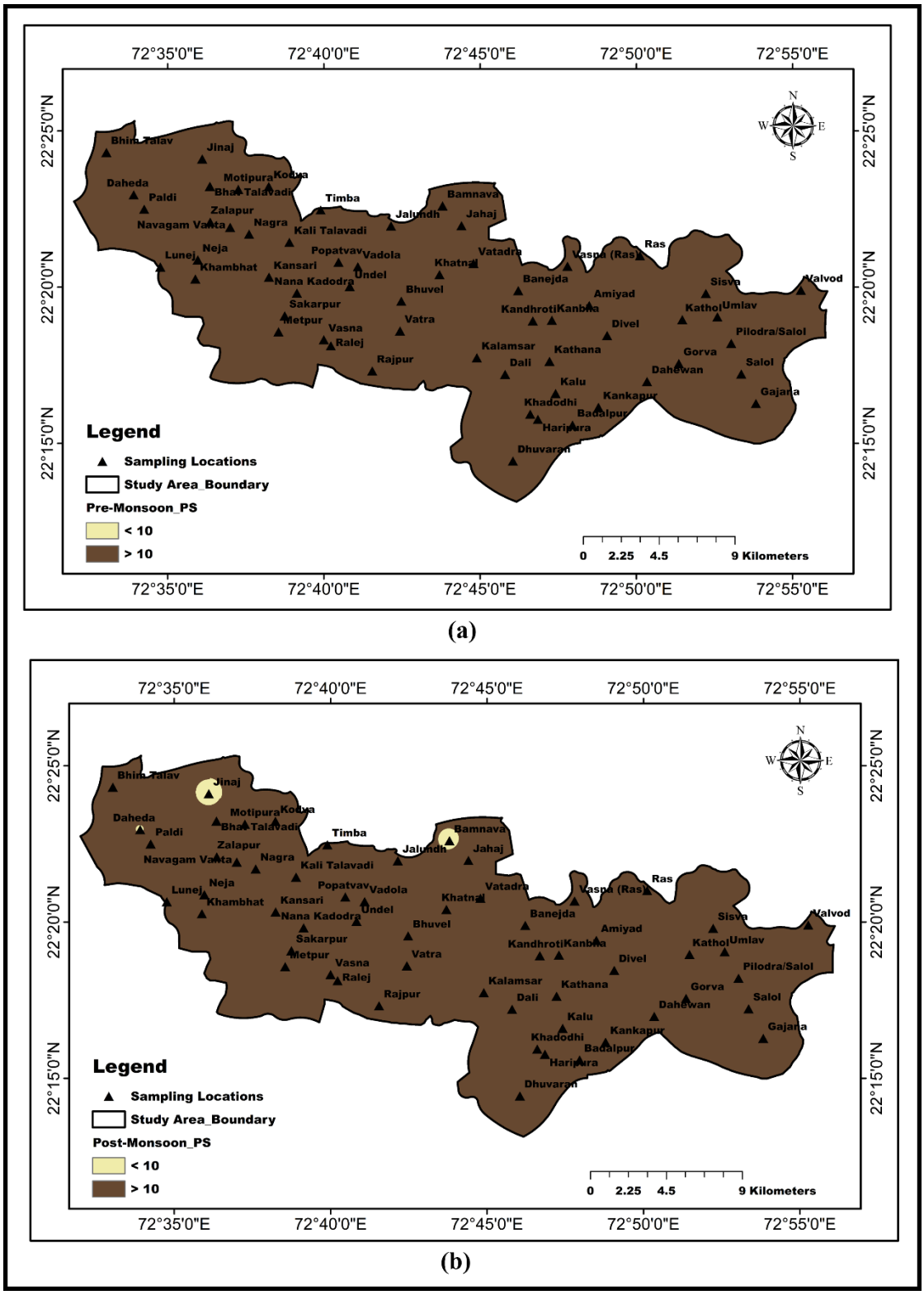

Figure 5.5 (a) Spatial Map of PS for the PRM Season (b) Spatial Map of PS for the POM Season

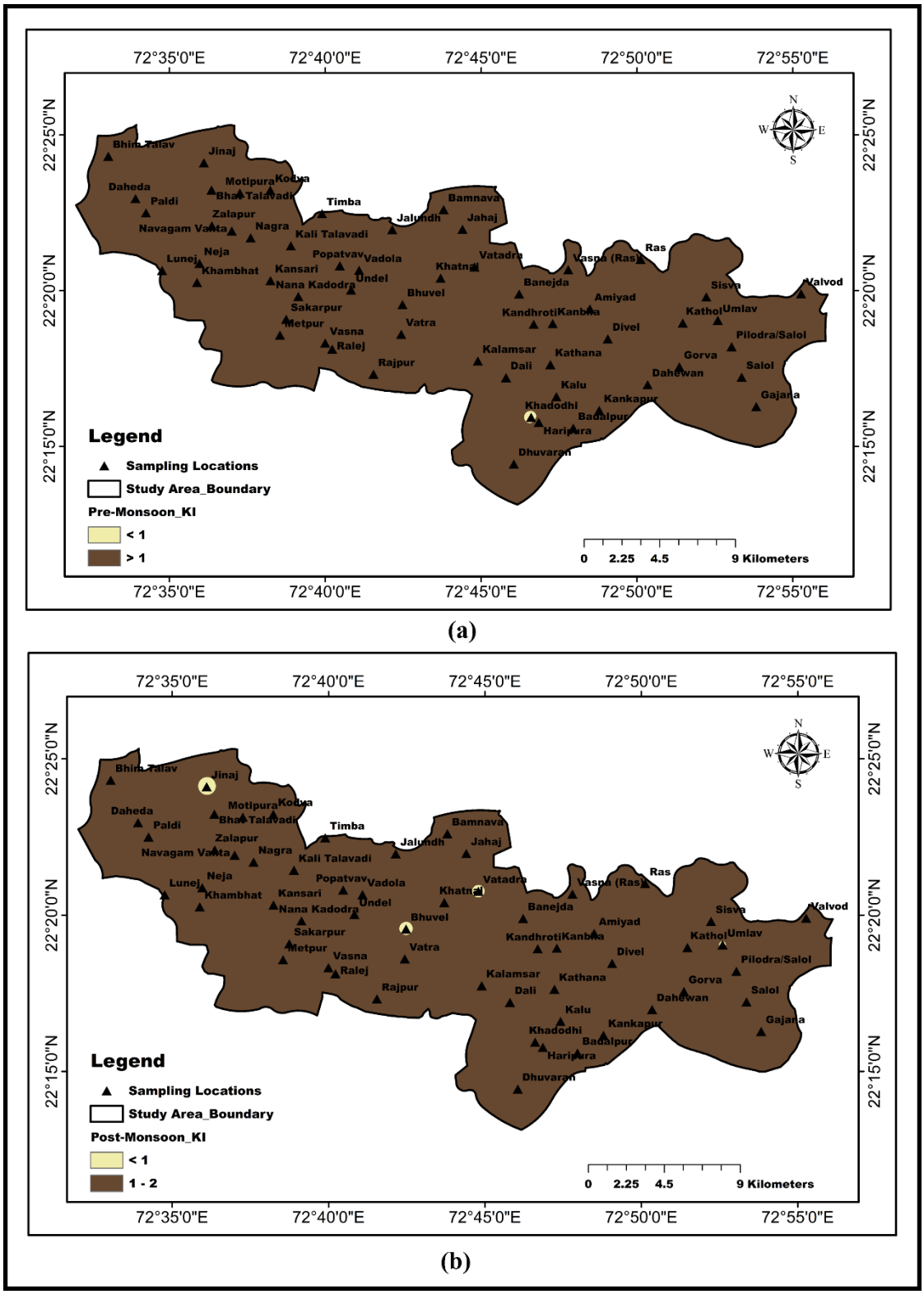

Figure 5.6 (a) Spatial Map of KI for the PRM Season (b) Spatial Map of KI for the POM Season

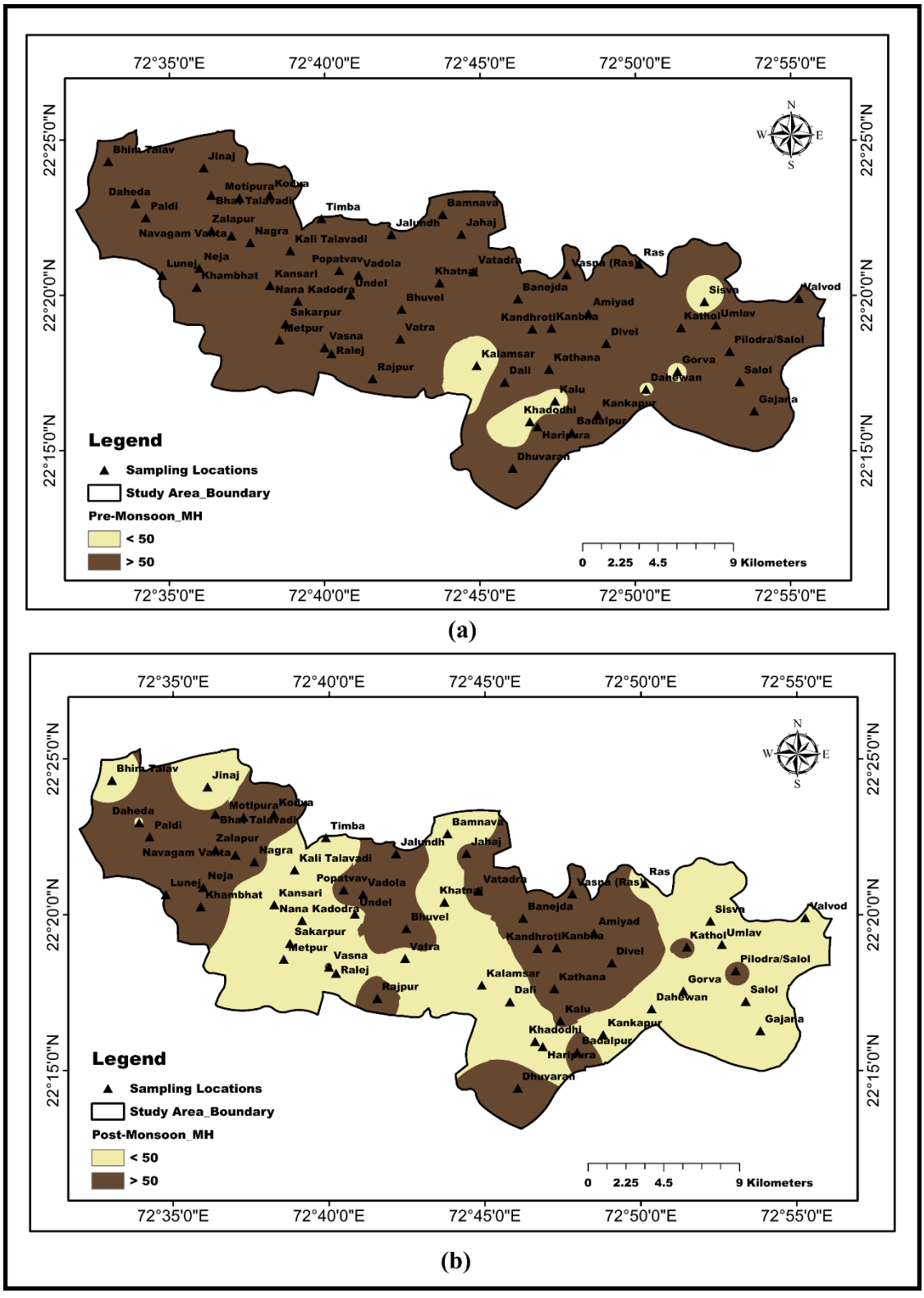

Figure 5.7 (a) Spatial Map of MH for the PRM Season (b) Spatial Map of MH for the POM Season

5.3 Entropy Weighted Irrigation Groundwater Quality Index (EIRWQI) calculation

For the current study region, the groundwater quality index for agriculture is calculated for each sampling location by employing objective methods for allocating weight to each quality parameter. To mitigate the impact of subjective decision-maker understanding in evaluating groundwater suitability for irrigation, the Entropy approach is adopted to assign weight to parameters for computing the Entropy Weighted Irrigation Water Quality Index (EIRWQI).

The calculation involves the following six steps, which were discussed in the previous chapter:

(1) A total of nine irrigation water quality parameters were selected to generate the index: Electrical Conductivity, sodium, chloride, bicarbonate, Sodium Absorption Ratio, Percentage Sodium, Potential Salinity, Kelley's Index, and Magnesium Hazard

(2) Generate a matrix of agricultural water quality:

$$P=\begin{bmatrix} p_{11} & p_{12} & \cdots & p_{1y} \\ p_{21} & p_{22} & \cdots & p_{2y} \\ \vdots & \vdots & \ddots & \vdots \\ p_{x1} & p_{x2} & \cdots & p_{xy} \end{bmatrix}$$

where, x (i=1,2,3,…,x) is the number of groundwater samples; y (j=1,2,3,…,y) is the number of indicator parameters of each groundwater sample.

(3) Employing a method known as "generating quotient after range pretreatment", compute standardized values (R_{ij}), in which standardized values are computed by first determining Q_{ij} (Eq. 5) and then determining R_{ij} (Eq. 6) and generating a standardized matrix (Subba Rao et al. 2020) :

$$(a)\ Q_{ij} = \frac{(P_{ij})_{highest} - (P_{ij})}{(P_{ij})_{highest} - (P_{ij})_{least}} \qquad \text{……...….(Eq.5)}$$

where,$(P_{ij})_{least}$ and $(P_{ij})_{highest}$ is the lowest and greatest values of individual parameters in the samples, respectively.

$$Q=\begin{bmatrix} q_{11} & q_{12} & \cdots & q_{1y} \\ q_{21} & q_{22} & \cdots & q_{2y} \\ \vdots & \vdots & \ddots & \vdots \\ q_{x1} & q_{x2} & \cdots & q_{xy} \end{bmatrix}$$

where, Q is a standardized matrix.

(b) $R_{ij} = \frac{Q_{ij}}{\sum_{i=1}^{m} Q_{ij}}$ ……(Eq.6)

$$R = \begin{bmatrix} r_{11} & r_{12} & \dots & r_{1y} \\ r_{21} & r_{22} & \dots & r_{2y} \\ \vdots & \vdots & \ddots & \vdots \\ r_{x1} & r_{x2} & \dots & r_{xy} \end{bmatrix}$$

where, R is the final standardized matrix.

(4) Compute the entropy (E_j) of each parameter by applying (Eq. 7) and then the entropy weight (W_j) of each parameter by using (Eq. 8) (Bao et al., 2020):

$E_j = \frac{1}{\ln(m)} \sum_{i=1}^{m} R_{ij} * \ln(R_{ij})$ (When $R_{ij} = 0$, $R_{ij} * \ln(R_{ij})$ is defined to be 0)..…….(Eq.7)

$W_j = \frac{(1-E_j)}{\sum_{j=1}^{m} (1-E_j)}$ ……..(Eq.8)

(5) Estimate the quality scoring (Q_j) of each parameter (Adimalla 2021)

$Q_j = \frac{C_j}{Bj} X\ 100$ ……(Eq.9)

$Q_{pH} = \frac{C_{pH} - 7}{8.5 - 7} \text{ x } 100 \quad C_{pH} > 7$

$Q_{pH} = \frac{7 - C_{pH}}{8.5 - 7} \text{ x } 100 \quad C_{pH} < 7$

where, C_j specifies the amount of parameter j in mg/l, Bj specifies the irrigation water quality standard of j^{th} parameter.

(6) Calculate the entropy-weighted irrigation water quality index (EIRWQI) by first determining the sub-index of each parameter ($SIRWQI_i$) by taking the product of entropy weight to its quality scoring. The final EIRWQI for each sample is calculated by adding all SIRWQI values of all parameters at that location (Li et al., 2021). The following equations are applied:

$SIRWQI_j = Q_j * W_j$ ……(Eq.10)

$EIRWQI = \sum_{j=1}^{m} SIRWQI$ ……..…(Eq.11)

Ultimately, the irrigation water quality of each sampling location is classified into five categories according to the calculated value of EIRWQI at that location: Excellent quality: EIRWQI ≤ 50, Good quality: 50 < EIRWQI ≤100, Poor quality: 100 < EIRWQI

≤ 200, Very poor quality: 200 < EIRWQI ≤ 300 and Unsuitable to use: EIRWQI > 300 (Abbasnia et al., 2018).

5.4 Groundwater suitability analysis based on calculated EIRWQI

The EIRWQI values and corresponding groundwater quality class for agriculture are calculated for 57 groundwater sampling locations in the PRM and 54 groundwater sampling locations in the POM seasons and are graphically represented in Fig. 5.8. The average of EIRWQI in the PRM season is 213.70, while in the POM season is 173.08. In the PRM season, the lowest and highest calculated values of EIRWQI are 115.16 and 369.46, respectively; on the other hand, in the POM season, the lowest and highest values are 51.05 and 525.65, respectively.

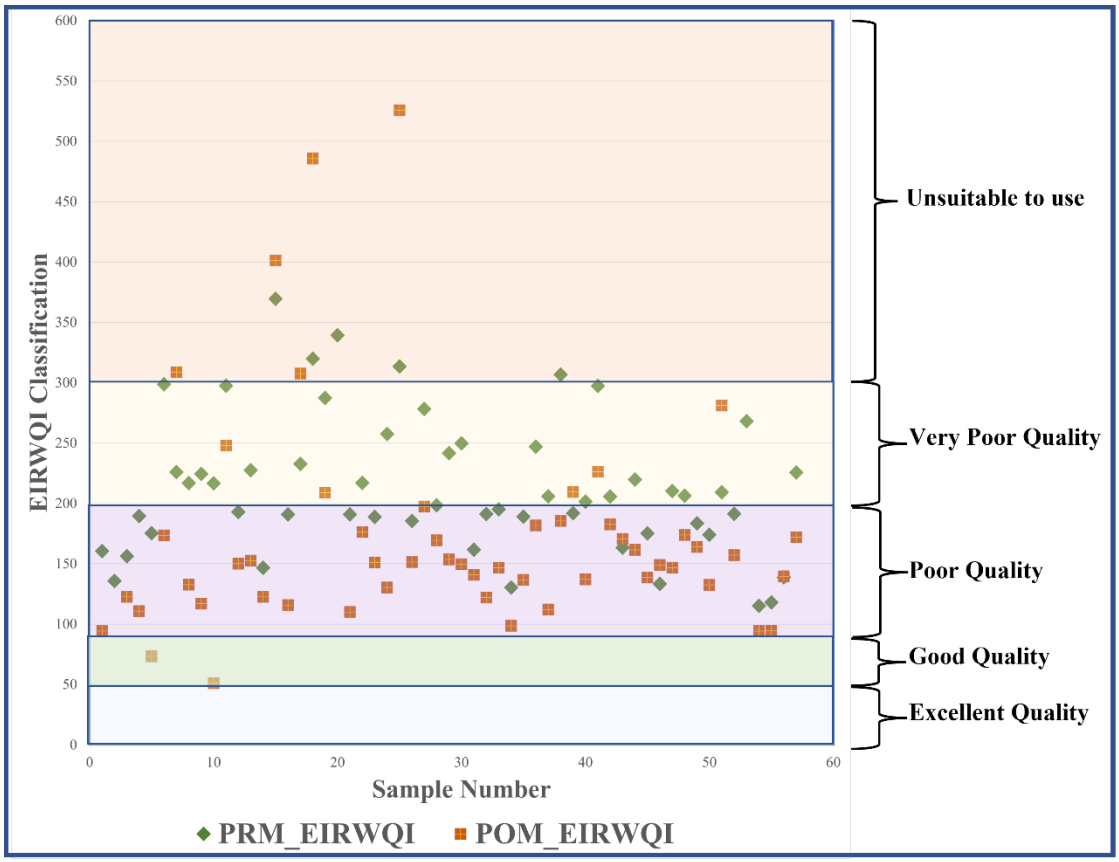

Figure 5.8 Graphical representation of EIRWQI value and associated irrigation water quality class for PRM and POM seasons

EIRWQI values of 8.77% of samples (5 samples) in the PRM and 9.26% of samples (5 samples) in the POM period are greater than 300, signifying that the groundwater is inappropriate for irrigation. In the PRM season, 25 samples (43.86%) are classified as very poor water quality, while 27 samples (47.37%) are considered poor water quality, representing that the groundwater quality in the region during this period is unsuitable

for agricultural use. However, Due to the recharge of the groundwater, the count of samples that are categorized as very poor quality is reduced to 5 (9.26% samples) during the POM season, while 70.37% samples (38 samples) fall into the class of poor-quality water for irrigation. It is observed that no sample during the PRM season falls under the category of good quality water for irrigation, while six samples (11.11% samples) during the POM season fall under good quality water. Furthermore, not even a single sample belongs to the "Excellent water quality" class for both seasons (Table 5.10).

Moreover, to create a spatial map illustrating the geographic distribution of EIRWQI value at each sampling location for both PRM and POM seasons (Fig. 5.9), the "Inverse Distance Weighted (IDW)" spatial analyst function, which is founded on a non-geostatistical spatial interpolation technique, was utilized within ArcGIS 10.4.1. The Summary of Spatial Interpretation of groundwater quality class according to EIRWQI Maps for both PRM and POM Seasons are recorded in Table 5.11.

Table 5.10 Summary of groundwater quality class for agriculture according to EIRWQI for both PRM and POM seasons

Season	EIRWQI Range	Groundwater quality class	Count of samples	% Samples
PRM	EIRWQI ≤ 50	Excellent Quality	0	0.00
	50 < EIRWQI ≤ 100	Good Quality	0	0.00
	100 < EIRWQI ≤ 200	Poor Quality	27	47.37
	200 < EIRWQI ≤ 300	Very Poor Quality	25	43.86
	EIRWQI > 300	Unsuitable to use	5	8.77
POM	EIRWQI ≤ 50	Excellent Quality	0	0.00
	50 < EIRWQI ≤ 100	Good Quality	6	11.11
	100 < EIRWQI ≤ 200	Poor Quality	38	70.37
	200 < EIRWQI ≤ 300	Very Poor Quality	5	9.26
	EIRWQI > 300	Unsuitable to use	5	9.26

Table 5.11 Summary of Spatial Interpretation of Groundwater Quality Class according to EIRWQI Maps for both PRM and POM Seasons

Season	EIRWQI Range	Groundwater quality class	Area (Sq.km)	% Area
PRM	EIRWQI ≤ 50	Excellent Quality	0	0
	50 < EIRWQI ≤ 100	Good Quality	0	0
	100 < EIRWQI ≤ 200	Poor Quality	170.31	39.32
	200 < EIRWQI ≤ 300	Very Poor Quality	254.74	58.81
	EIRWQI > 300	Unsuitable to use	8.11	1.87
POM	EIRWQI ≤ 50	Excellent Quality	0	0
	50 < EIRWQI ≤ 100	Good Quality	4.54	1.05
	100 < EIRWQI ≤ 200	Poor Quality	356.96	82.41
	200 < EIRWQI ≤ 300	Very Poor Quality	55.96	12.92
	EIRWQI > 300	Unsuitable to use	15.71	3.63

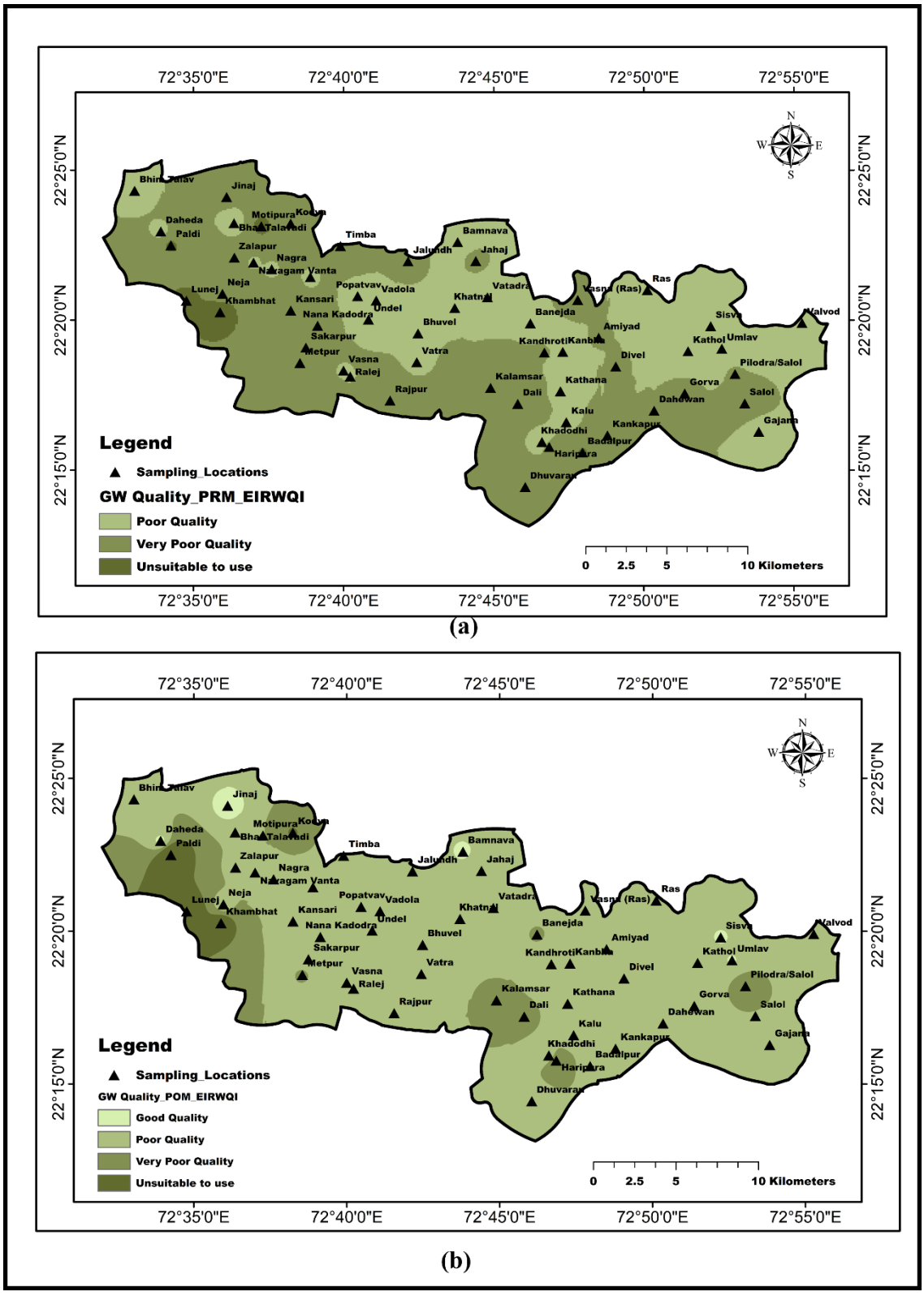

Figure 5.9 (a) Spatial Map groundwater quality class according to EIRWQI for the PRM season (b) Spatial Map groundwater quality class according to EIRWQI for the POM season

Chapter - 6

Vulnerability Assessment of Seawater Intrusion

6.1 General

Seawater intrusion can be described as saline water encroachment into coastal aquifers governed by natural and anthropogenic factors (Bordbar, Neshat, and Javadi 2019). The SWI pattern has a strong correlation with the attributes of related locations. In particular, the intrusion of saltwater has a considerable effect on how water is used and managed in the coastal stretch, where groundwater serves as the crucial source of freshwater (Chang et al., 2019). The term "groundwater vulnerability to saltwater intrusion" describes how the aquifer's intrinsic features make it susceptible to the impacts of groundwater extraction, rising sea levels, or both in coastal areas (Saravanan, Parthasarathy, and Sivaranjani 2019). The conventional SWI vulnerability evaluation methodology for groundwater resources entails superimposing thematic maps associated with rated geographic data, employing the overlay technique, and demarcating various vulnerability zones based on the assigned values (Kim, Chung, and Chang 2021). The selection of the suitable assessment method depends on the research objectives and the geological parameters of the study region. Various index-based methodologies, such as DRASTIC, PI, SI, EPIK, SANTIC, GOD, AVI, and GALDIT, have been developed to evaluate saline water intrusion. GALDIT is an extensively employed method among the specially developed techniques for assessing saltwater intrusion. (Yang et al., 2022). The chapter includes a step-by-step process for demarking seawater intrusion zones in the study region employing the GALDIT method.

6.2 GALDIT Method

The GALDIT method is an empirical ranking technique that integrates overlay and indexing methods. The model evaluates six hydrogeological indicators: Groundwater occurrence/type of aquifer (G), Aquifer hydraulic conductivity (A), Level of groundwater above sea level (L), Distance from shoreline/vicinity to coastline (D), Impact of prevailing salinity (I), and thickness/depth of aquifer pertinent to extensive salinity intrusion (T), with the abbreviation GALDIT derived from the characters of these parameters (Chang et

al., 2019). Each GALDIT indicator is first divided into different classes based on the range. The ratings of 10, 7.5, 5, and 2.5 are assigned to each class based on their importance in seawater intrusion, where the rating value of 2.5 indicates the lowest effect on SWI. Furthermore, each indicator is assigned weight on a scale of 1 to 4 (less significant to most significant) according to its relevance in the SWI process. The rating and weight of the indicator are determined by the findings from research about saltwater intrusion conducted by field peers, which are given in Table 6.1 (Chachadi A.G. and J.P. 2007). Finally, the index (GI) is calculated by dividing the sum of the product of the allocated weight (W) and the allocated rating (R) of each indicator by the sum of the weights of all indicators.

$$GI = \frac{\sum_{n=1}^{6} (W_n \times R_n)}{\sum_{n=1}^{6} W_n} \quad \text{.....(Eq.1)}$$

After calculating the Index, the region can be categorized into distinct zones of seawater incursion vulnerability. The lowest and greatest GI values ranged from 2.5 to 10 and were categorized into four zones: Very high SWI vulnerable zone: GI range≥7.5, High SWI vulnerable zone: 5.0≥GI range<7.5, Moderate SWI vulnerable zone: 2.5≥GI range<5.0, and Low SWI vulnerable zone: index range <2.5 (Tasnim and Tahsin, 2016). Fig. 6.1 represents a flowchart illustrating the GALDIT method for seawater intrusion.

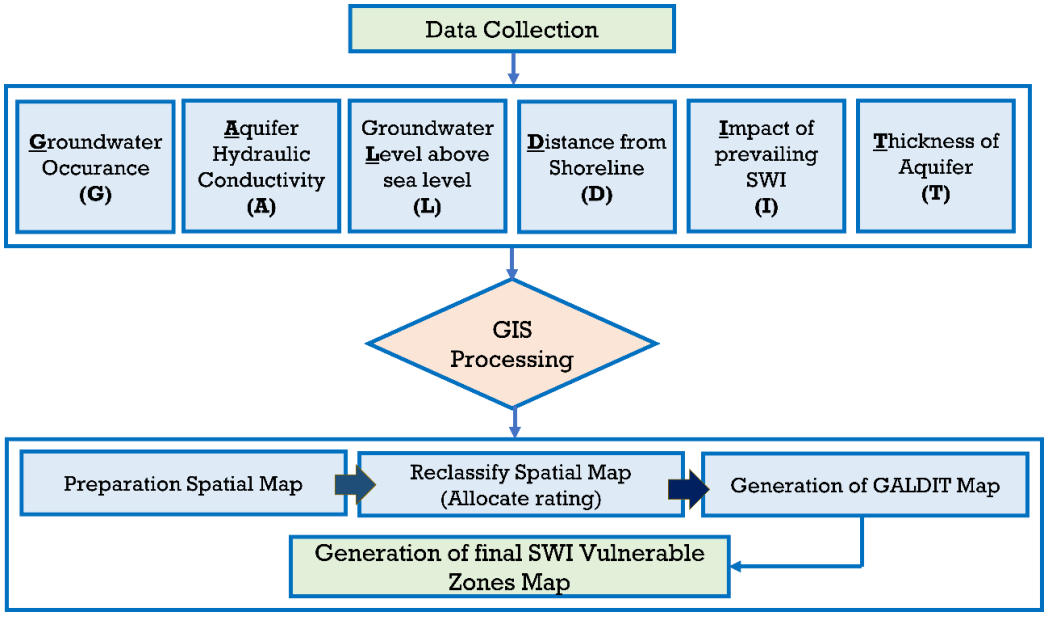

Figure 6.1 Flowchart for GALDIT Method

Table 6.1 Rating and Weight of GALDIT Indicators

Indicator	Allocated Weight	Range	Allocated Rating/ Importance
G:- Groundwater occurrence/Type of Aquifer	1	Confined	10
		Unconfined	7.5
		Leaky Confined	5
		Bounded	2.5
A:- Hydraulic conductivity of Aquifer (m/day)	3	> 40	10
		10 - 40	7.5
		5 - 10	5
		< 5	2.5
L:- Groundwater level above sea level (m)	4	< 1.0	10
		1.0 - 1.5	7.5
		1.5 - 2.0	5
		>2.0	2.5
D:- Vicinity to coastline /Distance from Shoreline (m)	4	< 500	10
		500 - 750	7.5
		750 - 1000	5
		> 1000	2.5
I:- Impact of prevailing salinity (Ratio = $Cl/[CO_3+HCO_3]$)	1	> 2.0	10
		1.5 - 2.0	7.5
		1.0 - 1.5	5
		< 1.0	2.5
T:- Depth/Thickness of aquifer (m)	2	> 10	10
		7.5 - 10	7.5
		5 - 7.5	5
		< 5	2.5

Source: (Chachadi A.G. and J.P. 2007)

6.3 GALDIT Indicators for Khambhat Coastal Region

Table 6.1 shows the comprehensive assessment standards for the GALDIT indicators. The range of each parameter value is categorized into four classes based on the importance during the vulnerability assessment.

6.3.1 Groundwater Occurrence/Type of Aquifer

The groundwater occurrences refer to the type of aquifer that influences groundwater salinization due to its intrinsic properties. A confined aquifer is intrinsically more vulnerable due to inadequate recharge circumstances, which can either accelerate or start the salinization process (Chronidou et al., 2022). For the

current research, data related to the type of aquifer were acquired from the Central Groundwater Board (CGWB). An unconfined aquifer covers 95.44 % of the study region, while a confined aquifer covers the rest (Fig. 6.2).

6.3.2 Hydraulic conductivity of Aquifer

Hydraulic conductivity is a key indicator for assessing the water flow rate within the aquifer. Hydraulic conductivity (HC) denotes an aquifer's capacity to transmit water and affects the extent of seawater intrusion. Higher conductivity correlates with a more significant inland movement of seawater. Areas exhibiting hydraulic conductivity exceeding 40 m/day received the maximum rating, whereas those with hydraulic conductivity below 5 m/day were assigned the lowermost rating (Chachadi A.G. and J.P. 2007). The hydraulic conductivity of the entire study region is 32.04 m/day (CGWB 2022) and assigned a rating of 7.5 for the indicator.

6.3.3 Groundwater Level above sea level

The groundwater level is essential for sustaining hydraulic pressure along the coastline to counteract salinity intrusion. When the water height above sea level reaches the highest level, the susceptibility ranking will attain its lowest level, and conversely. The height of the Water level below 1m from sea level constitutes the maximum significance grade of 10, indicating considerable susceptibility to saltwater intrusion. On the other hand, the height of a water level over 2m from the sea level is the least susceptible, rated at 2.5 (Saravanan et al., 2019). The groundwater level data were collected from Gujarat Water Resource Development Corporation Limited (GWRDC) for the pre-monsoon 2020. The value of the indicator in the study region ranges between 1.5 to 14.59m with a mean value of 7.5m. The entire study region is allocated the lowest rating of 2.5.

6.3.4 Vicinity to Coastline/Distance from Shoreline

The impact of saline water ingress diminishes as one travels inland in a direction perpendicular to the coast. We can achieve maximum influence near the coast (Chachadi A.G. and J.P. 2007). A distance map from the shoreline was generated using a spatial analyst tool, Euclidean distance, in ArcGIS software (Fig. 6.5). The map is categorized into 4 distinct classes, spanning from the high impact of salinization within 500m from the shoreline (rating 10) to the very low impact of salinization away from more than 1000m from the shoreline (rating 2.5).

6.3.5 Impact of Prevailing Salinity

To evaluate the susceptibility of the aquifer to intrusion of saline water, it is crucial to take into consideration the prevailing salinity scenario in the region. The chloride ion predominates in seawater but is in small amounts in groundwater. In contrast, Bicarbonate is present in substantial amounts in groundwater but is found in minimal levels in seawater. Hence, the ratio Cl^- / [CO_3^-+ HCO_3^-] can be employed to assess the prevailing scenario of salinization (Chachadi A.G. and J.P. 2007). The concentration of ions chloride, carbonate, and bicarbonate are obtained through the groundwater sampling and laboratory teasing of 57 locations in the study region during the pre-monsoon season. The map illustrating the spatial distribution of the ratio was generated using the spatial analyst tool IDW (Inverse Distance Weighting) in ArcGIS software (Fig. 6.6). The details of the indicator rating are given in Table 6.1.

6.3.6 Depth/Thickness of Aquifer

The thickness of an aquifer is vital in evaluating saltwater intrusion since the ingress of salt water is directly proportional to the thickness of the aquifer (Saravanan et al., 2019). The lithology data acquired from Gujarat Water Resource Development Corporation Limited (GWRDC) pertaining to the study region was used to acquire the depth of the aquifer. The depth of the aquifer of the study region ranges between 15 to 60m, and according to a rating of 10, is assigned to the whole study area, considering the high risk of salinization.

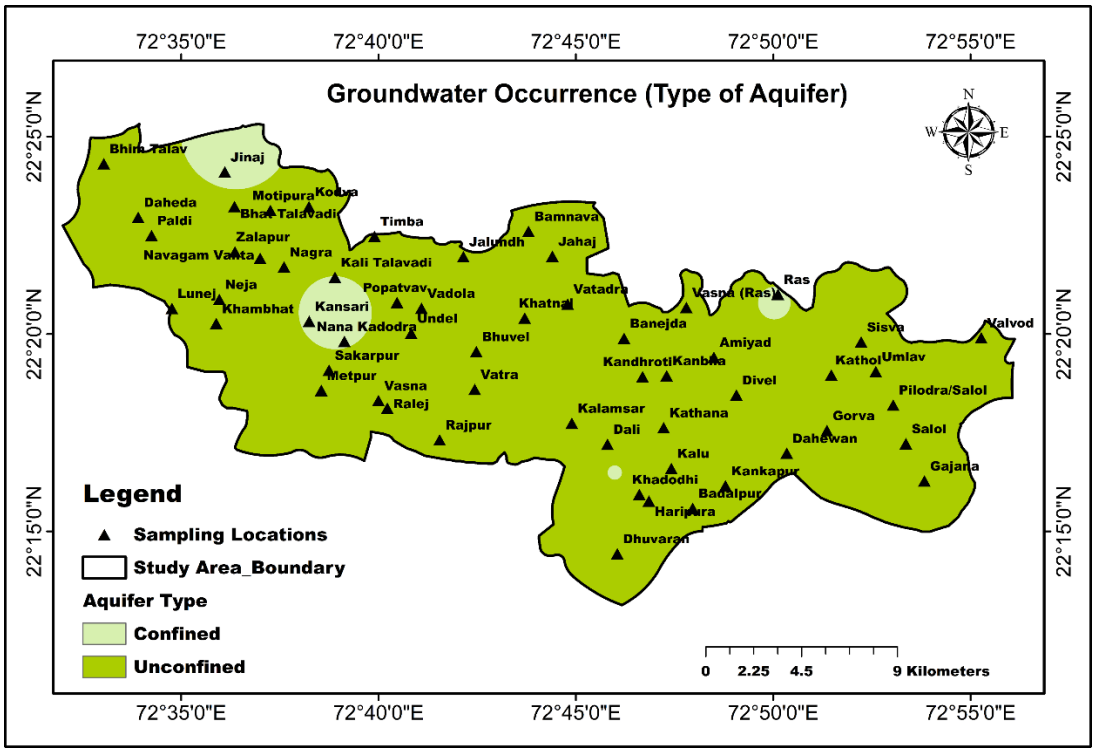

Figure 6.2 Groundwater Occurrence/Type of Aquifer

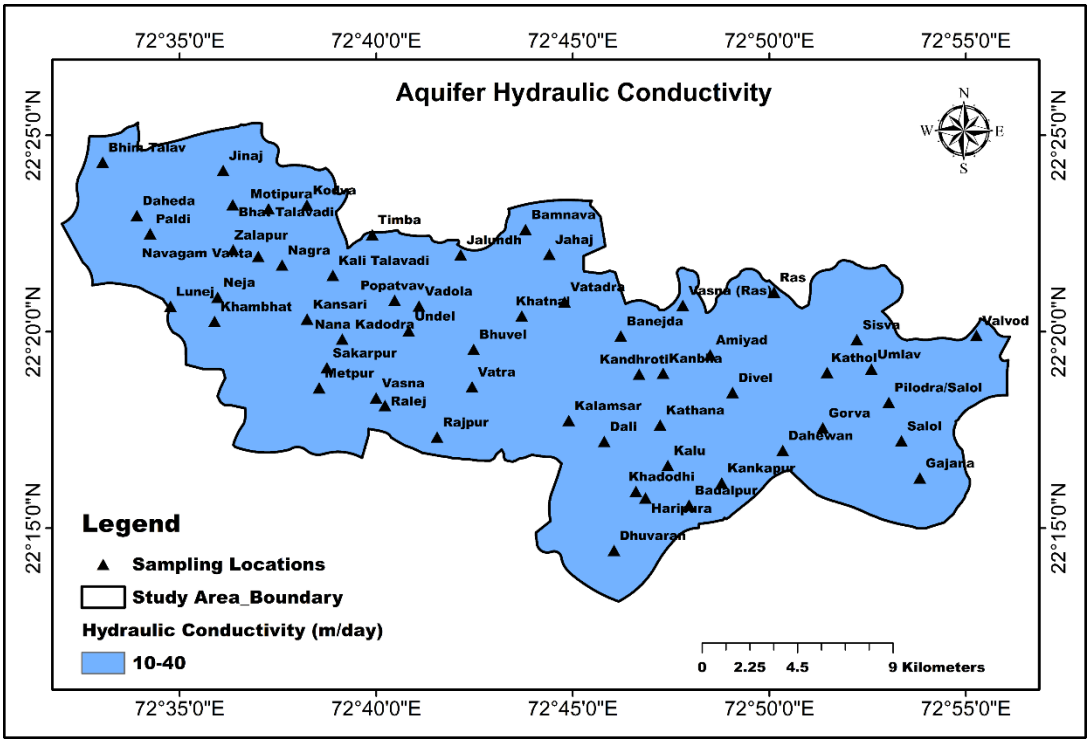

Figure 6.3 Aquifer Hydraulic Conductivity

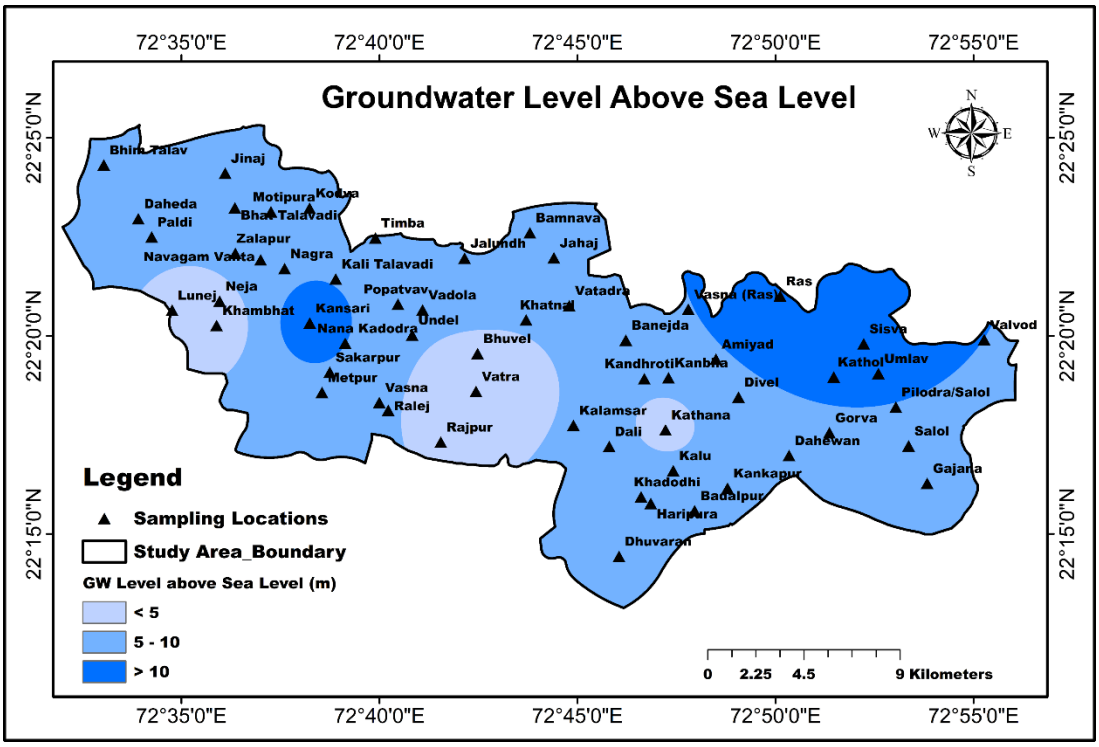

Figure 6.4 Groundwater Level above Sea Level

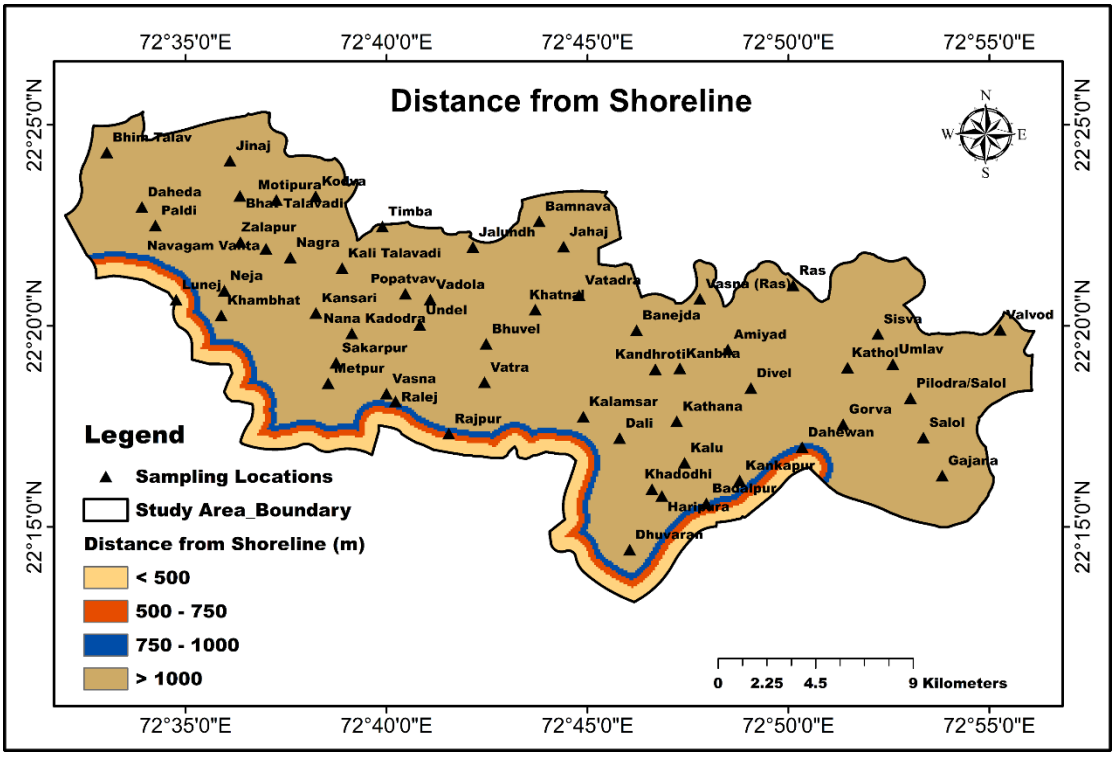

Figure 6.5 Vicinity to Coastline/Distance from the Shoreline

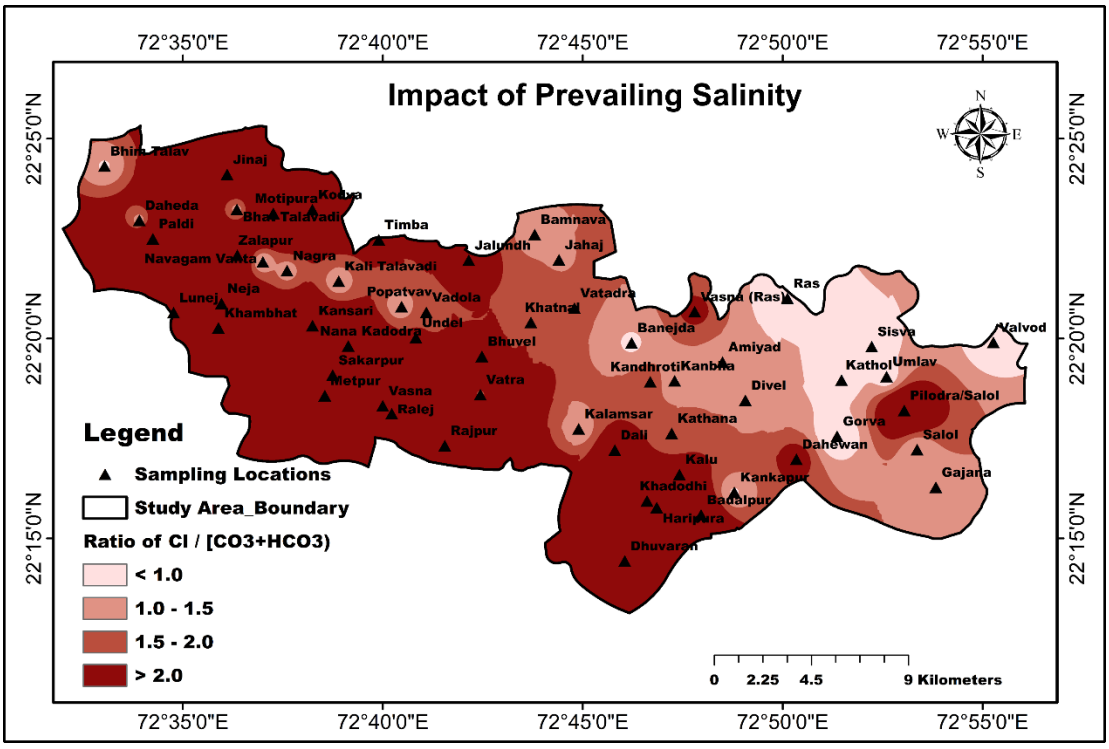

Figure 6.6 Impact of Prevailing Salinity

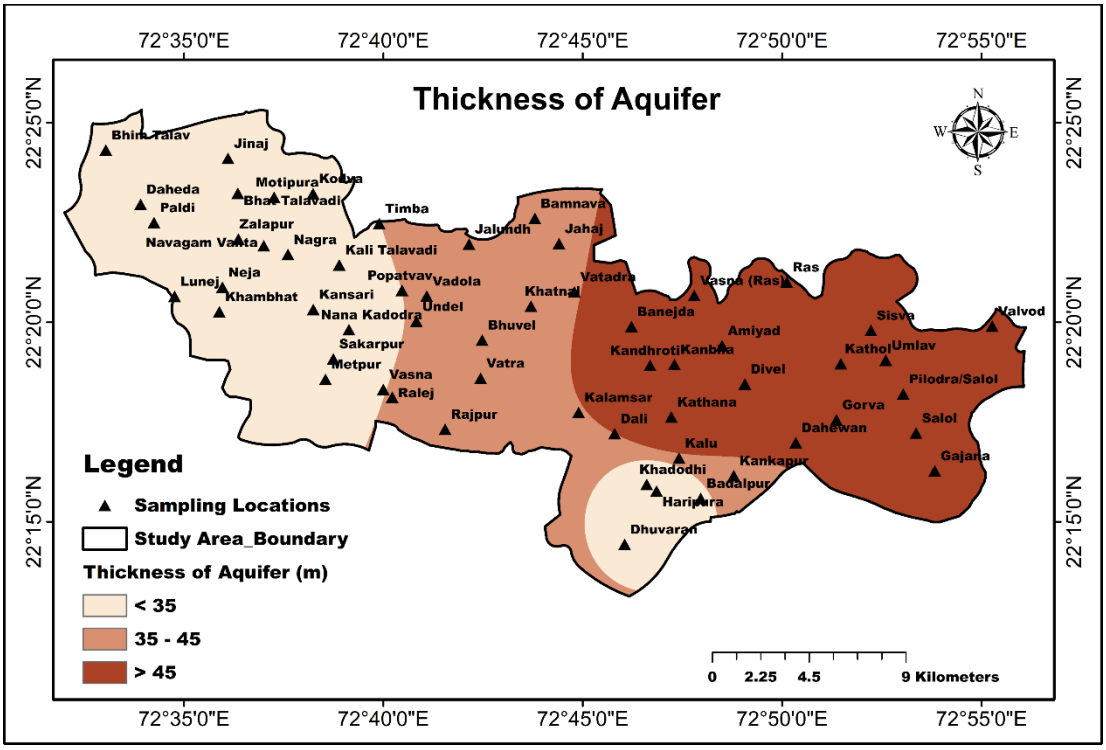

Figure 6.7 Depth/Thickness of Aquifer

6.4 Demarcation of SWI vulnerable zones

The demarcation of vulnerable zones to the ingress of saline water in the study region was done by developing a SWI vulnerable zones map in a GIS environment. Spatial maps of individual GALDIT indicators were generated and divided into distinct classes as per the rating guideline. In the next step, each spatial map was allocated a rating using a spatial analyst tool called Reclassify in ArcGIS software. Furthermore, six GALDIT indicator spatial maps were overlaid, and weight was allocated to individual indicators using the "Weighted sum" spatial analyst tool. The value of the calculated GALDIT index in the research region ranges from 4.04 to 7.27, with a mean of 5.18, illustrating that the index values can be grouped as highly vulnerable and moderately vulnerable. Ultimately, as per the classification of the GALDIT index, the GALDIT map was classified into two distinct zones: High vulnerable zones and Moderate vulnerable zones. Spatial interpretation of the GALDIT map shows that approximately 50% (216.45 sq.km) of the study region falls under high vulnerable zones, and the remaining 216.70 sq.km study region falls under moderate vulnerable zones. The GALDIT mapping reveals that highly vulnerable zones are more susceptible to saltwater intrusion than moderately and low vulnerable zones.

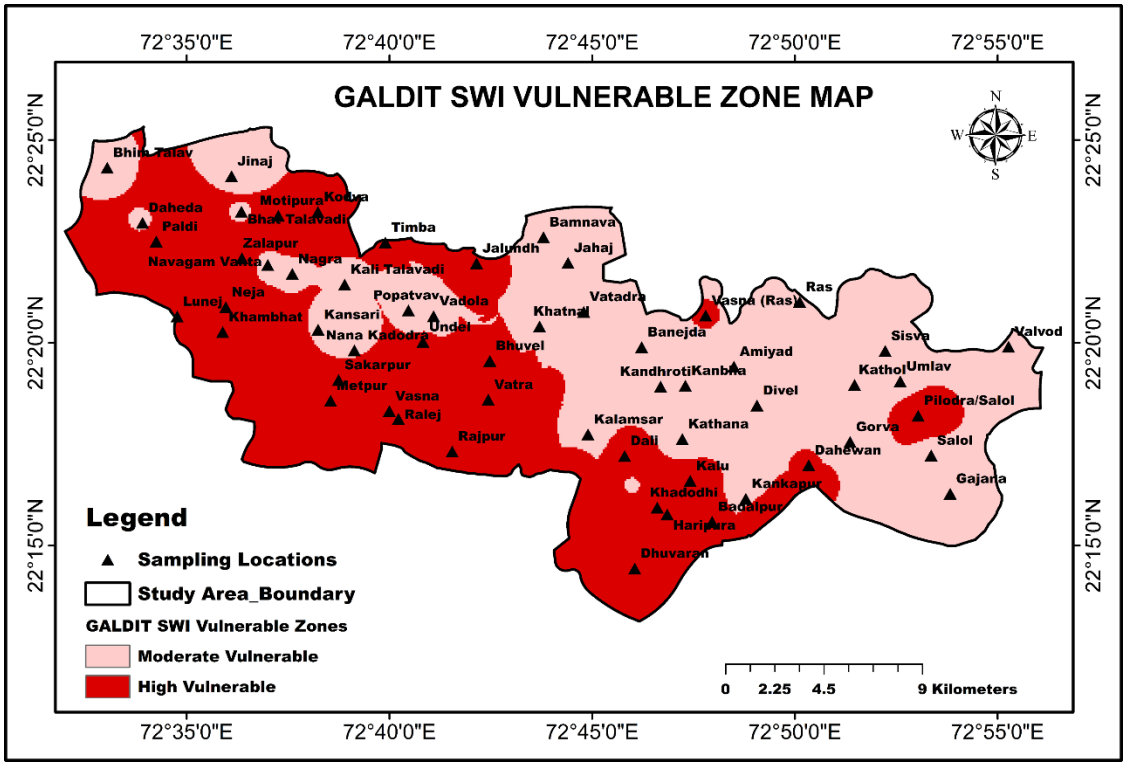

Figure 6.8 GALDIT SWI Vulnerable Zone Map

Chapter - 7

Conclusion

Groundwater is essential for the sustenance and welfare of rural coastal communities in India. It is the principal source of potable water, providing a dependable and comparatively safe supply in contrast to surface water. Additionally, it is vital for agriculture, facilitating the irrigation of products such as rice, vegetables, and cash crops, which are fundamental to rural economies. Consequently, the quality of groundwater plays a significant role in rural life. In this context, research has been conducted to examine the potability of groundwater and its appropriateness for agricultural application, as well as to identify seawater intrusion vulnerable zones in the Khambhat coastal region. The quality index approach was adopted to assess the potability of the groundwater, and the index was first computed by employing the subjective method for weighting parameters. Additionally, to address the constraints of the subjective technique for parameter weighting and to validate the weight assignment of the initial method, the index was also computed using the entropy approach, an objective method. This method assigns weights to each parameter using mathematical calculations. The Entropy weighted irrigation water quality index was calculated to examine the appropriateness of groundwater for agricultural use. Finally, according to susceptibility to saline water ingress, the research region was classified into two distinct vulnerable zones using the GALDIT method.

7.1 Conclusion

The following summarizes particular conclusions derived from the results of several components of this research:

- Chemical analysis (Laboratory testing) of the groundwater samples shows an increased level of EC, TDS, Na, and Cl in most of the samples during the PRM season, which denotes the impact of saline water mixing. However, the amount of the parameter during the POM season is reduced due to dilution instigated by groundwater recharge during the monsoon. Moreover, the increased amount of HCO_3 during the POM season was observed as a result of the infiltration of CO_2-rich rainwater, dissolution of carbonate minerals, and less evaporation. On average,

groundwater has an alkaline pH, which tends to rise during POM and fall during PRM.

- Interpretation of the Piper trilinear diagram for the PRM season reveals 92.98% of samples are of the Zone-II class of the diamond-shaped plot, indicating the dominance of Na and Cl ions in the groundwater, which in turn signifies the mixing of saline water. However, for the POM season, samples that fall under the Zone-II class decreased to 46.29% as a result of groundwater recharge.

- The correlation matrix represents a very high positive correlation of TDS with EC, Na, and Cl, indicating these ions are the primary contributors to the TDS in the groundwater. Also, a very high correlation among EC, Na, and Cl indicates a common source of ions.

- During the PRM season, the average GWQI value is 265.66, and on the other hand, the value during the POM season is 185.22. According to the classification of GWQI, During the PRM season, 15 samples (26.32%) and 28 samples (49.12%) are considered “Unsuitable to use” and “Very poor quality” for the drinking, while during the POM season, 4 samples (7.41%) and 8 samples (14.81%) are considered “Unsuitable to use” and “Very poor quality” for the drinking, illustrate improvement in the water quality after monsoon.

- During the PRM season, the average EGWQI value is 2.35, and on the other hand, the value during the POM season is 1.60. According to the classification of EGWQI, During the PRM season, 20 samples (35.09%) and 18 samples (31.58%) are considered “Unsuitable to use and “Very poor quality” for the drinking, while during the POM season, 5 samples (9.26%) and 3 samples (5.56%) are considered “Unsuitable to use and “Very poor quality” for the drinking, illustrate improvement in the water quality after monsoon.

- The interpretation of the spatial map of the groundwater quality class based on GWQI reveals that the 368.31 sq.km (85.03%) area of the region falls under the categories of “Very poor and Not suitable quality” during the PRM season for drinking, while during the POM season, 115.77 sq.km (26.73%) area of the region falls under the categories of “Very poor and Not suitable quality.” On the other hand, the

interpretation of the spatial map of the groundwater quality class based on EGWQI illustrates that the 316.25 sq.km (73.01%) area of the region falls under the categories of "Very poor and Not suitable quality" during the PRM season for drinking, while during the POM season, 52.36 sq.km (12.09%) area of the region falls under the categories of "Very poor and Not suitable quality."

- According to the computed values of various irrigation indices during the PRM season, the majority of the samples are not appropriate for agriculture. The mean value of EIRWQI during the PRM season is 213.70, while that of during the POM season is 173.08. According to the value of EIRWQI during the PRM season, 5 samples (8.77%) and 25 samples (43.86%) are considered "Unsuitable to use and "Very poor quality" for agriculture, while during the POM season, 5 samples (9.26%) and 5 samples (9.26%) are considered "Unsuitable to use and Very poor quality" for agriculture, illustrate improvement in the water quality after monsoon. During the PRM season, not even a single sample falls under the "Excellent or Good quality" category for agriculture.

- Moreover, the geospatial analysis depicts that the 262.85 sq.km (60.68%) area of the region falls under the categories of "Very poor and Not suitable quality," and the remaining 170.31 sq.km (39.32%) of the region falls under the "Poor quality" during the PRM season. On the other hand, during the POM season, 71.67 sq.km (16.55%) area of the region falls under the categories of "Very poor and Not suitable water quality," and 356.96 sq.km (82.41%) area is categorized as "Good quality" for the irrigation.

- The findings of the assessment of seawater intrusion using the GALDIT method reveal that approximately 50% (216.45 sq.km) area of the research region can be classified as a "High vulnerable zone." While the remaining 216.70 sq.km area can be classified as a "Moderate vulnerable zone."

7.2 Recommendations

- Extraction of the groundwater from the deep borewell for agriculture should be immediately controlled by implementing policy.
- Canals can facilitate the diversion of river water to areas impacted by seawater for the remediation of contaminated areas.

- Enhance the replenishment of coastal aquifers utilizing artificial recharge methods such as rainwater harvesting, the establishment of recharge wells, or the implementation of infiltration basins.
- Construct a sub-surface impermeable or low-permeability barrier to obstruct or impede the ingress of saltwater water into freshwater aquifers.
- Utilize injection wells for injecting freshwater into aquifers, establishing a hydraulic barrier that inhibits the ingress of seawater.
- Enhance knowledge within local populations regarding the causes and effects of saltwater intrusion and the significance of sustainable water use.

7.3 Scope for Future Research

- Continuous surveillance through cost-effective and advanced techniques such as remote sensing, IoT, etc., can be employed.
- Isotopic signatures may be utilized to investigate seawater intrusion, improving the comprehension of palaeosalinity and current intrusion.
- A geophysical survey can be done to delineate the underlying structure and identify salty and freshwater zones using the physical characteristics of the Earth.
- Artificial intelligence (AI) and machine learning (ML) methodologies can be employed to analyze extensive datasets and forecast forthcoming SWI trends.
- Evaluate the impact of climate change on seawater intrusion in the coastal region.
- Assess the impact of prevailing seawater intrusion on soil and crop production in the coastal region.
- Extend the current research from two-dimensional to three-dimensional, allowing a more precise simulation for most seawater intrusion issues in forthcoming research.

List of References

(1) Abbasnia, A., Radfard, M., Mahvi, A. H., Nabizadeh, R., Yousefi, M., Soleimani, H., & Alimohammadi, M. (2018). Groundwater quality assessment for irrigation purposes based on irrigation water quality index and its zoning with GIS in the villages of Chabahar, Sistan and Baluchistan, Iran. *Data in Brief*, *19*, 623–631. https://doi.org/10.1016/j.dib.2018.05.061

(2) Adagba, T., Kankara., A. I., & Idris, M. A. (2022). Evaluation of groundwater suitability for irrigation purpose using gis and irrigation water quality indices. *FUDMA Journal of Sciences*, *6*(8.5.2017), 63–80. www.aging-us.com

(3) Adimalla, N. (2021). Application of the Entropy Weighted Water Quality Index (EWQI) and the Pollution Index of Groundwater (PIG) to Assess Groundwater Quality for Drinking Purposes: A Case Study in a Rural Area of Telangana State, India. *Archives of Environmental Contamination and Toxicology*, *80*(1), 31–40. https://doi.org/10.1007/s00244-020-00800-4

(4) Adimalla, N., Li, P., & Venkatayogi, S. (2018). Hydrogeochemical Evaluation of Groundwater Quality for Drinking and Irrigation Purposes and Integrated Interpretation with Water Quality Index Studies. *Environmental Processes*, *5*(2), 363–383. https://doi.org/10.1007/s40710-018-0297-4

(5) Adimalla, N., Qian, H., & Li, P. (2020). Entropy water quality index and probabilistic health risk assessment from geochemistry of groundwaters in hard rock terrain of Nanganur County, South India. *Chemie Der Erde*, *80*(4). https://doi.org/10.1016/j.chemer.2019.125544

(6) Alessio Ishizaka, P. N. (2013). *Multi-criteria Decision Analysis: Methods and Software* (1st editio). Wiley; 1s.

(7) APHA. (2012). *Standard Methods for the Examination of Water and Wastewater* (22nd ed.). American Public Health Association.

(8) Aravinthasamy, P., Karunanidhi, D., Subba Rao, N., Subramani, T., & Srinivasamoorthy, K. (2020). Irrigation risk assessment of groundwater in a non-perennial river basin of South India: implication from irrigation water quality index (IWQI) and geographical information system (GIS) approaches. *Arabian Journal of Geosciences*, *13*(21). https://doi.org/10.1007/s12517-020-06103-1

(9) Arthur M. Piper. (1944). *A graphic procedure in geochemical interpretation of water analysis*. American Geophysical Union Transactions. https://doi.org/10.1029/TR025i006p00914

(10) Ayers, R.S., D. W. W. (1994). *Water quality for agriculture*. Food and Agriculture Organization of the United Nations.

(11) Baena-Ruiz, L., & Pulido-Velazquez, D. (2021). GIS-SWIAS: Tool to Summarize Seawater Intrusion Status and Vulnerability at Aquifer Scale. *Scientific Programming*, *2021*. https://doi.org/10.1155/2021/8818634

(12) Balasubramanian, M., Sridhar, S. G. D., Ayyamperumal, R., Karuppannan, S., Gopalakrishnan, G., Chakraborty, M., & Huang, X. (2022). Isotopic signatures, hydrochemical and multivariate statistical analysis of seawater intrusion in the coastal aquifers of Chennai and Tiruvallur District, Tamil Nadu, India. *Marine Pollution Bulletin*, *174*. https://doi.org/10.1016/j.marpolbul.2021.113232

(13) Bao, Q., Yuxin, Z., Yuxiao, W., & Feng, Y. (2020). Can Entropy Weight Method Correctly Reflect the Distinction of Water Quality Indices? *Water Resources Management*, *34*(11), 3667–3674. https://doi.org/10.1007/s11269-020-02641-1

(14) Barik, R., & Pattanayak, S. K. (2019). Assessment of groundwater quality for irrigation of green spaces in the Rourkela city of Odisha, India. *Groundwater for Sustainable Development*, *8*, 428–438. https://doi.org/10.1016/j.gsd.2019.01.005

(15) Batarseh, M., Imreizeeq, E., Tilev, S., Al Alaween, M., Suleiman, W., Al Remeithi, A. M., Al Tamimi, M. K., & Al Alawneh, M. (2021). Assessment of groundwater quality for irrigation in the arid regions using irrigation water quality index (IWQI) and GIS-Zoning maps: Case study from Abu Dhabi Emirate, UAE. *Groundwater for Sustainable Development*, *14*. https://doi.org/10.1016/j.gsd.2021.100611

(16) Beyene, G., Aberra, D., & Fufa, F. (2019). Evaluation of the suitability of groundwater for drinking and irrigation purposes in Jimma Zone of Oromia, Ethiopia. *Groundwater for Sustainable Development*, *9*. https://doi.org/10.1016/j.gsd.2019.100216

(17) Bhavsar, Z., & Patel, J. (2023). Assessing potability of groundwater using groundwater quality index (GWQI), entropy weighted groundwater pollution index (EGPI) and geospatial analysis for khambhat coastal region of Gujarat. *Groundwater for Sustainable Development*, *21*. https://doi.org/10.1016/j.gsd.2023.100916

(18) BIS. (2012). *Drinking Water Specifications IS 10500:2012*. Burea of Indian Standard.

(19) Bordbar, M., Neshat, A., & Javadi, S. (2019). Modification of the GALDIT framework using statistical and entropy models to assess coastal aquifer vulnerability. *Hydrological Sciences Journal*, *64*(9), 1117–1128. https://doi.org/10.1080/02626667.2019.1620951

(20) Brindha, K., & Michael schneider. (2019). Impact of urbanization on groundwater quality. In *GIS and Geostatistical Techniques for groundwater science* (pp. 179–196).

(21) CGWB. (2022). Technical report series- Aquifer Map and Management Plan, Anand District, Gujarat State. In *Central Groundwater Board* (Issue December).

(22) Chachadi A.G., & J.P., F. (2007). Assessing aquifer vulnerability to seawater intrusion using GALDIT method: Part 2-GALDIT indicators description. *IAHS - AISH Publication*, 172–180.

(23) Chandrasekar, N., Selvakumar, S., Srinivas, Y., John Wilson, J. S., Simon Peter, T., & Magesh, N. S. (2014). Hydrogeochemical assessment of groundwater quality along the coastal aquifers of southern Tamil Nadu, India. *Environmental Earth Sciences*, *71*(11), 4739–4750. https://doi.org/10.1007/s12665-013-2864-3

(24) Chang, S. W., Chung, I. M., Kim, M. G., Tolera, M., & Koh, G. W. (2019). Application of GALDIT in assessing the seawater intrusion vulnerability of Jeju Island, South Korea. *Water (Switzerland)*, *11*(9). https://doi.org/10.3390/w11091824

(25) Chronidou, D., Tziritis, E., Panagopoulos, A., Oikonomou, E. K., & Loukas, A. (2022). A Modified GALDIT Method to Assess Groundwater Vulnerability to Salinization—Application to Rhodope Coastal Aquifer (North Greece). *Water (Switzerland)*, *14*(22). https://doi.org/10.3390/w14223689

(26) Dash, S., & Kalamdhad, A. S. (2021). Discussion on the existing methodology of entropy-weights in water quality indexing and proposal for a modification of the expected conflicts. *Environmental Science and Pollution Research*, *28*(38), 53983–54001. https://doi.org/10.1007/s11356-021-14482-5

(27) Dhakate, R., Ratnalu, G. V., & Sankaran, S. (2020). Hydrogeochemical and isotopic study for evaluation of seawater intrusion into shallow coastal aquifers of Udupi District, Karnataka, India. *Chemie Der Erde*, *80*(4). https://doi.org/10.1016/j.chemer.2020.125647

(28) Doneen, L. D. (1964). *Notes on Water Quality in Agriculture, Part 1*. Department of Water Science and Engineering, University of California.

(29) Eaton, F. M. (1950). Significance of Carbonates in Irrigation Waters. *Soil Science*, *69*(2), 123–134. 10.1097/00010694-195002000-00004

(30) Edet, A. (2017). Hydrogeology and groundwater evaluation of a shallow coastal aquifer, southern Akwa Ibom State (Nigeria). *Applied Water Science*, *7*(5), 2397–2412. https://doi.org/10.1007/s13201-016-0432-1

(31) El Behairy, R. A., El Baroudy, A. A., Ibrahim, M. M., Kheir, A. M. S., & Shokr, M. S. (2021). Modelling and Assessment of Irrigation Water Quality Index Using GIS in Semi-arid Region for Sustainable Agriculture. *Water, Air, and Soil Pollution*, *232*(9). https://doi.org/10.1007/s11270-021-05310-0

(32) Gao, Y., Qian, H., Ren, W., Wang, H., Liu, F., & Yang, F. (2020). Hydrogeochemical characterization and quality assessment of groundwater based on integrated-weight water quality index in a concentrated urban area. *Journal of Cleaner Production*, *260*. https://doi.org/10.1016/j.jclepro.2020.121006

(33) Gautam, S. K., Singh, A. K., Tripathi, J. K., Singh, S. K., Srivastava, P. K., Narsimlu, B., & Singh, P. (2016). Appraisal of surface and groundwater of the subarnarekha river basin, Jharkhand, India: Using remote sensing, irrigation indices and statistical technique. *Geospatial Technology for Water Resource Applications*, *December*, 144–169. https://doi.org/10.1201/9781315370989-19

(34) Gopinath, S., Srinivasamoorthy, K., Saravanan, K., & Prakash, R. (2019). Tracing groundwater salinization using geochemical and isotopic signature in Southeastern coastal Tamilnadu, India. *Chemosphere*, *236*. https://doi.org/10.1016/j.chemosphere.2019.07.036

(35) Hem, J. D. (1985). *Study and interpretation of the chemical characteristics of natural water (3rd Edition)*. https://doi.org/10.3133/wsp2254

(36) Hinkle, D. E., Wiersma, W., , Jurs, S. G. (2003). *Applied statistics for the behavioral sciences (Vol. 663).* Houghton Mifflin Company.

(37) Islam, A. R. M. T., Al Mamun, A., Rahman, M. M., & Zahid, A. (2020). Simultaneous comparison of modified-integrated water quality and entropy weighted indices: Implication for safe drinking water in the coastal region of Bangladesh. *Ecological Indicators*, *113*. https://doi.org/10.1016/j.ecolind.2020.106229

(38) Ismail, A. H., Hassan, G., & Sarhan, A. H. (2020). Hydrochemistry of shallow groundwater and its assessment for drinking and irrigation purposes in Tarmiah district, Baghdad governorate, Iraq. *Groundwater for Sustainable Development*, *10*. https://doi.org/10.1016/j.gsd.2019.100300

(39) Kanagaraj, G., Elango, L., Sridhar, S. G. D., & Gowrisankar, G. (2018). Hydrogeochemical processes and influence of seawater intrusion in coastal aquifers south of Chennai, Tamil Nadu, India. *Environmental Science and Pollution Research*, *25*(9), 8989–9011. https://doi.org/10.1007/s11356-017-0910-5

(40) Karakuş, C. B., & Yıldız, S. (2020). Evaluation for Irrigation Water Purposes of Groundwater Quality in the Vicinity of Sivas City Centre (Turkey) by Using Gis and an Irrigation Water Quality Index. *Irrigation and Drainage*, *69*(1), 121–137. https://doi.org/10.1002/ird.2386

(41) Kavurmacı, M., & Karakuş, C. B. (2020). Evaluation of Irrigation Water Quality by Data Envelopment Analysis and Analytic Hierarchy Process-Based Water Quality Indices: the Case of Aksaray City, Turkey. *Water, Air, and Soil Pollution*, *231*(2). https://doi.org/10.1007/s11270-020-4427-z

(42) Kelley, W. P. (1941). Permissible Composition and Concentration of Irrigation Water. *Transactions of the American Society of Civil Engine*, *106*(1). https://doi.org/ttps://doi.org/10.1061/TACEAT.000538

(43) Khan, A. F., Srinivasamoorthy, K., Prakash, R., & Rabina, C. (2021). Hydrochemical and statistical techniques to decode groundwater geochemical interactions and saline water intrusion along the coastal regions of Tamil Nadu and Puducherry, India. *Environmental Geochemistry and Health*, *43*(2), 1051–1067. https://doi.org/10.1007/s10653-020-00713-0

(44) Kim, I. H., Chung, I. M., & Chang, S. W. (2021). Development of seawater intrusion vulnerability assessment for averaged seasonality of using modified galdit method. *Water (Switzerland)*, *13*(13). https://doi.org/10.3390/w13131820

(45) Kumar, K. S. A., Priju, C. P., & Prasad, N. B. N. (2015). Study on Saline Water Intrusion into the Shallow Coastal Aquifers of Periyar River Basin, Kerala Using Hydrochemical and Electrical Resistivity Methods. *Aquatic Procedia*, *4*, 32–40. https://doi.org/10.1016/j.aqpro.2015.02.006

(46) Kumar, P. J. S., & Augustine, C. M. (2022). Entropy-weighted water quality index (EWQI) modeling of groundwater quality and spatial mapping in Uppar Odai Sub-

Basin, South India. *Modeling Earth Systems and Environment*, *8*(1), 911–924. https://doi.org/10.1007/s40808-021-01132-5

(47) Kumari, M., & Rai, S. C. (2020). Hydrogeochemical Evaluation of Groundwater Quality for Drinking and Irrigation Purposes Using Water Quality Index in Semi Arid Region of India. *Journal of the Geological Society of India*, *95*(2), 159–168. https://doi.org/10.1007/s12594-020-1405-4

(48) Kumari, R., Kumar Singh, C., & Mukherjee, S. (n.d.-a). *Isotopes and ion chemistry to identify salinization of coastal aquifers of Sabarmati River Basin*. https://www.researchgate.net/publication/235566831

(49) Kumari, R., Kumar Singh, C., & Mukherjee, S. (n.d.-b). *Isotopes and ion chemistry to identify salinization of coastal aquifers of Sabarmati River Basin*. https://www.researchgate.net/publication/235566831

(50) Lakshmanan, E., Nair, I. S., Renganayaki, S. P., & Elango, L. (2013). Identification of Seawater Intrusion by Cl/Br Ratio and Mitigation through Managed Aquifer Recharge in Aquifers North of Chennai, India. In *JGWR* (Vol. 2). https://www.researchgate.net/publication/259263845

(51) Li, C., Gao, Z., Chen, H., Wang, J., Liu, J., Li, C., Teng, Y., Liu, C., & Xu, C. (2021). Hydrochemical analysis and quality assessment of groundwater in southeast North China Plain using hydrochemical, entropy-weight water quality index, and GIS techniques. *Environmental Earth Sciences*, *80*(16). https://doi.org/10.1007/s12665-021-09823-z

(52) Li, H., Smith, C. D., Wang, L., Li, Z., Xiong, C., & Zhang, R. (2019). Combining spatial analysis and a drinking water quality index to evaluate monitoring data. *International Journal of Environmental Research and Public Health*, *16*(3). https://doi.org/10.3390/ijerph16030357

(53) L.S., N., V.V.S., G. R., G., T. R., J., M., G., P., V.S., S., P.R., P., S.M., R., & B.M., R. R. (2013). An integrated approach to investigate saline water intrusion and to identify the salinity sources in the Central Godavari delta, Andhra Pradesh, India. *Arabian Journal of Geosciences*, *6*(10), 3709–3724. https://doi.org/10.1007/s12517-012-0634-2

(54) Magesh, N. S., Krishnakumar, S., Chandrasekar, N., & Soundranayagam, J. P. (2013). Groundwater quality assessment using WQI and GIS techniques, Dindigul district, Tamil Nadu, India. *Arabian Journal of Geosciences*, *6*(11), 4179–4189. https://doi.org/10.1007/s12517-012-0673-8

(55) Maurya, P., Kumari, R., & Mukherjee, S. (2019a). Hydrochemistry in integration with stable isotopes (δ18O and δD) to assess seawater intrusion in coastal aquifers of Kachchh district, Gujarat, India. *Journal of Geochemical Exploration*, *196*, 42–56. https://doi.org/10.1016/j.gexplo.2018.09.013

(56) Maurya, P., Kumari, R., & Mukherjee, S. (2019b). Hydrochemistry in integration with stable isotopes (δ18O and δD) to assess seawater intrusion in coastal aquifers of Kachchh district, Gujarat, India. *Journal of Geochemical Exploration*, *196*, 42–56. https://doi.org/10.1016/j.gexplo.2018.09.013

(57) Mohanty, A. K., & Rao, V. V. S. G. (2019). Hydrogeochemical, seawater intrusion and oxygen isotope studies on a coastal region in the Puri District of Odisha, India. *Catena*, *172*, 558–571. https://doi.org/10.1016/j.catena.2018.09.010

(58) Mostaza-Colado, D., Carreño-Conde, F., Rasines-Ladero, R., & Iepure, S. (2018). Hydrogeochemical characterization of a shallow alluvial aquifer: 1 baseline for groundwater quality assessment and resource management. *Science of the Total Environment*, *639*, 1110–1125. https://doi.org/10.1016/j.scitotenv.2018.05.236

(59) Mukate, S., Wagh, V., Panaskar, D., Jacobs, J. A., & Sawant, A. (2019). Development of new integrated water quality index (IWQI) model to evaluate the drinking suitability of water. *Ecological Indicators*, *101*, 348–354. https://doi.org/10.1016/j.ecolind.2019.01.034

(60) Narayan, K. A., Schleeberger, C., & Bristow, K. L. (2007). Modelling seawater intrusion in the Burdekin Delta Irrigation Area, North Queensland, Australia. *Agricultural Water Management*, *89*(3), 217–228. https://doi.org/10.1016/j.agwat.2007.01.008

(61) Naz, I., Fan, H., Aslam, R. W., Tariq, A., Quddoos, A., Sajjad, A., Soufan, W., Almutairi, K. F., & Ali, F. (2024). Integrated Geospatial and Geostatistical Multi-Criteria Evaluation of Urban Groundwater Quality Using Water Quality Indices. *Water (Switzerland)*, *16*(17). https://doi.org/10.3390/w16172549

(62) Odu, G. O. (2019). Weighting methods for multi-criteria decision making technique. *Journal of Applied Sciences and Environmental Management*, *23*(8), 1449. https://doi.org/10.4314/jasem.v23i8.7

(63) Omprakash, M. D., & Gadikar, N. (2018). *Salt Water Intrusion and Water Security Issues of Coastal Community: Case of Thane District (Maharashtra)* (pp. 167–177). https://doi.org/10.1007/978-981-10-5711-3_12

(64) P. Prusty, S. H. F. (2020). Seawater intrusion in coastal aquifer of india - A review. *HydroResearch*, 61–74. https://doi.org/10.1016/j.hydres.2020.06.001

(65) Rao, N. S., Dinakar, A., Sravanthi, M., & Kumari, B. K. (2021). Geochemical characteristics and quality of groundwater evaluation for drinking, irrigation, and industrial purposes from a part of hard rock aquifer of South India. *Environmental Science and Pollution Research*, *28*(24), 31941–31961. https://doi.org/10.1007/s11356-021-12404-z

(66) Rawat, K. S., Singh, S. K., & Gautam, S. K. (2018). Assessment of groundwater quality for irrigation use: a peninsular case study. *Applied Water Science*, *8*(8). https://doi.org/10.1007/s13201-018-0866-8

(67) Richard, L. A. (1954). *Diagnosis and Improvement of Saline and Alkali Soils*. US Department of Agriculture.

(68) Sahu, S. S. & P. (2020). Status of seawater intrusion in coastal aquifer of Gujarat, India: a review. *SN Applie Science*, *2*. https://doi.org/10.1007/s42452-020-03510-7

(69) Saikrishna, K., Purushotham, D., Sunitha, V., Reddy, Y. S., Linga, D., & Kumar, B. K. (2020). Data for the evaluation of groundwater quality using water quality index and regression analysis in parts of Nalgonda district, Telangana, Southern India. *Data in Brief*, *32*. https://doi.org/10.1016/j.dib.2020.106235

(70) Salil Kumar Gupta, Suresh Kumar Gupta, I. C. G. (1987). *Management of Saline Soils and Waters*. Oxford & IBH Publishing Company.

(71) Sarath Prasanth, S. V., Magesh, N. S., Jitheshlal, K. V., Chandrasekar, N., & Gangadhar, K. (2012). Evaluation of groundwater quality and its suitability for drinking and agricultural use in the coastal stretch of Alappuzha District, Kerala, India. *Applied Water Science*, *2*(3), 165–175. https://doi.org/10.1007/s13201-012-0042-5

(72) Saravanan, S., Parthasarathy, K. S. S., & Sivaranjani, S. (2019). Assessing Coastal Aquifer to Seawater Intrusion: Application of the GALDIT Method to the Cuddalore Aquifer, India. In *Coastal Zone Management: Global Perspectives, Regional Processes, Local Issues* (pp. 233–250). Elsevier. https://doi.org/10.1016/B978-0-12-814350-6.00010-0

(73) Satheeskumar, V., Subramani, T., Lakshumanan, C., Roy, P. D., & Karunanidhi, D. (2021). Groundwater chemistry and demarcation of seawater intrusion zones in the Thamirabarani delta of south India based on geochemical signatures. *Environmental*

Geochemistry and Health, *43*(2), 757–770. https://doi.org/10.1007/s10653-020-00536-z

(74) Singaraja, C., Chidambaram, S., Anandhan, P., Prasanna, M. V., Thivya, C., & Thilagavathi, R. (2015). A study on the status of saltwater intrusion in the coastal hard rock aquifer of South India. *Environment, Development and Sustainability*, *17*(3), 443–475. https://doi.org/10.1007/s10668-014-9554-5

(75) Singh, K. K., Tewari, G., & Kumar, S. (2020). Evaluation of Groundwater Quality for Suitability of Irrigation Purposes: A Case Study in the Udham Singh Nagar, Uttarakhand. *Journal of Chemistry*, *2020*. https://doi.org/10.1155/2020/6924026

(76) Solangi, G. S., Siyal, A. A., Babar, M. M., & Siyal, P. (2020). Groundwater quality evaluation using the water quality index (WQI), the synthetic pollution index (SPI), and geospatial tools: a case study of Sujawal district, Pakistan. *Human and Ecological Risk Assessment*, *26*(6), 1529–1549. https://doi.org/10.1080/10807039.2019.1588099

(77) Spandana, M. P., Suresh, K. R., & Prathima, B. (n.d.). *Developing an Irrigation Water Quality Index for Vrishabavathi Command Area*. www.ijert.org

(78) Subba Rao, N. (2012). PIG: a numerical index for dissemination of groundwater contamination zones. *Hydrological Processes*, *26*(22), 3344–3350. https://doi.org/10.1002/hyp.8456

(79) Subba Rao, N., Sunitha, B., Adimalla, N., & Chaudhary, M. (2020). Quality criteria for groundwater use from a rural part of Wanaparthy District, Telangana State, India, through ionic spatial distribution (ISD), entropy water quality index (EWQI) and principal component analysis (PCA). *Environmental Geochemistry and Health*, *42*(2), 579–599. https://doi.org/10.1007/s10653-019-00393-5

(80) Subbarao, M., Reddi, M., & Reddy, B. (2018). Groundwater Quality Assessment in Srikalahasthi Mandal, Chittoor District, Andhra Pradesh, South India. In *IOSR Journal of Engineering (IOSRJEN) www.iosrjen.org ISSN* (Vol. 08). www.iosrjen.org

(81) Sylus, K. J., & Ramesh, H. (2015). The Study of Sea Water Intrusion in Coastal Aquifer by Electrical Conductivity and Total Dissolved Solid Method in Gurpur and Netravathi River Basin. *Aquatic Procedia*, *4*, 57–64. https://doi.org/10.1016/j.aqpro.2015.02.009

(82) Tasnim, Z., & Tahsin, S. (2016). Application of the Method of Galdit for Groundwater Vulnerability Assessment: A Case of. *South Florida Asian Journal of Applied Science and Engineering*, *5*(1), 27–40. https://doi.org/10.18034

(83) Tejashvini, A., Subbarayappa, C. T., Mudalagiriyappa, M., Chowdappa, H. D., & Ramamurthy, V. (2024). Assessment of irrigation water quality for groundwater in Semi-Arid Region, Bangalore, Karnataka. Water Science, 38(1), 548–568. https://doi.org/10.1080/23570008.2024.2414131

(84) Thilagavathi, R., Chidambaram, S., Prasanna, M. V., Thivya, C., & Singaraja, C. (2012). A study on groundwater geochemistry and water quality in layered aquifers system of Pondicherry region, southeast India. *Applied Water Science*, *2*(4), 253–269. https://doi.org/10.1007/s13201-012-0045-2

(85) Todd, D. K., & Mays, L. W. (2005). *Groundwater Hydrology* (3rd Editio). John Wiley and Sons Ltd.

(86) Vasanthavigar, M., Srinivasamoorthy, K., Vijayaragavan, K., Rajiv Ganthi, R., Chidambaram, S., Anandhan, P., Manivannan, R., & Vasudevan, S. (2010). Application of water quality index for groundwater quality assessment: Thirumanimuttar sub-basin, Tamilnadu, India. *Environmental Monitoring and Assessment*, *171*(1–4), 595–609. https://doi.org/10.1007/s10661-009-1302-1

(87) Verma, P., Singh, P. K., Sinha, R. R., & Tiwari, A. K. (2020). Assessment of groundwater quality status by using water quality index (WQI) and geographic information system (GIS) approaches: a case study of the Bokaro district, India. *Applied Water Science*, *10*(1). https://doi.org/10.1007/s13201-019-1088-4

(88) WHO. (2017). *Guideline for Drinking Water Quality* (4th Editio). Worl Health Organization.

(89) Wilcox, L. V. (1955). *Classification and Use of Irrigation Waters*. US Department of Agriculture, Circular 969.

(90) Wondimu Musie, G. G. (2023). Fresh water resources, scarcity, water salinity challenges and possible remedies: A review. *Heliyon*. https://doi.org/10.1016/j.heliyon.2023.e18685

(91) Yang, J. S., Jeong, Y. W., Agossou, A., Sohn, J. S., & Lee, J. B. (2022). GALDIT Modification for Seasonal Seawater Intrusion Mapping Using Multi Criteria Decision Making Methods. *Water (Switzerland)*, *14*(14), 1–19. https://doi.org/10.3390/w14142258

(92) Zhe, W., Xigang, X., & Feng, Y. (2021). An abnormal phenomenon in entropy weight method in the dynamic evaluation of water quality index. *Ecological Indicators*, *131*. https://doi.org/10.1016/j.ecolind.2021.108137

List of Publications

(1) Zalak A. Bhavsar, Jayeshkumar S. Patel; “Assessing potability of groundwater using groundwater quality index (GWQI), entropy weighted groundwater pollution index (EGPI) and geospatial analysis for Khambhat coastal region of Gujarat,” Groundwater for Sustainable Development, Vol-21, May 2023. https://doi.org/10.1016/j.gsd.2023.100916 (Scopus)

(2) Zalak A. Bhavsar, Jayeshkumar S. Patel; “Understanding efficient seawater intrusion assessment in coastal region of India: a methodological review,” International Journal of Hydrology Science and Technology, Vol-16, No.4, November 2023. https://doi.org/10.1504/IJHST.2023.134626 (Scopus)

Appendix A
Laboratory testing results of the Pre-Monsoon Season

Village Name	Taluka Name	pH	TDS (mg/l)	Ca (mg/l)	Mg (mg/l)	Na (mg/l)	Cl (mg/l)	SO_4 (mg/l)	K (mg/l)	F (mg/l)	NO_3 (mg/l)	HCO_3 (mg/l)	CO_3 (mg/l)	EC (µƵ/cm)
Bamnava	Khambhat	7.8	2266	36	73	599	639	189	6.05	0.38	4.84	567	163	2300
Bhat Talavadi	Khambhat	8.2	1987	52	66	496	426	468	6.63	0.54	7.27	407	72	2600
Bhim Talav	Khambhat	9.0	1986	24	49	546	462	261	0.73	0.17	4.84	462	182	1190
Bhuvel	Khambhat	8.0	2720	38	62	796	852	389	9.52	0.38	4.84	439	144	2790
Daheda	Khambhat	8.2	2539	36	57	713	568	547	3.78	0.18	4.84	476	142	3800
Dhuvaran	Khambhat	7.8	4199	48	32	1105	2059	0	3.8	0.55	7.27	753	202	5730
Haripura	Khambhat	7.5	4665	88	303	1053	1527	1064	2.17	0.65	7.27	582	48	7230
Jahaj	Khambhat	7.4	3534	33	80	1020	923	556	4.84	0.49	7.27	764	158	3890
Jalundh	Khambhat	7.8	3352	34	94	1000	1314	253	6.12	0.91	7.27	549	108	3650
Jinaj	Khambhat	8.1	3583	56	94	1038	1136	701	11.34	0.55	7.27	467	91	5900
Kalamsar	Khambhat	7.6	3937	58	2	1235	1136	10	5.06	0.55	7.27	1244	252	6300
Kali Talavadi	Khambhat	8.4	2970	37	60	840	710	370	4.42	1.02	7.27	744	209	3100
Kansari	Khambhat	7.7	3393	58	86	1025	1491	147	8.29	1.02	7.27	488	98	4620
Khadodhi	Khambhat	7.5	3012	74	0	15	1740	0	14.82	1.02	9.69	1116	67	7750
Khambhat	Khambhat	8.4	5951	35	106	1954	2485	688	15.61	0.95	7.27	515	168	13500
Khatnal	Khambhat	8.3	2407	24	59	636	959	0	5.9	0.33	4.84	590	139	2450
Kodva	Khambhat	8.3	3901	35	157	1089	1420	560	6.73	0.9	7.27	434	206	7000
Lunej	Khambhat	8.1	4848	60	191	1097	2840	0	109.31	0.55	7.27	473	187	15400
Metpur	Khambhat	7.6	5174	140	276	1320	2485	401	24.58	1.02	7.27	461	91	11900
Motipura	Khambhat	8.0	5689	65	305	1546	3195	0	13	0.71	7.27	453	125	12300
Nagra	Khambhat	8.5	2904	36	48	840	568	712	4.72	0.95	7.27	575	125	3000
Nana Kadodra	Khambhat	7.8	4580	72	277	1067	1314	1301	28.27	1	7.27	472	77	6770
Navagam Vanta	Khambhat	8.3	3364	49	51	954	462	1102	4.66	0.65	7.27	600	146	3400
Neja	Khambhat	8.2	3693	39	65	1018	1775	0	2.05	0.6	7.27	662	134	3750
Paldi	Khambhat	7.8	4932	144	198	1097	2840	0	16.23	0.82	7.27	447	206	18500
Popatvav	Khambhat	7.9	2639	32	44	754	533	492	6.6	0.95	7.27	671	113	2650
Rajpur	Khambhat	7.5	4660	128	292	1079	2840	0	26	0.65	7.27	256	65	7320
Ralej	Khambhat	7.5	3697	60	118	1025	923	1280	18.64	1.02	7.27	221	70	5230
Sakarpur	Khambhat	7.9	4271	62	239	1089	1775	505	13.73	0.9	7.27	498	103	7700
Timba	Khambhat	7.8	3664	43	67	1075	1491	0	5.03	0.77	7.27	813	175	5210
Undel	Khambhat	7.7	3343	44	291	617	817	1001	6.68	0.9	7.27	484	89	3350
Vadola	Khambhat	7.7	2859	35	69	818	781	473	7.14	0.95	7.27	621	62	2850
Vasna	Khambhat	7.5	3424	50	94	978	888	1049	13.08	0.82	7.27	231	134	3800
Vatadra	Khambhat	7.8	1696	36	79	244	675	0	3.13	0.49	7.27	590	72	1720
Vatra	Khambhat	7.8	3392	58	114	907	888	778	9.41	0.71	7.27	517	130	4150
Zalapur	Khambhat	8.3	3601	52	74	1033	1704	0	8.1	0.42	4.84	601	137	5100
Amiyad	Borsad	7.5	3812	54	103	1047	888	801	3.21	0.54	7.27	689	230	5100
Badalpur	Borsad	7.5	5048	54	99	1136	2663	0	3.19	1.02	7.27	904	192	5710
Banejda	Borsad	7.2	3801	48	91	1037	533	1297	5.05	0.22	4.84	548	247	4800
Dahewan	Borsad	7.6	3419	97	56	1002	1243	304	6.97	0.38	4.84	537	180	3510

Dali	Borsad	7.6	5878	136	290	1481	2485	216	2.41	0.55	7.27	1008	262	10300
Divel	Borsad	8.0	3506	57	49	1014	781	606	3.19	0.6	7.27	795	204	3600
Gajana	Borsad	8.3	1805	26	39	513	533	107	4	0.43	4.84	479	108	3000
Gorva	Borsad	8.2	3541	40	21	1007	178	1101	2.72	0.71	7.27	1031	163	4300
Kalu	Borsad	7.7	2570	75	27	775	923	227	6.75	0.49	7.27	368	175	2600
Kanbha	Borsad	8.4	1893	61	38	496	497	141	4.29	0.33	4.84	449	211	1900
Kandhroti	Borsad	7.1	2761	16	68	713	1101	0	4.49	0.23	4.84	717	146	2810
Kankapur	Borsad	7.3	3894	55	117	1050	1065	373	1.44	0.55	7.27	548	686	5200
Kathana	Borsad	7.6	2678	44	70	754	888	142	52.52	0.77	7.27	578	202	2800
Kathol	Borsad	8.4	3042	26	94	775	426	582	1.84	0.33	4.84	921	218	3060
Pilodra/Salol	Borsad	7.7	4130	152	185	1003	1420	944	4.24	0.38	4.84	356	70	7800
Ras	Borsad	7.8	3615	41	58	1005	355	1161	2.45	0.55	7.27	647	348	3610
Salol	Borsad	8.2	3635	34	26	1025	1065	0	1.29	0.38	7.27	1231	254	5100
Sisva	Borsad	8.3	1426	39	8	286	355	0	5.04	0.38	7.27	421	317	1700
Umlav	Borsad	8.4	1397	22	59	216	355	0	1.63	0.27	7.27	584	161	1800
Valvod	Borsad	8.2	1993	45	51	496	355	203	1.32	0.88	7.27	637	206	2700
Vasna (Ras)	Borsad	7.8	3329	42	69	1011	1278	132	4.51	0.54	4.84	605	192	3350

Appendix B
Laboratory testing results of the Post-Monsoon Season

Village Name	Taluka Name	pH	TDS (mg/l)	Ca (mg/l)	Mg (mg/l)	Na (mg/l)	Cl (mg/l)	SO_4 (mg/l)	K (mg/l)	F (mg/l)	NO_3 (mg/l)	HCO_3 (mg/l)	CO_3 (mg/l)	EC (µ℧/cm)
Bamnava	Khambhat	7.8	1237	70	26	225	291	0	4.54	0.33	4.84	570	55	1750
Bhim Talav	Khambhat	8.1	1938	55	31	216	724	0	0.13	0.25	4.84	838	74	2480
Bhuvel	Khambhat	7.9	2050	34	58	116	710	0	7.25	0.23	4.84	1053	79	2300
Daheda	Khambhat	7.6	1280	102	61	150	284	0	9.55	0.25	4.84	592	91	1330
Dhuvaran	Khambhat	7.7	2692	42	72	664	432	102	2.52	0.70	9.69	1272	108	4400
Haripura	Khambhat	7.4	6425	119	24	1116	1995	0	1.50	0.47	7.27	3056	115	6800
Jahaj	Khambhat	7.7	2103	40	26	216	568	0	3.38	0.80	4.84	1191	62	3900
Jalundh	Khambhat	7.8	2083	52	66	225	452	0	3.86	0.90	7.27	1175	113	3300
Jinaj	Khambhat	7.8	892	58	28	44	142	0	18.67	0.36	4.84	550	70	750
Kalamsar	Khambhat	7.7	3664	98	24	1067	1456	0	3.91	0.33	4.84	925	94	5550
Kali Talavadi	Khambhat	7.6	2356	124	18	546	710	0	3.10	0.64	7.27	776	182	4020
Kansari	Khambhat	7.6	2534	124	18	546	710	0	7.42	0.42	7.27	932	204	4020
Khadodhi	Khambhat	7.7	2446	146	61	286	866	0	6.63	0.36	4.84	897	190	3100
Khambhat	Khambhat	7.2	9458	123	136	1084	3607	0	12.87	0.48	4.84	4302	206	12200
Khatnal	Khambhat	8.1	1921	96	20	308	575	0	5.30	0.20	4.84	732	190	2100
Kodva	Khambhat	7.6	7099	152	154	1244	2009	0	6.80	0.54	7.27	3329	211	7700
Lunej	Khambhat	8.6	10935	139	146	1775	3997	0	89.08	0.32	4.84	4736	142	15600
Metpur	Khambhat	7.7	3753	148	72	1000	1122	485	11.24	0.81	9.69	777	149	5000
Nagra	Khambhat	8.3	1628	49	38	216	504	0	2.80	0.18	2.42	665	156	2120
Nana Kadodra	Khambhat	7.3	3263	112	33	546	947	0	23.13	0.70	7.27	1423	202	5100
Navagam Vanta	Khambhat	8.6	2865	20	19	216	914	0	3.67	0.54	7.27	702	994	2900
Neja	Khambhat	7.9	1883	28	17	189	647	0	3.88	0.59	9.69	978	24	1900
Paldi	Khambhat	7.9	4440	16	12	1331	1429	0	12.13	0.19	7.27	1335	317	14000
Popatvav	Khambhat	7.7	1805	27	19	308	670	0	5.16	0.48	7.27	745	36	3000
Rajpur	Khambhat	7.2	3779	168	116	884	913	672	23.63	0.48	7.27	978	48	7400
Ralej	Khambhat	7.4	2450	92	48	617	780	0	16.03	0.65	9.69	882	31	4900
Sakarpur	Khambhat	7.6	1889	58	20	529	435	332	13.18	0.82	9.69	484	31	3900
Timba	Khambhat	7.5	1838	55	25	513	444	346	6.45	0.60	9.69	421	34	3500
Undel	Khambhat	7.3	2616	63	36	244	913	0	5.29	0.53	7.27	1319	41	2600
Vadola	Khambhat	7.5	1645	44	32	286	385	0	6.34	0.55	7.27	780	118	2800
Vasna	Khambhat	7.5	2108	56	35	420	534	0	12.26	0.63	9.69	1008	55	3400
Vatadra	Khambhat	7.7	2120	50	42	110	528	0	2.07	0.47	7.27	1155	235	1900
Vatra	Khambhat	7.4	2011	66	30	331	703	0	8.63	0.51	7.27	852	29	3000
Zalapur	Khambhat	7.5	2658	38	25	496	790	0	5.01	0.33	4.84	1153	156	3700
Amiyad	Borsad	7.7	1776	20	19	84	646	0	7.29	0.42	4.84	978	29	2100
Badalpur	Borsad	7.4	2724	50	39	754	575	188	2.31	0.82	9.69	628	490	4500
Banejda	Borsad	7.4	3836	56	34	546	1369	0	4.66	0.40	4.84	1591	240	3900
Dahewan	Borsad	7.4	2160	78	28	365	646	0	6.17	0.26	7.27	1007	36	2800
Dali	Borsad	6.9	3631	72	32	1032	396	1248	2.86	0.27	7.27	825	26	9400
Divel	Borsad	7.8	2760	24	30	378	1075	0	2.46	0.24	4.84	1210	43	2600

Gajana	Borsad	7.4	2402	52	29	513	711	0	7.26	0.23	4.84	1063	34	3800
Gorva	Borsad	7.9	2082	20	12	308	575	0	1.50	0.38	4.84	1054	113	2100
Kalu	Borsad	7.8	2272	36	23	265	548	0	6.07	0.64	7.27	1166	134	2900
Kanbha	Borsad	7.9	2218	18	13	189	741	0	4.12	0.29	7.27	1147	110	2300
Kandhroti	Borsad	8.0	2771	58	43	343	807	0	2.10	0.32	7.27	1030	490	3100
Kankapur	Borsad	7.5	2429	39	21	420	912	0	1.48	0.44	7.27	939	98	3400
Kathana	Borsad	7.6	2191	15	14	254	701	0	47.69	0.44	4.84	1041	166	2800
Kathol	Borsad	7.8	2577	130	85	435	649	0	0.96	0.42	4.84	1057	221	2900
Pilodra/Salol	Borsad	7.2	3922	18	12	563	1730	0	3.87	0.43	50.86	1537	62	5400
Ras	Borsad	7.7	2413	26	15	244	780	0	1.39	0.27	4.84	1319	29	2800
Sisva	Borsad	7.7	1564	78	25	165	439	0	38.28	0.38	4.84	631	226	2600
Umlav	Borsad	7.8	1988	78	29	116	648	0	0.91	0.35	4.84	858	259	2030
Valvod	Borsad	7.6	2146	30	15	207	684	0	1.32	0.62	9.6	1083	127	2900
Vasna (Ras)	Borsad	7.6	2284	24	20	406	679	0	2.78	0.30	4.84	836	319	3500

Appendix C
Irrigation Indices Values Pre-Monsoon Season

Village Name	Taluka Name	SAR	% Na	RSC (meq/l)	RSBC (meq/l)	KI	MH (meq/l)	PS (meq/l)
Bamnava	Khambhat	13.19	77.06	6.92	7.50	3.34	76.98	19.99
Bhat Talavadi	Khambhat	10.77	73.04	1.04	4.08	2.69	67.67	16.89
Bhim Talav	Khambhat	14.69	81.97	8.41	6.37	4.54	77.10	15.75
Bhuvel	Khambhat	18.51	83.29	5.00	5.30	4.95	72.90	28.08
Daheda	Khambhat	17.22	82.75	6.05	6.01	4.78	72.31	21.72
Dhuvaran	Khambhat	30.31	90.55	14.05	9.95	9.56	52.37	58.08
Haripura	Khambhat	11.96	61.00	-18.19	5.15	1.56	85.03	54.15
Jahaj	Khambhat	21.87	84.39	9.56	10.88	5.39	79.99	31.83
Jalundh	Khambhat	20.03	82.23	3.17	7.30	4.61	82.01	39.70
Jinaj	Khambhat	19.68	81.19	0.16	4.86	4.29	73.46	39.34
Kalamsar	Khambhat	43.44	94.63	25.73	17.49	17.56	5.38	32.15
Kali Talavadi	Khambhat	19.84	84.38	12.38	10.35	5.39	72.78	23.88
Kansari	Khambhat	19.97	81.79	1.29	5.10	4.47	70.97	43.59
Khadodhi	Khambhat	0.48	21.84	16.83	14.60	0.18	0.00	49.09
Khambhat	Khambhat	37.15	89.08	3.57	6.69	8.12	83.32	77.26
Khatnal	Khambhat	15.90	82.13	8.25	8.47	4.57	80.21	27.05
Kodva	Khambhat	17.49	76.42	-0.69	5.37	3.23	88.09	45.89
Lunej	Khambhat	15.60	72.97	-4.73	4.76	2.55	84.00	80.12
Metpur	Khambhat	14.90	66.15	-19.11	0.57	1.93	76.48	74.28
Motipura	Khambhat	17.86	70.45	-16.75	4.18	2.37	88.56	90.13
Nagra	Khambhat	21.56	86.45	7.84	7.63	6.36	68.74	23.44
Nana Kadodra	Khambhat	12.78	64.11	-16.08	4.14	1.76	86.38	50.61
Navagam Vanta	Khambhat	22.77	86.24	8.06	7.39	6.25	63.19	24.50
Neja	Khambhat	23.19	85.87	8.02	8.90	6.07	73.32	50.07
Paldi	Khambhat	13.93	67.21	-9.29	0.14	2.03	69.40	80.12
Popatvav	Khambhat	20.31	86.34	9.55	9.40	6.29	69.40	20.16
Rajpur	Khambhat	12.04	61.01	-24.05	-2.19	1.54	79.00	80.12
Ralej	Khambhat	17.69	78.01	-6.75	0.63	3.51	76.43	39.36
Sakarpur	Khambhat	14.04	67.71	-11.17	5.07	2.08	86.41	55.33
Timba	Khambhat	23.90	85.96	11.50	11.18	6.11	71.99	42.06
Undel	Khambhat	7.42	50.82	-15.24	5.74	1.03	91.60	33.47
Vadola	Khambhat	18.47	82.81	4.82	8.43	4.79	76.48	26.96
Vasna	Khambhat	18.81	80.74	-1.98	1.29	4.16	75.61	35.97
Vatadra	Khambhat	5.21	56.31	3.77	7.87	1.28	78.35	19.04
Vatra	Khambhat	15.93	76.38	0.53	5.58	3.21	76.42	33.15
Zalapur	Khambhat	21.56	83.87	5.73	7.26	5.17	70.12	48.07
Amiyad	Borsad	19.27	80.33	7.79	8.60	4.08	75.88	33.39
Badalpur	Borsad	21.22	82.03	10.37	12.12	4.56	75.15	75.12
Banejda	Borsad	20.29	82.07	7.33	6.59	4.56	75.77	28.54
Dahewan	Borsad	20.05	82.24	5.35	3.96	4.61	48.77	38.23
Dali	Borsad	16.46	67.78	-5.40	9.73	2.10	77.86	72.35

Divel	Borsad	23.79	86.53	12.95	10.19	6.41	58.64	28.34
Gajana	Borsad	14.87	83.26	6.94	6.55	4.95	71.21	16.15
Gorva	Borsad	32.10	92.18	18.61	14.90	11.76	46.40	16.48
Kalu	Borsad	19.52	85.03	5.90	2.29	5.65	37.25	28.40
Kanbha	Borsad	12.28	77.85	8.22	4.32	3.50	50.67	15.49
Kandhroti	Borsad	17.35	82.96	10.22	10.95	4.85	87.51	31.06
Kankapur	Borsad	18.36	78.70	19.47	6.24	3.69	77.82	33.93
Kathana	Borsad	16.44	81.10	8.25	7.28	4.12	72.40	26.53
Kathol	Borsad	15.86	78.89	13.33	13.80	3.73	85.64	18.08
Pilodra/Salol	Borsad	12.92	65.73	-14.64	-1.75	1.91	66.75	49.89
Ras	Borsad	23.68	86.52	15.38	8.56	6.41	70.00	22.10
Salol	Borsad	32.19	92.08	24.81	18.48	11.62	55.77	30.04
Sisva	Borsad	10.90	82.84	14.86	4.95	4.78	25.28	10.01
Umlav	Borsad	5.45	61.32	8.98	8.47	1.58	81.56	10.01
Valvod	Borsad	12.00	77.00	10.86	8.19	3.34	65.14	12.13
Vasna (Ras)	Borsad	22.31	85.01	8.54	7.82	5.66	73.04	37.43

Appendix D
Irrigation Indices Values Post-Monsoon Season

Village Name	Taluka Name	SAR	% Na	RSC (meq/l)	RSBC (meq/l)	KI	MH (meq/l)	PS (meq/l)
Bamnava	Khambhat	5.83	63.75	5.54	5.85	1.74	37.99	8.21
Bhim Talav	Khambhat	5.77	63.96	10.91	10.99	1.77	48.17	20.42
Bhuvel	Khambhat	2.81	44.71	13.42	15.56	0.78	73.78	20.03
Daheda	Khambhat	2.90	40.11	2.63	4.61	0.65	49.65	8.01
Dhuvaran	Khambhat	14.42	78.30	16.43	18.75	3.60	73.87	13.25
Haripura	Khambhat	24.41	85.99	46.01	44.15	6.13	24.96	56.28
Jahaj	Khambhat	6.53	69.63	17.45	17.52	2.27	51.74	16.02
Jalundh	Khambhat	4.89	55.19	15.00	16.66	1.22	67.67	12.75
Jinaj	Khambhat	1.19	31.51	6.15	6.12	0.37	44.32	4.01
Kalamsar	Khambhat	25.05	87.14	11.43	10.27	6.76	28.77	41.07
Kali Talavadi	Khambhat	12.13	75.65	11.12	6.53	3.10	19.31	20.03
Kansari	Khambhat	12.13	75.74	14.41	9.09	3.10	19.31	20.03
Khadodhi	Khambhat	5.02	50.61	8.73	7.42	1.01	40.79	24.43
Khambhat	Khambhat	16.02	73.26	60.05	64.37	2.72	64.58	101.75
Khatnal	Khambhat	7.47	67.77	11.89	7.21	2.08	25.57	16.22
Kodva	Khambhat	17.00	72.83	41.34	46.98	2.67	62.56	56.67
Lunej	Khambhat	25.08	80.75	63.41	70.69	4.07	63.40	112.76
Metpur	Khambhat	16.86	76.69	4.39	5.35	3.27	44.51	36.70
Nagra	Khambhat	5.63	62.95	10.53	8.45	1.69	56.12	14.22
Nana Kadodra	Khambhat	11.66	74.56	21.75	17.73	2.86	32.70	26.71
Navagam Vanta	Khambhat	8.30	78.75	42.07	10.51	3.67	61.04	25.78
Neja	Khambhat	6.95	74.85	14.03	14.63	2.94	50.03	18.25
Paldi	Khambhat	61.27	97.02	30.66	21.08	32.42	55.29	40.31
Popatvav	Khambhat	11.11	82.30	10.50	10.86	4.60	53.71	18.90
Rajpur	Khambhat	12.84	68.54	-0.30	7.65	2.14	53.24	32.75
Ralej	Khambhat	12.99	76.14	6.95	9.87	3.14	46.25	22.00
Sakarpur	Khambhat	15.27	83.72	4.43	5.04	5.07	36.25	15.73
Timba	Khambhat	14.40	82.40	3.23	4.16	4.65	42.84	16.13
Undel	Khambhat	6.07	63.77	16.88	18.47	1.74	48.52	25.76
Vadola	Khambhat	8.01	72.30	11.89	10.59	2.58	54.53	10.86
Vasna	Khambhat	10.85	76.61	12.68	13.73	3.22	50.76	15.06
Vatadra	Khambhat	2.77	44.84	20.81	16.44	0.80	58.08	14.89
Vatra	Khambhat	8.48	71.73	9.17	10.67	2.50	42.84	19.83
Zalapur	Khambhat	15.35	84.59	20.14	17.00	5.46	52.04	22.29
Amiyad	Borsad	3.23	59.99	14.43	15.03	1.43	61.04	18.22
Badalpur	Borsad	19.42	85.21	20.92	7.80	5.75	56.26	18.18
Banejda	Borsad	14.20	81.02	28.48	23.28	4.25	50.03	38.62
Dahewan	Borsad	9.02	72.13	11.51	12.61	2.56	37.19	18.22
Dali	Borsad	25.44	87.84	8.16	9.93	7.21	42.29	24.16
Divel	Borsad	12.14	81.83	17.60	18.63	4.48	67.33	30.33
Gajana	Borsad	14.14	81.87	13.57	14.83	4.48	47.91	20.06

Gorva	Borsad	13.45	87.13	19.06	16.28	6.75	49.74	16.22
Kalu	Borsad	8.49	76.00	19.89	17.31	3.12	51.30	15.46
Kanbha	Borsad	8.29	80.88	20.50	17.90	4.18	54.36	20.90
Kandhroti	Borsad	8.32	69.95	26.78	13.99	2.32	55.01	22.77
Kankapur	Borsad	13.48	83.29	14.98	13.44	4.97	47.03	25.73
Kathana	Borsad	11.33	86.59	20.69	16.31	5.81	60.62	19.78
Kathol	Borsad	7.29	58.43	11.21	10.84	1.40	51.88	18.31
Pilodra/Salol	Borsad	25.22	92.88	25.37	24.29	12.99	52.37	48.80
Ras	Borsad	9.43	80.79	20.05	20.32	4.19	48.75	22.00
Sisva	Borsad	4.16	57.82	11.93	6.45	1.21	34.58	12.38
Umlav	Borsad	2.85	44.67	16.42	10.17	0.80	38.01	18.28
Valvod	Borsad	7.71	76.79	19.25	16.25	3.30	45.19	19.30
Vasna (Ras)	Borsad	14.81	86.18	21.49	12.50	6.21	57.88	19.15

Appendix E
GWQI, EGWQI and EIRWQI and corresponding groundwater quality class Pre-Monsoon Season

Sample Number	Village Name	Taluka Name	GWQI	EGWQI	EIRWQI
1	Bamnava	Khambhat	168.17	1.51	160.59
2	Bhat Talavadi	Khambhat	161.38	1.54	135.67
3	Bhim Talav	Khambhat	142.36	1.29	156.32
4	Bhuvel	Khambhat	207.14	1.79	189.47
5	Daheda	Khambhat	186.84	1.67	175.41
6	Dhuvaran	Khambhat	294.58	2.31	298.73
7	Haripura	Khambhat	398.09	3.90	225.96
8	Jahaj	Khambhat	255.45	2.27	216.85
9	Jalundh	Khambhat	262.13	2.29	224.37
10	Jinaj	Khambhat	282.43	2.50	216.73
11	Kalamsar	Khambhat	247.87	1.99	297.54
12	Kali Talavadi	Khambhat	216.28	2.02	192.84
13	Kansari	Khambhat	269.88	2.29	227.50
14	Khadodhi	Khambhat	205.06	1.81	146.75
15	Khambhat	Khambhat	458.22	3.79	369.46
16	Khatnal	Khambhat	175.32	1.48	190.88
17	Kodva	Khambhat	315.30	2.88	232.63
18	Lunej	Khambhat	428.99	3.42	319.94
19	Metpur	Khambhat	449.23	4.02	287.30
20	Motipura	Khambhat	479.57	4.13	339.36
21	Nagra	Khambhat	219.33	2.08	190.82
22	Nana Kadodra	Khambhat	404.32	3.97	216.95
23	Navagam Vanta	Khambhat	248.27	2.35	188.86
24	Neja	Khambhat	270.91	2.21	257.58
25	Paldi	Khambhat	405.81	3.43	313.57
26	Popatvav	Khambhat	195.78	1.84	185.50
27	Rajpur	Khambhat	419.73	3.64	278.17
28	Ralej	Khambhat	314.68	2.95	198.48
29	Sakarpur	Khambhat	364.46	3.38	241.58
30	Timba	Khambhat	264.08	2.20	249.67
31	Undel	Khambhat	303.96	3.23	161.63
32	Vadola	Khambhat	221.44	2.04	191.22
33	Vasna	Khambhat	281.23	2.57	195.13
34	Vatadra	Khambhat	131.94	1.26	130.30
35	Vatra	Khambhat	269.26	2.51	189.03
36	Zalapur	Khambhat	268.61	2.17	247.08
37	Amiyad	Borsad	280.92	2.57	205.83
38	Badalpur	Borsad	369.54	3.08	306.70
39	Banejda	Borsad	278.16	2.58	191.93
40	Dahewan	Borsad	252.74	2.08	201.55

41	Dali	Borsad	457.88	4.10	297.35
42	Divel	Borsad	246.40	2.21	205.76
43	Gajana	Borsad	133.92	1.18	163.45
44	Gorva	Borsad	236.47	2.29	219.77
45	Kalu	Borsad	192.97	1.57	175.16
46	Kanbha	Borsad	137.03	1.20	133.31
47	Kandhroti	Borsad	193.92	1.60	210.32
48	Kankapur	Borsad	272.34	2.39	206.37
49	Kathana	Borsad	287.09	1.84	183.39
50	Kathol	Borsad	209.88	2.04	173.99
51	Pilodra/Salol	Borsad	344.35	3.18	209.22
52	Ras	Borsad	253.12	2.39	191.37
53	Salol	Borsad	226.84	1.89	268.08
54	Sisva	Borsad	93.45	0.80	115.16
55	Umlav	Borsad	98.79	0.96	117.99
56	Valvod	Borsad	144.71	1.42	138.71
57	Vasna (Ras)	Borsad	243.82	2.03	225.65

Appendix F
GWQI, EGWQI and EIRWQI and corresponding groundwater quality class Post-Monsoon Season

Sample Number	Village Name	Taluka Name	GWQI	EGWQI	EIRWQI
1	Bamnava	Khambhat	89.28	0.83	94.18
2	Bhim Talav	Khambhat	126.57	1.08	122.65
3	Bhuvel	Khambhat	132.49	1.17	110.74
4	Daheda	Khambhat	99.01	0.95	73.36
5	Dhuvaran	Khambhat	177.10	1.65	173.47
6	Haripura	Khambhat	367.58	3.21	308.72
7	Jahaj	Khambhat	130.69	1.24	132.68
8	Jalundh	Khambhat	137.99	1.35	116.97
9	Jinaj	Khambhat	70.03	0.72	51.05
10	Kalamsar	Khambhat	251.10	1.97	247.94
11	Kali Talavadi	Khambhat	161.24	1.42	150.04
12	Kansari	Khambhat	165.92	1.45	152.65
13	Khadodhi	Khambhat	169.46	1.50	122.59
14	Khambhat	Khambhat	560.33	4.73	401.19
15	Khatnal	Khambhat	125.34	1.11	115.85
16	Kodva	Khambhat	431.27	3.87	307.61
17	Lunej	Khambhat	687.18	5.91	485.65
18	Metpur	Khambhat	282.88	2.37	208.89
19	Nagra	Khambhat	107.78	0.94	110.06
20	Nana Kadodra	Khambhat	211.24	1.91	176.43
21	Navagam Vanta	Khambhat	157.17	1.22	151.14
22	Neja	Khambhat	122.05	1.09	130.37
23	Paldi	Khambhat	276.51	2.16	525.65
24	Popatvav	Khambhat	123.78	1.03	151.42
25	Rajpur	Khambhat	290.98	2.53	197.41
26	Ralej	Khambhat	181.36	1.59	169.48
27	Sakarpur	Khambhat	150.41	1.31	153.62
28	Timba	Khambhat	144.45	1.29	149.80
29	Undel	Khambhat	164.90	1.46	140.73
30	Vadola	Khambhat	111.13	1.02	122.06
31	Vasna	Khambhat	144.04	1.32	146.63
32	Vatadra	Khambhat	124.68	1.16	98.67
33	Vatra	Khambhat	140.36	1.22	136.67
34	Zalapur	Khambhat	162.69	1.38	181.82
35	Amiyad	Borsad	111.65	0.98	112.19
36	Badalpur	Borsad	181.94	1.51	185.57
37	Banejda	Borsad	230.24	1.91	209.51
38	Dahewan	Borsad	140.76	1.25	137.01
39	Dali	Borsad	255.01	2.12	226.33
40	Divel	Borsad	171.87	1.40	182.70

41	Gajana	Borsad	154.69	1.33	170.56
42	Gorva	Borsad	122.87	1.08	161.55
43	Kalu	Borsad	134.89	1.25	138.66
44	Kanbha	Borsad	129.93	1.12	149.11
45	Kandhroti	Borsad	164.16	1.39	146.61
46	Kankapur	Borsad	157.36	1.28	173.79
47	Kathana	Borsad	193.82	1.32	163.93
48	Kathol	Borsad	173.50	1.60	132.56
49	Pilodra/Salol	Borsad	253.58	1.96	281.16
50	Ras	Borsad	139.72	1.22	157.11
51	Sisva	Borsad	116.81	1.09	94.18
52	Umlav	Borsad	122.27	1.07	94.34
53	Valvod	Borsad	130.59	1.15	139.52
54	Vasna (Ras)	Borsad	137.47	1.12	171.99